

Development of Nanoparticles Based Assays for the Direct
Detection of Unamplified Nucleic Acids in Clinical
Specimens

Ontwikkeling van op nanodeeltjes gebaseerde tests voor de directe
detectie van ongeamplificeerde nucleïne-zuren in klinische monsters

THESIS

to obtain the degree of Doctor from the

Erasmus University Rotterdam

by command of the

rector magnificus

Prof.dr. H.A.P. Pols

and in accordance with the decision of the Doctorate Board

The public defense shall be held on

Tuesday 28 October 2014 at 13.30 o'clock

by

Sherif Mohamed Shawky Abdou

born in Cairo, Egypt



ERASMUS UNIVERSITEIT ROTTERDAM

Doctoral Committee

Promoter: Prof.dr. F. Grosveld

Other members: Prof.dr. D.F.E. Huylebroeck

Dr. T.L.M. Ten Hagen

Dr. N.J. Galjart

Copromoter: Prof.dr. H.M.E. Azzazy

The studies in this thesis were performed in Youssef Jamel for Science and Technology Research Center (STRC) and chemistry department, School of Science and Engineering. The American University in Cairo (AUC), Cairo, Egypt.

Cover design: Dr. Tamer Samir & Sherif Mohamed Shawky

Cover illustration: Schematic diagram represents double stranded DNA, non-aggregated red gold nanoparticles conjugated to oligonucleotide and blue aggregated gold nanoparticles as a result of hybridization to the target nucleic acid

Copyright © 2014 by Sherif Mohamed Shawky Abdou

ISBN 978-94-6203-678-9

Printed by WÖhrmann Print Service, Zutphen

Table of Contents

Table of Contents.....	i
List of Acronyms	v
1 Introduction.....	1
1.1 Gold nanoparticles (AuNPs)	3
1.1.1 Structure and physical properties of gold nanoparticles	3
1.1.2 Synthesis of gold nanoparticles.....	5
1.1.3 Selected nucleic acids detection strategies using AuNPs.....	8
1.1.3.1 Cross-linking method.....	8
1.1.3.2 Non- Cross-linking method	10
1.1.3.3 Unmodified AuNPs method	12
1.1.3.4 Fluorescence energy transfer and Quenching.....	15
1.1.3.5 Selected Immuno-assays by gold nanoparticles.....	20
1.2 Iron oxide nanoparticles	21
1.2.1 Synthesis of iron oxide nanoparticles.....	21
1.2.2 Magnetic nanoparticles applications.....	23
1.2.2.1 In-Vitro Diagnostics	23
1.2.2.2 Biomolecules Separation	26
1.3 Hepatitis C virus (HCV)	27
1.3.1 HCV life cycle.....	28
1.3.2 Current therapeutic options	28
1.3.3 Current diagnostic methods.....	29
1.3.3.1 Biochemical markers and serological tests	29
1.3.3.2 Nucleic acid testing (NAT).....	31
1.4 Tumor Markers	34
1.4.1 Urinary Bladder Cancer.....	34
1.4.1.1 Hepatoma Up-Regulated Protein (HURP)	36
1.4.2 Breast Cancer	36
1.4.2.1 Histidine-Rich Glycoprotein (HRG)	38
1.5 Scope of the thesis.....	39

2	Direct Detection of Unamplified Hepatitis C Virus RNA Using Unmodified Gold Nanoparticles	41
2.1	Abstract.....	42
2.2	Introduction	43
2.3	Materials and Methods:.....	45
2.3.1	Synthesis of AuNPs.....	45
2.3.2	Characterization of AuNPs	46
2.3.3	Serum Samples.....	46
2.3.4	HCV RNA Extraction.....	46
2.3.5	RT-PCR and Real Time RT-PCR.....	47
2.3.6	Colorimetric AuNPs Assay for Detecting Full Length HCV RNA in Clinical Samples.....	47
2.3.7	Detection Limit Measurements.....	48
2.4	Results.....	48
2.4.1	Size Distribution and Surface Plasmon Band of the Prepared AuNPs	48
2.4.2	Suitability of RNA Extraction Method	50
2.4.3	Colorimetric AuNPs Assay: Development & Optimization.....	50
2.5	Conclusions.....	53
3	Detection of Unamplified HCV RNA in Serum Using A Novel Two Metallic Nanoparticle Platform	55
3.1	Abstract.....	56
3.2	Introduction	57
3.3	Materials and Methods:.....	60
3.3.1	Iron oxide magnetic nanoparticles: synthesis and functionalization	60
3.3.2	Characterization of Magnetic Nanoparticles (MNP).....	60
3.3.3	Conjugation of HCV specific probe to the amino functionalized MNP.....	60
3.3.4	Synthesis of Positively Charged AuNPs.....	61
3.3.5	Characterization of synthesized AuNPs	62
3.3.6	Serum specimens	62
3.3.7	Real-time RT-PCR	62

3.3.8	Colorimetric two nanoparticles HCV assay:	63
3.4	Results:.....	64
3.4.1	Characterization of magnetic nanoparticles	64
3.4.2	Characterization of synthesized AuNPs	65
3.4.3	Detection of HCV RNA in Serum Using Real-time RT-PCR and Two Nanoparticles HCV Assay	67
3.5	Discussion and Conclusions	69
4	Development and evaluation of gold nanoparticles assays for direct detection of urinary bladder cancer and breast cancer biomarkers	73
4.1	Abstract.....	74
4.2	Introduction	75
4.3	Materials and methods	78
4.3.1	Study Population	78
4.3.1.1	Urinary Bladder Cancer.....	78
4.3.1.2	Breast Cancer	78
4.3.2	Amino functionalized MNP synthesis, functionalization and characterization	79
4.3.3	Synthesis and characterization of Gold Nanoparticles	80
4.3.4	Total RNA extraction	81
4.3.4.1	Urinary Bladder Cancer.....	81
4.3.4.2	Breast Cancer	81
4.3.5	HURP & HRG RNA purification by MNP functionalized by a target specific probe	81
4.3.6	RT-PCR for HURP and HRG RNA	82
4.3.7	The developed colorimetric AuNPs based assay for target RNA detection.....	82
4.3.8	Detection Limit Measurement	83
4.3.9	Statistical Analysis	83
4.4	Results.....	84
4.4.1	Size Distribution of amine functionalized magnetic nanoparticles	84
4.4.2	Size distribution and surface Plasmon band of the prepared AuNPs.....	85

Table of Contents

4.4.3	RT-PCR for HURP and HRG	86
4.4.4	AuNPs assay: development and optimization.....	88
4.4.5	AuNPs assay: performance characteristics	88
4.5	Discussion.....	89
5	Dissertation Discussion.....	96
5.1	Unmodified AuNPs in HCV RNA detection in serum samples.....	96
5.2	Cationic AuNPs in detection of HCV in serum samples	98
5.3	Unmodified AuNPs in tumor marker detection	99
6	Bibliography.....	101
7	Summary.....	118
8	Samenvatting.....	122
9	curriculum vitae	126
10	PhD Portfolio.....	128
11	Acknowledgements.....	130

List of Acronyms

ACS	American Chemical Society
AFM	Atomic Force Microscope
ALT	alanine amino transferase
aM	ato Molar
APES	Amino-propyl tri-ethoxysilane
APMS	Amino-propyl tri-methoxysilane
AST	Aspartate Transaminase
AuNPs	gold nanoparticles
BCA	Bio barcode assay
BDAC	Benzyl di-methyl hexadecyl ammonium chloride
b-DNA	branched DNA
BTA	bladder tumor antigen
CTAB	Cetyl-tri methyl ammonium bromide
ds-DNA	double stranded DNA
E1	Envelope protein 1
E2	Envelope protein 2
EIA	Enzyme Linked Immune-assays
ERLs	Extrinsic Raman labels
fcc	face centered cube
FDA	Food and Drug Administration
FM	femto molar
fmole	femto mole
FRET	Forster Resonance Energy Transfer
FT-IR	Fourier Transform Infra-Red Spectroscopy

List of Acronyms

GOBO	Gene-expression based outcome for breast cancer online (http://co.bmc.lu.se/gobo)
HAuCl₄.3H₂O	Tetra-chlorauric acid
HCV	Hepatitis C virus.
HRG	Histidine-rich glycoprotein
HURP	Hepatoma up regulated protein
IC	internal conversion
IDC	invasive duct carcinoma
IFN	Interferon
ILC	invasive lobular carcinoma
ISC	inter system crossing
IU/ml	International unit per one millimeter
IUPAC	International union of pure and applied chemistry
M⁻¹cm⁻¹	Molar extinction coefficient unit. Molar concentration of the substance
Maghemite	γ -Fe ₂ O ₃
Magnetite	Fe ₃ O ₄
MBS	3- maleimido benzoic acid N-hydroxyl succinimide
mi-RNA	micro- RNA
MP	magnetic particles
MNP	Magnetic nanoparticles
m-RNA	messenger RNA
NATs	Nucleic Acid Testings
nm	nano meter
nmole	nano mole
NPV	negative predictive value

List of Acronyms

NS	non-structural
NSET	Nanoparticle Surface Energy Transfer
ORF	open reading frame
PBS	phosphate buffer saline
PPV	positive predictive value
RIBA	Recombinant immune blot assays
RT-PCR	Reverse Transcriptase- Polymerase Chain Reaction
SCC	squamous cell carcinoma
SEM	Scanning electron microscope
SERS	surface enhanced Raman scattering
SNPs	Single Nucleotide Polymorphisms
SPR	Surface Plasmon Resonance
ss-DNA	single stranded DNA
TCC	transitional cell carcinoma
TEM	Transmission electron microscope
TMA	Transcriptional mediated amplification
5'UTR	5' Untranslated region
UV	ultra violet
WHO	World Health Organization

1 Introduction

Patient safety and effective disease management are major aspects of healthcare strategies. Consequently, over the last two decades there has been an increase in communication between clinical diagnostic laboratories and clinical decision makers as to what would be the optimum therapeutic agent to use. The two main arms of medicine and, by extension also personalized medicine, are laboratory based tests and the choice of suitable treatments.

The early detection of nucleic acids of different natures (such as DNA, RNA and miR) obtained from different sources such as serum, plasma, infectious diseases (e.g. viral and bacterial), and cells is typically crucial for successful patient management. Consequently, clinical laboratory medicine strives for the development of molecular assays with high sensitivity, specificity, and multiplexing capabilities, with short turnaround times and lower costs. Despite the recent progress in this, some major challenges remain. These still include the rapid delivery of results within 24 hours, which is especially essential in hospitals and in particular their intensive care units. In addition, some types of analysis deal with very small sample quantities/volumes, as occurs often in forensic medicine laboratories and neonatal screening units. Furthermore, there is often a narrow concentration range of the analytes between healthy and the diseased states, and detection methods inevitably require the dilution of samples that are only available in small volumes (Schleicher 2006). Currently used techniques, such as DNA microarrays, real-time and conventional PCR, and branched DNA assay, requires multistep procedures that are time-consuming, labor-intensive, expensive, and sophisticated equipment.

Several criteria, such as specificity, sensitivity, reproducibility, simplicity and cost, should be taken into consideration for the development of new and optimized molecular assays. These challenges drive a constant search for alternative and improved assays, and have triggered the introduction of novel and often innovative approaches and technologies. Nanotechnology is one of those approaches.

Nanotechnology is the creation and utilization of materials, devices, and systems on the nanometer-length scale (10^{-9} meter) (Hood 2004, Jain 2005) that can be applied to molecular diagnostics, with the overall outcome

leading to an enhancement in clinical health care, and patient safety. The use of materials and chemicals at the nano-scale dimensions allows the utilization of unique properties that are not observed in bulk form, and include new colors and electronic, magnetic and mechanical properties. These depend on the type of the particle used, i.e. at nano-scale dimensions there is ideally an enhancement in the physical and chemical properties of the materials used. The blooming field of nanotechnology has generated several nanostructures with remarkable diagnostic applications over the past few years, which will almost inevitably propel clinical diagnostics to new frontiers. An assortment of nanoparticles, of various sizes, shapes, compositions, chemical and surface properties, and functionalized with various ligands (such as oligonucleotides, antibodies, cross linkers, polymers), has already been constructed. The evolving use of nanoparticles in diagnostic applications shows great promise to meet the rigorous demands of the clinical laboratory mainly in regard to sensitivity, specificity and cost-effectiveness (Azzazy et al. 2006). The unique optical and physical properties of nanoparticles and their extremely small size allows them to interact with bio-molecules and cellular structures, on a one-to-one level. This enables obtaining information on the single molecule level rather than data averaged over an ensemble of molecules, thereby leading to great assay sensitivity. The utility of nanoparticles would result in efficient, accurate, cost-effective diagnostic assays and would aid the development of point-of-care test, in line with the wanted paradigm shift of clinical laboratory medicine.

The most promising nanoparticles that may have a positive influence on clinical diagnostics are gold, iron oxide nanoparticles and quantum dots, due to their unique optical, magnetic and fluorescent properties respectively. My PhD research is focused on the magnetic and gold nanoparticles (AuNPs) and their role in the purification and detection of various nucleic acids.

1.1 Gold nanoparticles (AuNPs)

1.1.1 Structure and physical properties of gold nanoparticles

AuNPs are typical, solid spherical particles having either a negative or positive charge. Other shapes can also be synthesized, e.g. prisms, rods or a thin gold shell surrounding a dielectric core (an insulating material such as silica) and each with dimensions ranging from 0.8-250 nm (Liu 2006).

AuNPs have found their way into clinical diagnostics due to their unique optical properties. They have large molar extinction coefficients ($>10^8 \text{ M}^{-1} \text{ cm}^{-1}$) (Xie 2004). AuNPs exhibit a unique feature known as Surface Plasmon Resonance (SPR), which is responsible for the large absorption and cross-sectional scattering of AuNPs. These properties are about five orders of magnitude greater than that of conventional organic dyes (Huang et al. 2007). SPR is due to the collective resonant oscillations of free electrons at the surface of nanoparticles, which is induced by the alternating electromagnetic field of the incoming light, which has a wavelength greater than the AuNPs' diameter. This gives rise to intense colors for those particles within the visible frequencies, and is responsible for the strong optical and scattering properties of the AuNPs (Figure 1.1).

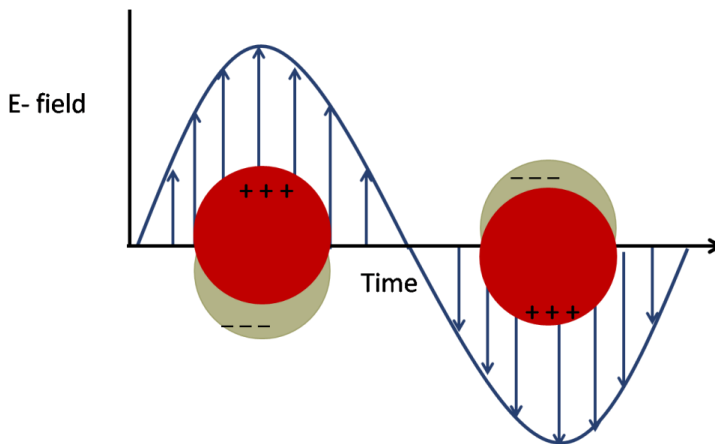


Figure 1.1: The surface Plasmon Resonance of AuNPs. Collective dipolar oscillations of the AuNPs surface electrons are induced by the oscillating electric field of the light.

AuNPs' high absorption coefficient is determined by the size and shape of the particles. The variation in relative thickness of the core and outer shell allows changes in the optical resonance of gold, shifting it as far

as the mid-infrared region (West et al. 2003, Rosi et al. 2005, Baptista et al. 2007). These optical properties are indeed influenced by the particle size and shape, but also by the dielectric constant of the medium and by the temperature (Daniel et al. 2004), which gives gold nanoparticles the advantages of multi-color tracking for assays using one light source, without any need for filters (Liu et al. 2007).

However, with gold nanoparticles smaller than 2 nm in diameter, the SPR disappears or decreases due to surface scattering of the conducting electrons, which decreases the intensity of the SPR as particle size decreases and is accompanied by broadening of the Plasmon bandwidth (Haiss et al. 2007). SPR however, increases with decreasing size when the particle diameter is smaller than 25 nm, and increases with increasing size when the particle diameter is larger than 25 nm (Daniel et al. 2004). A closely related process, called plasmon-plasmon interaction, allows the use of gold nanoparticles as labels for the colorimetric detection of biomolecules. Colloidal solutions of negatively charged, aggregated AuNPs are mainly achieved using sodium chloride salt as salt, a process also known as salt-induced aggregation (Baptista et al. 2008). When nanoparticles aggregate, the interaction of locally adjacent AuNPs (plasmon-plasmon interaction) shifts the color of a colloidal solution of spherical AuNPs from red to blue. Thus, the binding of labeled entities to their respective target could lead to aggregation of the nanoparticles and a detectable shift in the optical signal (West et al. 2003, Azzazy et al. 2006, Baptista et al. 2007, Jain et al. 2007). Additionally, the SPR of AuNPs shifts to higher wavelengths with an increase in the refractive index of the medium (Lucia 2006). Thus, this would allow the detection of the binding or adsorption of AuNPs to surfaces or targets (Jain et al. 2007). Most importantly in clinical applications is that different biological molecules, such as peptides, proteins, DNA and polymers (Daniel et al. 2004), could be conjugated easily to the surface of AuNPs, where their number as well as conformation could be easily controlled (Kenji Suzuki 2009). Moreover, AuNPs exhibit good conductivity of electrical and thermal energy. Owing to the aforementioned properties AuNPs have indeed meanwhile found their way into nucleic acid detection.

1.1.2 Synthesis of gold nanoparticles

Several methods have been established for preparing colloidal solutions of gold nanoparticles, either chemically or physically, and different shapes, sizes and charges have been produced (Daniel et al. 2004, Cheng et al. 2006, Radha Narayanan 2008). Preparation of gold nanoparticles is dependent mainly on the reduction of gold (III) ions, as chloroaurate, into metallic gold using a reducing agent; the latter is generally the capping agent that coats the formed metallic gold. The particle diameter is usually controlled by varying the reducing/capping agent concentration (Jana et al. 2001, Rao Cn et al. 2004). Reduction of gold ions has been chemically achieved using several reducing agents, such as sodium borohydride, phosphonium chloride and sodium citrate (Frens 1973, Duff et al. 1993, Brust et al. 1994). Also, AuNPs have been synthesized by more ecologically sustainable methods using bacteria, fungi, and plant extracts (Shiyong He et al. 2007, Bhambure et al. 2009, Castro L et al. 2010). In addition, the Brust-Schiffrin and seeding growth methods, respectively are two common techniques used in AuNPs synthesis (Jana et al. 2001, Daniel et al. 2004). The **Brust-Schiffrin** method was first published in 1995 (Brust et al. 1995). This method resulted in thermally and air stable AuNPs with a narrow size distribution ranging from 1.5 to 5.2 nm in diameter. These AuNPs could be easily isolated, re-dissolved in organic solvents, and made to function without aggregation or decomposition. They were obtained by reduction of gold (III) ions by an aqueous solution of sodium borohydride in the presence of dodecanethiol. This reduction step is done after transferring the gold ion precursors to toluene using tetra-octyl-ammonium bromide. As a result, the organic phase changes its color from orange to deep brown upon reduction by the borohydride. Brust and co-workers then succeeded in synthesizing AuNPs stabilized by p-mercaptophenol in one single step, thereby opening a path for the production of AuNPs stabilized by a variety of functional thiol ligands (Chen et al. 1998, Chen 1999). The size of the particles is controlled by adjusting the number of thiols to the gold ions in the reaction (Daniel et al. 2004, Zhenxin Wang et al. 2009). The most popular and simple method used for preparing gold nanoparticles is the **citrate reduction method**. Preparation of colloidal gold nanoparticles of 20 nm was first introduced and proposed by (Turkevich et al. 1951), and further developed by Frens (Frens 1973). As a result, a controlled particle size, ranging from 16 and 147 nm, was obtained. The mechanism of the citrate reduction of gold (III) ions into

gold nanoparticles is meanwhile fully understood (Turkevich 1985b, Turkevich 1985a). Synthesis of AuNPs by citrate reduction method is performed by the rapid addition of tri-sodium citrate to a boiling yellow solution of chlorauric acid. This changes the color of the solution from yellow over white to deep red within seconds, which indicates the formation of the AuNPs. The roles of citrate in the reaction are to serve as a reducing agent for the gold chloride and cap the produced nanoparticles. The citrate in the reaction is oxidized and reduces the gold ions to gold atoms. Nucleation occurs on the formed gold atoms, followed by growth of the nanoparticles capped with citrate ions, yielding an overall negative charge of the AuNPs. The difference in concentrations of the citrate and the gold ions, in addition to other reaction parameters such as temperature and pH, controls the size of the particles that are formed; the larger the citrate to gold ion ratio, the smaller the particles will be (Storhoff et al. 1998, Daniel et al. 2004, Kimling et al. 2006). The **seeding growth method** is another common technique for synthesizing AuNPs and to control their size distribution, and is used especially when large particles are needed (Belloni 1996, Brown et al. 1998, Jana et al. 2001, Perrault et al. 2009). The method is usually performed by firstly preparing the seed solution by reducing the gold ions with a reducing agent such as citrate or sodium borohydride (similar as above). As a result, small mono-disperse particles are produced that are then used as seeds for producing larger particles by adding them to a solution in which gold ions were previously reduced to metallic gold by a weak reducing agent, such as ascorbic acid or hydroquinone. The particle size is controlled by the amount of the seed nanoparticles added. Moreover, the shape and size of the AuNPs can be controlled in this seeding growth procedures by adding a surfactant, such as cetyl-tri-methyl-ammonium bromide (CTAB) and/or benzyl-dimethyl-hexa-decyl-ammonium chloride (BDAC), and silver nitrate. This has for example been used in the synthesis of gold nanorods with different aspect ratios, primarily by changing the concentrations of the surfactants (micelle formed) and silver nitrate, and was also used to produce positively charged gold nanoparticles (Carrot et al. 1998, Nikoobakht et al. 2001, Murphy et al. 2002, Busbee et al. 2003, Huang et al. 2007).

There are many methods for characterizing the produced AuNPs, such as Transmission Electron Microscopy (TEM), Scanning Electron Microscopy (SEM), and Atomic Force Microscopy (AFM) (Daniel et al. 2004, Sun et al. 2009). All are used for the size and morphology determination of

the nanoparticles. Also, the conventional UV/visible spectrophotometer is still commonly used for estimating particle size [according to the extinction coefficients of the nanoparticles (Liu et al. 2007)], and the particle concentration [from the intensity of the surface Plasmon band of the colloidal solution according to Beer-Lambert law (Jain et al. 2006, Haiss et al. 2007)]. As mentioned elsewhere (Maeland et al. 1964), the gold atom has a cubic closed-packed fcc crystal structure. A detailed study has been performed (Liu et al. 2007) for the calculation of the molar concentration of spherical nanoparticles with different caps and for the determination of their extinction coefficients using a UV-Vis spectrophotometer. The authors proposed two equations for calculating the molar concentration of the AuNPs, and then used the calculated concentration in the Beer-Lambert law to determine the extinction coefficient. They obtained a linear relationship between the extinction coefficient and the AuNPs diameter independent of the solvent used in the preparation or even the capping of the molecules. Also, their results are compatible with the theoretical calculations of the AuNPs, and with another study that determined particle concentration and size using UV-Vis spectra (Haiss et al. 2007). Calculations were performed by first calculating the average number of gold atoms in the prepared spherical nanoparticles, from the density of the fcc gold and the atomic weight of gold (Cui et al. 2002, Zhang et al. 2004), using this equation:

$$N = \frac{\pi \rho D^3}{6 M} = 30.89602 D^3$$

Where: **N** is the average number of gold atoms, **ρ** is the density for fcc gold (19.3 g/cm³), **M** is the atomic weight of gold (197 g/mole), and **D** is the diameter calculated from TEM or SEM.

Then, the molar concentration is calculated according to this equation:

$$C = \frac{N_{Total}}{NVN_A}$$

In which: the **N_{total}** is equivalent to the initial amount of gold salt used in the preparation reaction, **N** is the average number of gold atoms calculated from the previous equation, while **V** is the volume of the reaction solution in liters, and **N_A** is Avogadro's number.

The concentration is then used in the Beer-Lambert law equation to determine the nanoparticles' extinction coefficient as shown in the following equation (Liu et al. 2007).

$$A = \epsilon cl$$

In which, **A**: is the actual absorbance of the sample, **ϵ** : is the molar extinction coefficient, **C**: is the concentration of the sample in Molarity, and **l**: is the path length, which is 1 cm³.

Gold nanoparticles can be modified with different functional groups that allow the particles to be functionalized with different ligands, such as DNA, antigens, and antibodies. The sensitivity of the SPR of AuNPs to adsorption led to their use as labels in bioassays. We focus here on the different methods for using AuNPs to detect nucleic acids.

1.1.3 Selected nucleic acids detection strategies using AuNPs

Nucleic acid detection using AuNPs is based on two main mechanisms: (i) the unmodified AuNPs method, and (ii) the modified AuNPs method. The latter requires covalent modification of the AuNPs with an oligonucleotide specific to the target to be detected. AuNPs have been conjugated to oligonucleotides, and the attached DNA still has the ability to hybridize to its complementary sequence. The hybridization is selective, and the detection limit can reach 20 fmol/L (Jain 2007). The unique hybridization of the AuNPs probe with its complementary target sequence allows the assembly of the AuNPs, and a network of AuNPs is formed and detected by a color change (Storhoff et al. 1998) (e.g., a red to blue color change, with a red shift from 520 to 600 nm of the SPR). The advantage of using AuNPs as molecular recognition probes is the variety of the analytical techniques that can be used for their detection, including optical absorption, Raman scattering and electrical conductivity.

1.1.3.1 Cross-linking method

The modified AuNPs method involves the conjugation of a biological molecule to the nanoparticles surface for target detection. Detection of nucleic acids using AuNPs using cross-linking has been used (Elghanian et al. 1997, Storhoff et al. 1998). The method is based on using two probes specific

to the target nucleic acid, one probe (oligonucleotide) being conjugated to a set of AuNPs via thiol oligonucleotides, while the other is conjugated to another set of AuNPs; both oligonucleotides are complementary to the target DNA sequence at two different sites. Upon the addition of both modified AuNPs to the complementary DNA target, hybridization occurs between the target and the AuNPs modified with the specific target sequence, which leads to a decrease in the distance between the AuNPs. This results in the formation of a nanoparticles network, and thereby generates a red shift in the AuNPs SPR from 520 nm to ≥ 590 nm, which results in a change in the AuNPs color from red to purple, blue and then black according to the concentration of the target DNA (Figure 1.2). This method could be used in single-nucleotide polymorphisms (SNPs) detection by optimizing the annealing temperature at which the reaction occurs. Despite the high sensitivity and specificity of this method, which are obtained because the aggregation is based solely on the presence of the target, it suffers from many drawbacks, including AuNPs' modification with oligonucleotides being a labor-intensive procedure, and the hybridization conditions of the target nucleic acid with the probe-modified AuNPs' requiring optimization of the conditions regarding the kinetics and thermodynamics of nucleic acid binding, which on its turn requires tightly controlled conditions. Most importantly, this method cannot be used with long DNA and/or RNA sequences due to the steric hindrances associated with the probe-functionalized surface. To date, the cross-linking method has not been used for the detection of any nucleic acid from clinical samples, and more optimization is definitely needed for its application to the clinical diagnostics of nucleic acids from clinical specimens.

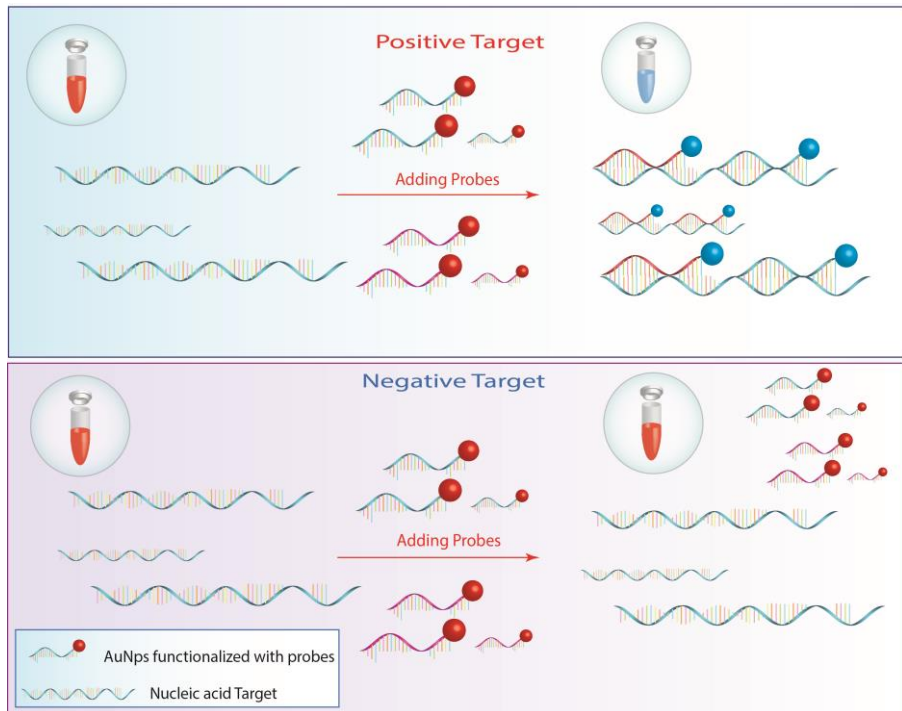


Figure 1.2: AuNPs cross-linking principle. The AuNPs are functionalized with DNA specific probes, then the target is added to the AuNPs solution and after denaturation and annealing, the nucleic acid target is hybridized with AuNPs modified probes leading to a formation of network of AuNPs/target shifting the color from red to blue indicating positive results. In absence of the target, the solution color remains red indicating negative results.

1.1.3.2 Non- Cross-linking method

As mentioned above, AuNPs have a high affinity for thiol groups. The non-cross-linking method is based on preparing AuNPs conjugated to a thiol-modified probe in which the aggregation of probe-modified AuNPs is induced by the addition of high salt (more than 2 M NaCl). Upon addition of the complementary target nucleic acid, hybridization occurs. When the high salt-induced aggregation of AuNPs is prevented the solution remains red, indicating a positive result. In contrast, in the absence of a complementary sequence, the aggregation of AuNPs occurs after the addition of at least 2 M NaCl solution. In the absence of a complementary sequence to the AuNPs modified probe, the solution will turn blue upon the addition of a high salt concentration, while in the presence of a complementary target sequence, hybridization occurs, which prevents the high salt-induced aggregation and,

thus, the solution remains red. The non-cross-linking method is superior to the cross-linking method in that it is used mainly for the detection of longer nucleic acids more than 1500 bases. It has been used by many groups to detect different nucleic acids targets and SNPs (Baptista et al. 2006, Doria et al. 2007, Baptista et al. 2008, Liandris et al. 2009, Conde et al. 2010, Costa et al. 2010). The principle of the non-cross-linking method is shown in Figure 1.3.

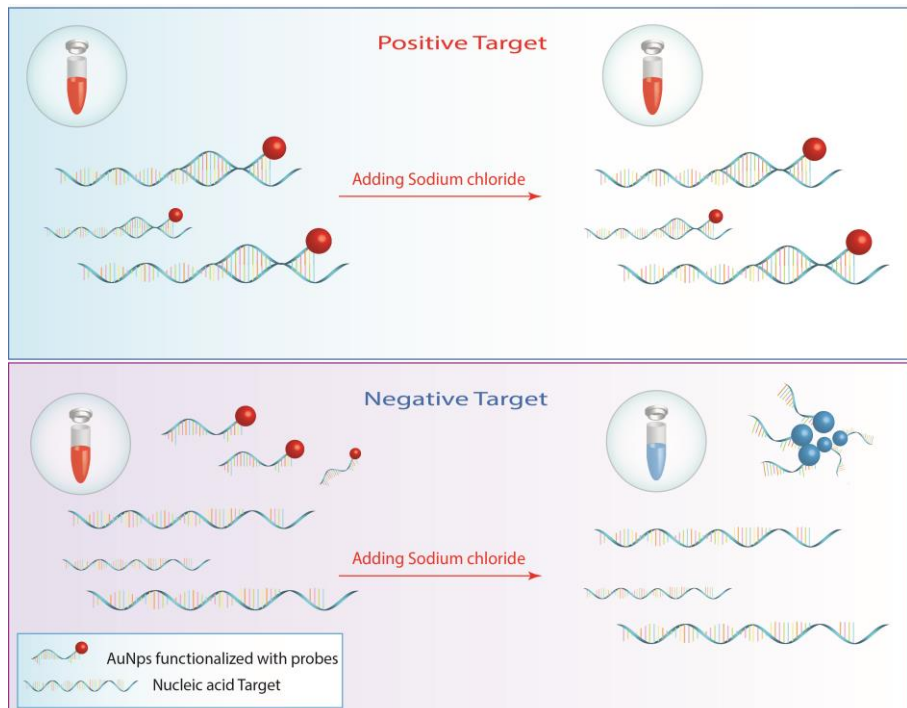


Figure 1.3: Principle of non-cross-linking assay for the detection of nucleic acids. The method depends on addition of high salt concentration to the AuNPs modified with target specific probe. In the presence of complementary target, hybridization occurs and no aggregation observed to the AuNPs and the solution remains red in color indicating positive sample. On the other hand, in the absence of complementary sequence, the AuNPs colloidal solution aggregates turning the color from red to blue indicating a negative sample. These color changes can be detected visually or spectrophotometrically.

1.1.3.3 Unmodified AuNPs method

The addition of salt shields the surface charges of the AuNPs, which are typically negative due to the adsorption of negatively charged citrate ions to their surfaces, leads to aggregation of the AuNPs and a red-to-blue color shift (see above) (Li et al. 2004a). The unmodified AuNPs method is based on the principle that single-stranded DNA (ssDNA) adsorbs the negatively charged citrate-coated AuNPs, thereby preventing their salt-induced aggregation and retention of their red color, even in the presence of sodium chloride. In contrast, double-stranded DNA (dsDNA) does not adsorb to AuNPs due to the repulsion between its negatively charged phosphate backbone and the negatively charged coating of citrate ions on the surfaces of the AuNPs. The idea behind this adsorption behavior of ssDNA on the negatively charged AuNPs is the fact that ssDNA can change its conformation by uncoiling, which results in the exposure of its nitrogenous bases to the surface of the AuNPs. Consequently, the attractive electrostatic forces between the DNA's nitrogenous bases and the AuNPs allow the adsorption of the ssDNA, which prevents the salt-induced aggregation of the AuNPs. Double stranded DNA does not adsorb to AuNPs due to the repulsion between its negatively charged phosphate backbone and the negatively charged surface of the AuNPs. Therefore, when AuNPs are added to a saline solution containing the target DNA and its complementary unlabeled primer, the AuNPs aggregate (because the primers are not free to stabilize the AuNPs) and the solution color changes from red to blue to black according to the concentration of the target added. However, in the absence of the target nucleic acid or in the presence of a non-complementary sequence, the primers are free to stabilize the AuNPs, thus preventing their aggregation and the solution color remains red (Figure 1.4). This method and concept were first introduced by Li et al., who developed colorimetric assay using unmodified AuNPs to detect different nucleic acid targets (Li et al. 2004a, Li et al. 2004b, Li et al. 2005). They used this method to detect amplified DNA and SNPs in (PCR-amplified) genomic DNA of fatal cardiac arrhythmia known as long QT syndrome extracted from clinical serum samples. They also applied this method to detect synthetic DNA sequences reaching a detection limit of 100 fmol. Furthermore, our group has used this method to detect hepatitis C virus (HCV) RNA amplified by (RT-PCR) for producing 250 bp amplicons in the 5-untranslated region of HCV genome in 10 HCV-positive serum samples. In our experiment, we

diluted the amplicons 30 times and attempted to detect the diluted samples using agarose gel electrophoresis stained with ethidium bromide, but no bands appeared. In contrast, these diluted samples were all detected using the unmodified AuNPs assay with a detection limit of 3 fmol (S. M. Shawky et al. 2009). The unmodified AuNPs-based nucleic acids detection method is superior to the modified methods because there is no need to functionalize the AuNPs with specific probes or oligonucleotides, which is labor-intensive and requires alkanethiol oligonucleotides that are expensive. In addition to the time needed for optimizing and functionalizing the AuNPs, which takes at least two days, the unmodified method allows the use of any primer without modification. Also, hybridization of the oligonucleotide and the target in the unmodified method is an independent step of the assay that eliminates the hassle of hybridization steps in the modified AuNPs assay. Finally, the unmodified method is simple, takes little time (less than 10 minutes), and is sensitive, specific and cost-effective.

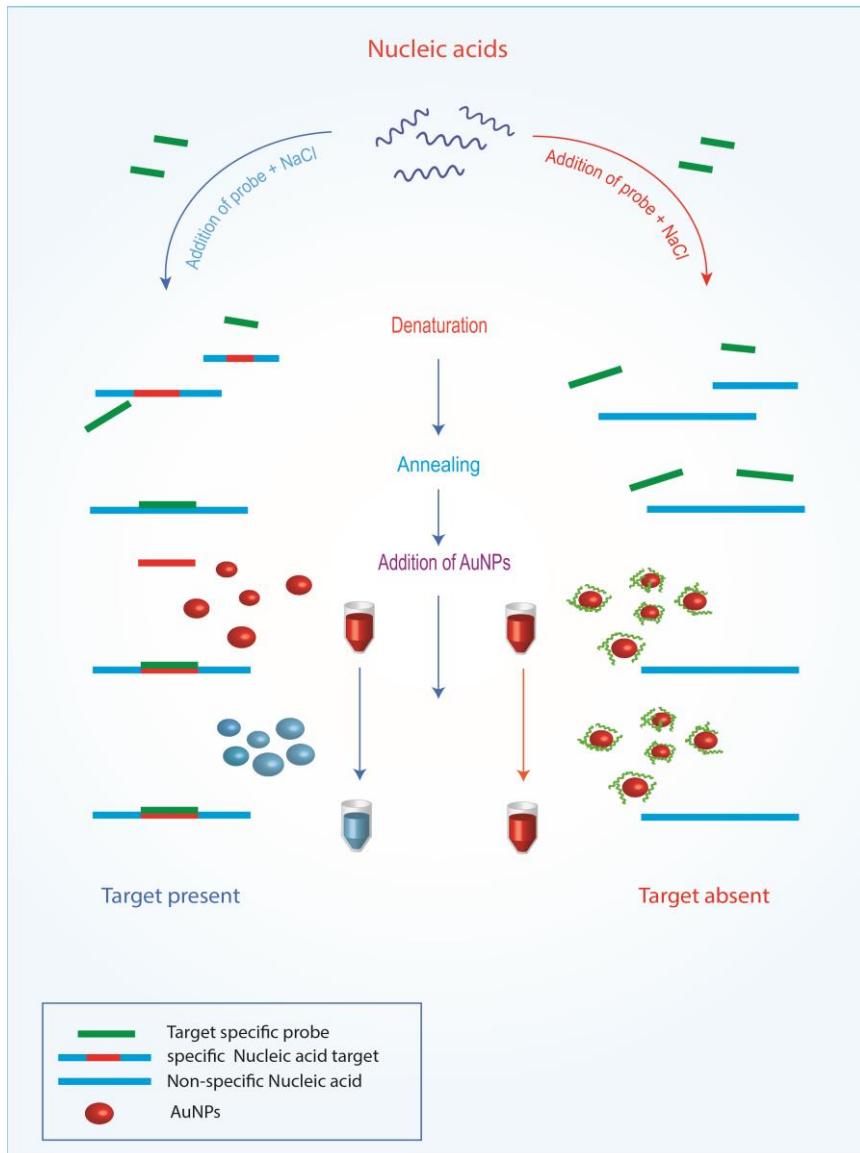


Figure 1.4: The principle of the unmodified AuNPs nucleic acids detection method. The target specific probes stabilize the AuNPs and prevent salt induced aggregation. Upon addition the complementary nucleic acid target, the probe hybridizes with its target, and the AuNPs aggregates by the action of the salt and color change occurs from red to blue. In absence of the target, the color solution remains red.

1.1.3.4 Fluorescence energy transfer and Quenching

Light is a form of electromagnetic energy that has a dual wave/particle nature, and is emitted in discrete quantities called photons (Schulman, 1985). Molecules that are able to absorb light are known as chromophores. A process known as luminescence, which is the collective name for processes in which light is emitted from an electronically excited state. Luminescence is divided into two categories: fluorescence and phosphorescence. The difference between them is that fluorescence (fluorophores), their release of energy is immediate typically in order of 1-10 nano-seconds. On the other hand, phosphorescence release of energy occurs with a much lower rate in the order of milliseconds to second (Figure 1.5). Absorption of light photons (energy) by a molecule occurs in about 10^{-15} seconds, which causes changes in the electron states of the molecule, thereby exciting the molecules' ground state electrons to a higher electron state above their thermal equilibrium. This excess energy will be lost via 1) chemical processes such as dissociation and photo-induced reaction and 2) physical processes. These physical processes fall within three categories: (i) excess energy emitted spontaneously (*fluorescence and phosphorescence*), (ii) excess energy that is thermalized by vibrational and rotational energy transfer (*intersystem crossing (ISC), internal conversion (IC), and vibrational relaxation*), and (iii) collisional quenching (*static and dynamic quenching*). Fluorescence and phosphorescence are the spontaneous emissions of this excess energy after 10^{-9} and $(10^{-3}-1)$ second, respectively. At longer wavelengths, the molecule stays in the excited state for about 1-10 nanoseconds. This loss of excess energy is illustrated in Figure 1.5.

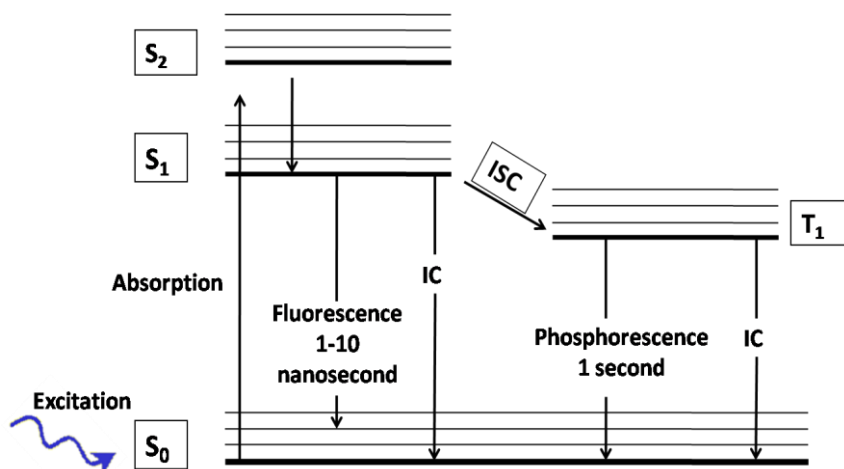


Figure 1.5: A modified Jablonski diagram showing the transitions between the excited and the ground state of the radiative energy loss (Fluorescence and phosphorescence) and the energy loss after excitation by light. S₀: ground state, S₁ & S₂: excited states, T₁: Triplet state, ISC: Intersystem crossing, IC: Internal conversion.

There is a well-known phenomenon in fluorescence-based assays for nucleic acid detection, which is called FRET (Fluorescence or Förster Resonance Energy Transfer). The basic mechanism of FRET is that there are two molecules (one donor and one acceptor). When the donor is excited by light, instead of emitting this energy, the energy is transferred to the other molecule (acceptor), whose maximum absorption wavelength is within the range of the donor emission wavelength. This leads to the excitation of the acceptor molecule and, consequently, the energy is emitted at a longer wavelength. Simply, the FRET phenomenon occurs by exciting a donor molecule whose emission wavelength overlaps the excitation wavelength of the acceptor molecule and, thus, the emission of the acceptor is detected instead of the emission of the donor. The excitation energy of the donor is transferred to the acceptor via an induced dipole-dipole interaction. The efficiency of this energy transfer is dependent mainly on the distance between the two molecules used, which should not be more than 10 nm, and is governed by the equation: $E = \frac{R_0^6}{R_0^6 + r^6}$ (Yeh et al. 2005), Where R_0 is the Förster transfer distance at which 50% of the energy transfer occurs, r is the donor-acceptor distance, and E is the energy transfer efficiency.

Quenching, on the other hand, refers to a process that leads to a reduction of the fluorescence intensity of the fluorophore. This is due to a variety of molecular interactions, such as interactions of a quencher with a fluorophore in its excited state, which prevents the fluorophore energy transitioning to the ground state, and, therefore, deactivation occurs through collision between the fluorophore and the quencher. This is called *collisional quenching*. On the other hand, there is another type of quenching in which the fluorophore forms a stable complex with the quencher. In this case, the free fluorophore molecules number is reduced and no emission is observed (Eftink et al. 1981, Lakowicz 1999, Lakowicz 2006). The FRET and quenching phenomena are very convenient to use in several applications as, cell imaging and, single cell detection, and nucleic acid detection as Real-Time PCR (Somogyi et al. 1985, Schroter et al. 2001, Shen et al. 2005, Rupcich et al. 2006, Bartolome et al. 2007, Slavoff et al. 2011). Despite the use of FRET and quenching in various biological techniques, including nucleic acids detection, there are two huge limitations that restrain their use in a wide range of molecular diagnostics. The first is that the Förster distance between the donor and the acceptor molecules should not exceed 10 nm. Secondly the emission maximum spectra of the donor should overlap with the maximum excitation spectra of the acceptor, which requires the precise selection of the donor and acceptor molecules in the FRET reactions.

The energy transfer of a fluorescent dye to nanoparticles, including AuNPs, is termed Nanoparticle Surface Energy Transfer (NSET). AuNPs have the property of quenching the fluorescent dyes. The use of AuNPs as a quencher or acceptor of the energy transfer from a fluorophore is superior to that of conventional quenchers used in FRET because the distance needed for this transfer can reach approximately 100 nm, which is 10 times greater than that of the conventional FRET phenomenon. Additionally, it is able to quench several dyes with different emission spectra at the same time, which enables the development of multiplexing detection tools (Ray et al. 2006, Paresh Chandra Ray et al. 2007). The NSET interaction resembles FRET in that its energy transfer interaction is dipole-dipole in nature, although it is more efficient due to the free oscillating electrons on the surfaces of the AuNPs that leads to an increase in the probability of donor energy transfer. Thus, NSET is an improvement over FRET (Jares-Erijman et al. 2003, Zheng et al. 2004, Jennings et al. 2006, Ray et al. 2006).

Because of the aforementioned properties of NSET, AuNPs have been used in many studies for the detection of many targets, including nucleic acids (Li et al. 2007). It has been employed to detect synthetic HCV RNA sequences using both non-cross-linking and/or unmodified AuNPs techniques with a detection limit of about 300 fM, by using a probe tagged with a fluorescent tag (Griffin et al. 2009a). It has also been used to detect the cleavage of dsDNA by nucleases (Ray et al. 2006). Moreover, AuNPs have been used as quenchers in a molecular beacon design (Dubertret et al. 2001), which is a common chemistry used in real-time PCR. The design is based on ssDNA having a hairpin structure, with one end attached to a fluorophore and the other end to AuNPs. The close proximity between the fluorophores and the nanoparticles leads to NSET, and the fluorophores are quenched by the action of the AuNPs. In the presence of the target DNA, the beacon structure opens for hybridization with its target, and the distance between the AuNPs and the fluorophores increases, leading the latter to restore its fluorescence. The most interesting aspect of these experiments is that the use of AuNPs has increased the sensitivity of molecular beacons by about 100 fold. Also, our group has used the NSET phenomenon to detect HCV RNA in serum samples using fluorescein as a fluorescent dye and AuNPs of different sizes as quenchers (Shawky et al. 2011). The principle used in the assay was the same as for the unmodified AuNPs detection described previously; however, the probe used in the hybridization is tagged with fluorescein. In the absence of the target HCV RNA, fluorescein was quenched by the attachment of the probe to the surfaces of the AuNPs. Once hybridization occurs upon addition of the target, the tagged probe will hybridize with the target (HCV RNA), leaving the AuNPs' surface and its emission is measured (Figure 1.6). This preliminary study was done on 12 HCV-positive samples and 12 normal individuals, yielding a sensitivity and specificity of 92%, with a detection limit of 10 fM. Moreover, we have measured the quenching effect of AuNPs of different sizes (15, 40 and 70 nm) on fluorescein labeled probes, and found that as the size of the AuNPs increases, the quenching efficiency increases. This study is still in progress and more experiments are needed to identify the optimum conditions for the detection.

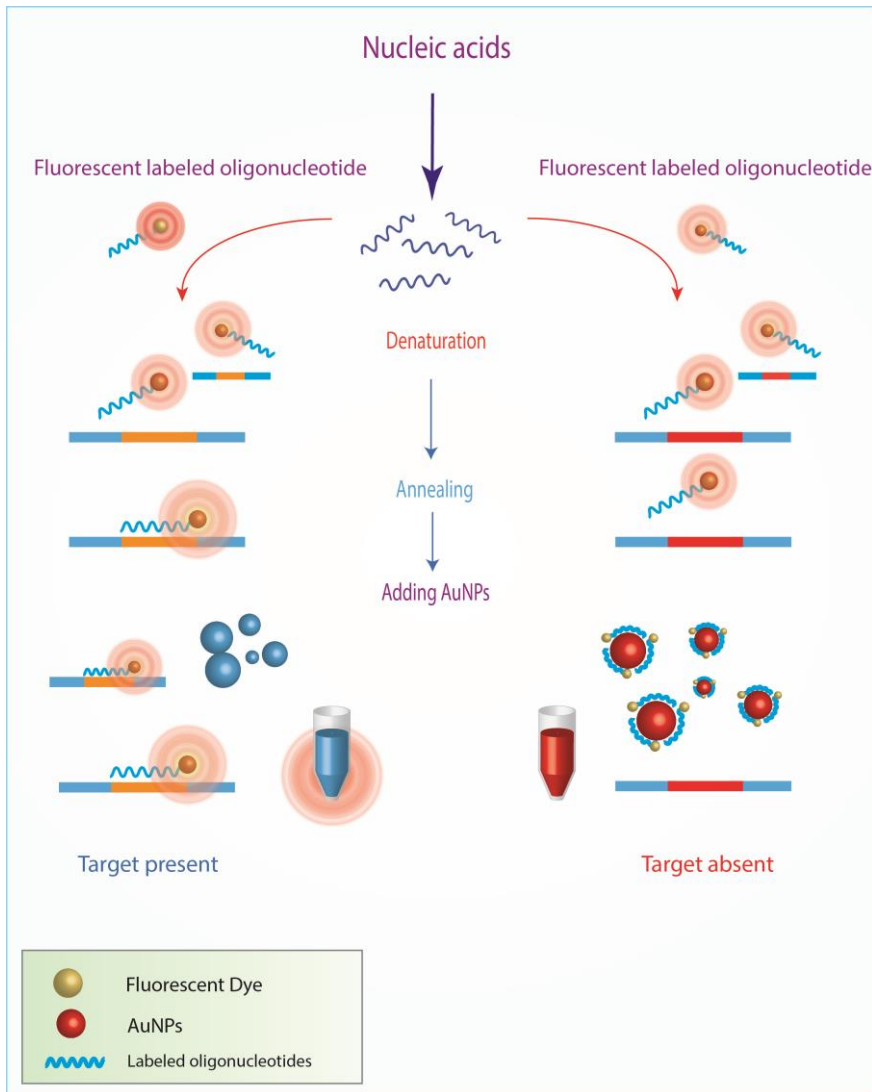


Figure 1.6 Schematic diagram of the NSET based detection. The fluorophore conjugated probes adsorbed on AuNPs leading to quenching the fluorescence signal of fluorophore due to the vicinity of the fluorophore and AuNPs. The target RNA binds to the probe and forms a double stranded RNA, thus increasing the fluorophore/AuNPs distance after hybridization, and decreasing NSET efficiency, leading to an enhanced fluorescence signal as the output signal. Moreover, the AuNPs aggregated by the action of the salt leading to a color change from red to blue.

1.1.3.5 Selected Immuno-assays by gold nanoparticles

Gold nanoparticles can be conjugated to antibodies or antigens for use in immuno-assays, and protein chips can also be developed. For example, several antibodies against HCV and HBV have been detected using gold nanoparticles, and silver enhancement staining was used for the amplification of the detection signal. This method has high sensitivity and specificity with a detection limit of 3 ng of antibody/ml, it is time saving as the results are available in less than 40 min.; it is also less costly than currently used methods (Duan et al. 2005). This method has been applied to detect antibodies against cytomegalovirus (CMV), *Toxoplasma gondii* (Tox), rubella virus (RBV), herpes simplex virus (HSV), and coxsackie virus B6 (CVB6) (Liang et al. 2004). The results showed that this method is sensitive (with detection limit of 1 pg of IgG immobilized on slides or 2.75 ng/ml IgG in solution), specific, with multiplexing capabilities, and saves time and money, hence it is attractive for clinical applications. The sensitivity of the AuNPs' based assays is due to the aforementioned properties of the gold nanoparticles such as their Surface Plasmon Resonance (SPR) that lies within the visible frequencies and the main reason in AuNPs' strong optical absorption and scattering properties. This in turn, have been used in colorimetric detection of different analytes by measuring changes in the refractive index of AuNPs' caused by the absorption of the target. Moreover, the high surface to volume ratio of the AuNPs' allows signal detection enhancement and high sensitivity of the assay (Baptista et al. 2008, Ambrosi et al. 2010, Sau et al. 2010).

Recently, gold nanoparticles with a different surface modification and shape were compared for evaluating the most sensitive method for immuno-assays (Radha Narayanan 2008). When used as extrinsic Raman labels (ERLs) in immuno-assays based on surface enhanced Raman Scattering, it was found that the limit of detection of cetyl-tri-methyl-ammonium bromide (CTAB) cubic gold nanoparticles is about 340 times below that for the spherical citrate gold nanoparticles, and 200 fold more sensitive. These results show that new immuno-assays could be developed using cubic gold nanoparticles that are capped with CTAB to set up more sensitive and yield lower detection limit assays.

1.2 Iron oxide nanoparticles

Iron oxides exist in a variety of chemical compositions, such as goethite, akaganéite, lepidocrocite, ferrihydrite, magnetite and maghemite (Rochelle M. Cornell et al. 2003). The most important iron oxides used in biomedical applications are the magnetite (Fe_3O_4) and its oxidized form maghemite ($\gamma\text{-Fe}_2\text{O}_3$) (Cao et al. 2005). Magnetic nanoparticles have unique physical, chemical, and mechanical properties at nano-scale, although the most important advantage of magnetic nanoparticles is their magnetism. Magnetic properties (*coercivity, susceptibility, crystallographic structure, magnetic anisotropic energy, and vacancies*) have been enhanced at the nano-scale level, which led to an emergence of magnetic nanoparticles with precisely tuned sizes and shapes. The two latter properties are parameters that greatly affect magnetism (Jun et al. 2008). The decrease in the size of magnetic particles to the nano-scale level has led to what is called superparamagnetism as a result of changing the magnetic spin direction, which leads to a net magnetization of zero. Moreover, nano-scale size affects the magnetic coercivity, which is the measure of the ability of the ferromagnetic material to withstand an external magnetic field. Magnetic nanoparticles have a high coercivity and low Curie temperature. Both magnetite and maghemite have supermagnetism properties at room temperature (Amin S. Teja et al. 2009). Furthermore, the saturation of the magnetization of nanoparticles is dependent on their size, which in turn affects their magnetic resonance signal enhancement capabilities (Lee et al. 2007). Also, as magnetic nanoparticles, they possess large magnetic moments when a magnetic field is applied, and they are attracted to a high magnetic flux density. This can be useful for applications in drug targeting, bio-separations, and hyperthermia treatments.

1.2.1 Synthesis of iron oxide nanoparticles

Different strategies are followed for the synthesis and preparation of magnetic nanoparticles. The most important is the **Co-Precipitation method**, which is based on the mixing of ferric and ferrous ions in a basic medium at room or elevated temperature. The salt type, ratio of ferric and ferrous ions, pH, stirring rate, and reaction temperature affect the morphology, structure, size, and the magnetic properties of the produced nanoparticles (Vu Thien Binh et al. 1998, Wu et al. 2008). The **thermal**

decomposition method has the main advantage of producing highly mono-dispersed particles with a narrow size distribution. The method is based on the decomposition and oxidation of iron salts, such as cobalt, N-nitroso-phenyl-hydroxylamine, acetyl-acetonate and nitrate salts, in an organic phase solution under high temperature (Rockenberger et al. 1999, Hyeon et al. 2001, Sun et al. 2002, Woo et al. 2004). However, the particles produced by this method are dissolved only in organic solvents, which is the main disadvantage of the thermal decomposition method. The **micro-emulsion method** is one of the methods used in the synthesis of magnetic nanoparticles. According to the IUPAC definition, a micro-emulsion is a liquid mixture in which water, oil and a surfactant are dispersed. The system is isotropic and thermodynamically stable, and the dispersed domain size is between 1 and 100 nm (Stanislaw Slomkowski et al. 2011). A variety of self-assembled structures (spherical, cylindrical and lamellar) can be produced based on the phase transition that occurs during the emulsification process (Solans et al. 2005). This concept has been utilized for the production of magnetic nanoparticles having high saturation magnetization values, controlled size, and a highly dispersed size range with very narrow size distribution (Tourinho et al. 1990, Vidal-Vidal et al. 2006, Chin et al. 2007). However, the process needs several washing steps and further particle stabilization is required in addition to the high temperature needed during the synthesis process. The **hydrothermal method** is a synthesis technique for producing single crystals from substances in a high temperature aqueous solution at high vapor pressure. The advantage of this method is the ability to achieve remarkable structures, such as nano-cubes and hollow sphere iron oxides (Titirici et al. 2006, Wang et al. 2007). However, a drawback of this method is the need for an expensive autoclave (K. Byrappa et al. 2001). Hydrothermal synthesis has been reported by several groups for the production of magnetic nanoparticles with good magnetization value, mono-dispersity and controlled size and morphology (Wang et al. 2003, Jing et al. 2004, Giri et al. 2005, Daou et al. 2006, Zheng et al. 2006, Hu et al. 2007). A number of strategies have been developed for the surface modification of iron oxide nanoparticles with oligonucleotides, antibodies, peptides, small molecules and carbohydrates.

Due to the aforementioned properties, magnetic nanoparticles have numerous medical applications, including *in vitro* diagnostics and molecular recognition in immuno-assays, bio-separation, and cell sorting, and *in vivo*

imaging as a result of their potential usefulness as contrast agents for magnetic resonance imaging. Finally, they can serve as drug/gene delivery systems (Zhao M. et al. 2002, Catherine C Berry et al. 2003, Shinkai et al. 2004, Ito et al. 2005, Laconte et al. 2005, Weissleder et al. 2005, S. c. Wuang et al. 2006).

1.2.2 Magnetic nanoparticles applications

1.2.2.1 In-Vitro Diagnostics

Superparamagnetic nanoparticles have positive properties due to their small size, high surface area, stability, and ease of surface functionalization. When bound to an antibody, antigen or oligonucleotide, they can easily detect specific (bio) molecules, structures, or microorganism. Additionally, their magnetic property has the advantage of eliminating or reducing the time needed for adsorption and separation steps, thus decreasing the overall time needed for the assay. Upon exposure to an external magnetic field, the magnetic signal is detected with a sensitive magnetometer and the target bound to the magnetic nanoparticles can be identified because the unbound molecules will disperse in all directions and no net magnetic signal is produced (Jain 2005). In an immuno-assay for allergen-specific immunoglobulin E detection, a novel magnetophoretic immuno-assay was developed based on the magnetophoretic deflection velocity of a micro-bead, which is proportional to the associated magnetic nanoparticles under an enhanced magnetic field gradient in a micro-channel (Hahn et al. 2007). The test was performed by conjugating polystyrene micro-beads to *Dermatophagoides farinae* (*D. farinae*) and *D. pteronyssinus*, and incubation with serum samples. The mixture was then reacted with magnetic nanoparticles conjugated with anti-human IgE using a sandwich immune reaction. When an external magnetic field is applied perpendicularly to the flow direction of a micro-fluidic channel, the magnetic particles exert a magnetic force, which drives their magnetophoretic lateral movement. This velocity correlated well with the concentration of allergen-specific IgE in serum (Figure 1.7). The detection limits of the allergen-specific human IgEs for *D. farinae* and *D. pteronyssinus* were 565 fM (0.045 IU/mL) and 268 fM (0.021 IU/mL), respectively. This method is fast, sensitive, and only tiny amounts (~10 μ l) of serum are needed. Also, magnetic nanoparticles have been used to screen telomerase activity in biological

samples in which, upon annealing of the nanoparticles with telomerase-associated TTAGGG repeats, the magnetic state of the nanoparticles was switched and detected by a magnetic reader (Grimm J 2004). Moreover, magnetic nanoparticles have been used for cell tracking and for calcium sensing (Jain 2007). Also, dextran-coated iron oxide nanoparticles (70 nm) have been used for the development of an immuno-assay for the detection of whole blood C-reactive protein (CRP). The output signal of the detector was proportional to the CRP concentration in the whole blood sample (4 μ l), with a detection limit of 3 mg/L (Ibraimi et al. 2006).

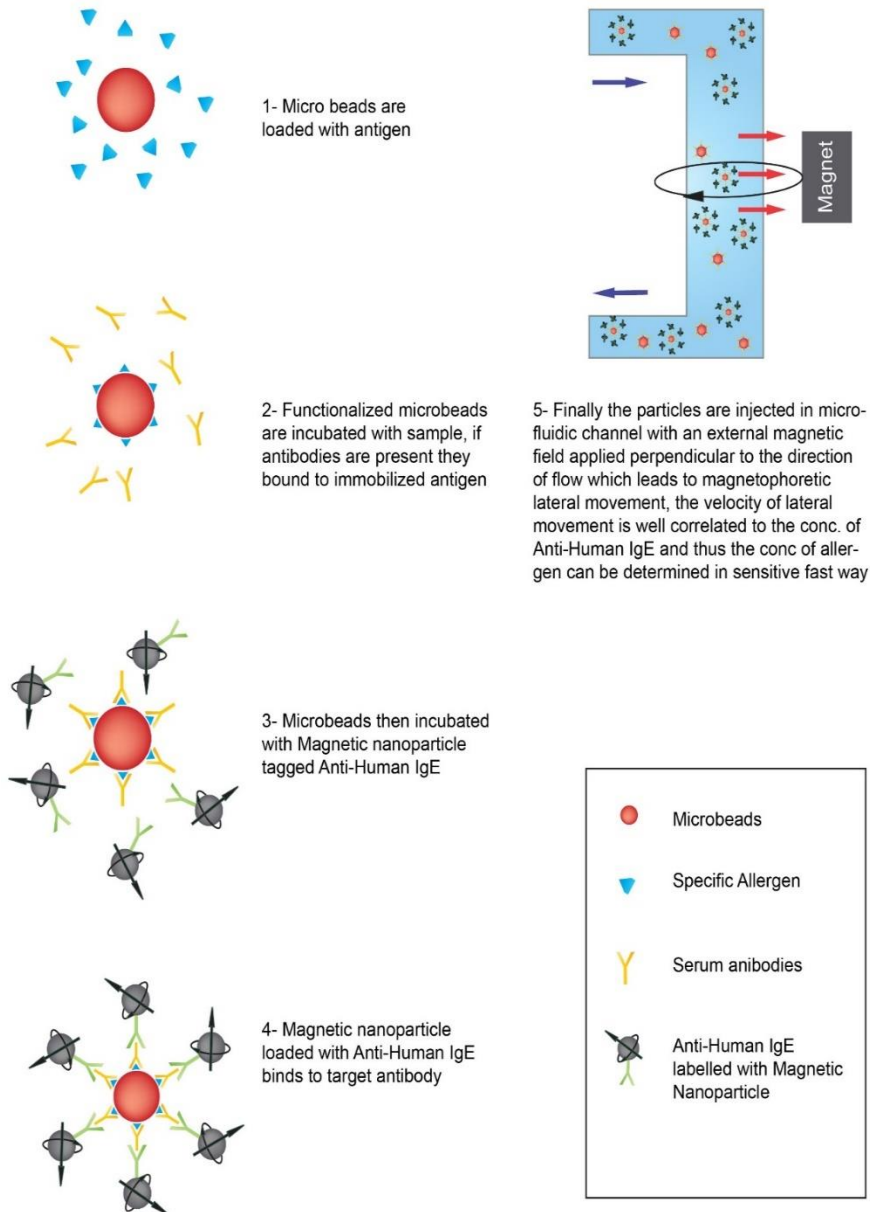


Figure 1.7 Schematic diagram showing the detection of Dermatophagoides Farinae antigens in serum samples using magnetic nanoparticles. The steps of the assay is described in the diagram.

1.2.2.2 Biomolecules Separation

Magnetic nanoparticles are currently used commercially for the separation of various biomolecules from clinical specimens. They are used in the separation of DNA, RNA, proteins, antigens, antibodies and viruses. The introduction of magnetic separation of biomolecules from a mixture was a breakthrough by increasing sample purity, selectivity and purity of the target needed to be analyzed, and, at the same time, decreasing the overall time taken for the completion of the assay. Magnetic separation can be used as a separate step for target capturing and purification from a sample, and it could also be used as a diagnostic tool.

Table 1.1 Examples of some commercially available magnetic particles, their uses and suppliers

Vendor	Products Examples	Clinical use	Website
Solulink	Magnetic beads range in size from 0.8 to 2.8 um in diameter, functionalized with amino, Streptavidin, and hydrophilic polymers	Purification of different biomolecules such as nucleic acids and antibodies	http://store.solulink.com
Thermo Scientific Pierce	Magna beads ranging in diameter from 1 to 4 um. Available with various coating as: protein A, Protein G, Streptavidin, anti-mouse & anti-rabbit Ab. Also, functionalized with amino or carboxyl groups.	Cell sorting, immuno-assays, proteins purification, and nucleic acid purification	http://www.piercenet.com/cat/pierce-magnetic-beads
Invitrogen	Dynabeads ranging in size from 1to 2.8 um in diameter. Available with different coatings as: Streptavidin, Protein A or G, secondary antibodies, and amino groups.	Cell separation & sorting, immuno-precipitation assays, nucleic acid capturing & purification.	http://www.lifetechnologies.com/dynabeads
Nanocs	Magnetic nanoparticles from 10 nm to 1 um. Available functionalized with hydroxyl, amine and carboxyl groups. In addition with folic acid, Streptavidin, protein A & protein G and fluorescent tags nanoparticles such as fluorescein , cy3, cy5 and Rhodamine B.	Used in different biomolecules separations, diagnostics, cell imaging and cells separation.	http://www.nanocs.net/nanoparticle/magnetic_nanoparticles.html

1.3 Hepatitis C virus (HCV)

Hepatitis C is a blood-borne liver disease caused by the hepatitis C virus (HCV), which was identified in 1989 and prior to that was described as non-A-non B hepatitis (Choo et al. 1989). It is a major public health problem. According to the World Health Organization, about 200 million people, or 3% of the world population, are currently infected with HCV as the result of blood transfusions in times where the virus was not identified yet, but 3-4 million persons are still newly infected each year. Additionally, there are 170 million chronic carriers at risk of developing liver cirrhosis and/or liver cancer due to HCV infection only (Who). Moreover, a recent study found that Egypt has the highest prevalence of HCV in the world. About 14.7% of the Egyptian population is chronically infected with HCV, and it is estimated that more than 500,000 new HCV infections occur per year in Egypt (Miller et al. 2010), i.e. between one sixth and one eighth of the estimated new cases in the world, and which translates to a rate of ~6.9/1,000 persons per year in Egypt being newly infected with the virus.

HCV is a small, enveloped RNA virus belonging to the *Flaviviridae* family, genus *Hepacivirus*, which comprises a group of highly variable strains or isolates. They are classified into six groups or clades based on a phylogenetic analysis of full-length or partial sequences of different HCV strains. The clades differ by 31 to 34% in their nucleotide sequence and about 30% of their amino acids sequence (Simmonds et al. 1993, Higuchi et al. 2002). Each clade contains one or more genotypes. Until now, 11 genotypes and more than 70 subtypes have been described. Different genotypes differ by more than 30% of their nucleotide sequence, while subtypes have a nucleotide difference of 20-25% (Simmonds 2004). HCV genotypes are distributed worldwide, with different genotypes being more common or predominant in different areas. HCV undergoes constant mutation in newly replicating viruses within chronically infected patients. This results in high numbers of HCV populations with diverse nucleotide sequences (Simmonds 2004). These newly formed viruses are termed HCV quasi-species. It is believed that certain quasi-species are responsible for the development of chronic hepatitis, vaccine failure and the rapid development of drug resistance (Boyer et al. 2000).

1.3.1 HCV life cycle

The HCV genome is a 9.5 Kb-long, single-stranded RNA molecule of positive polarity, which means that the HCV RNA is similar to the mRNA in that it can be immediately translated by the host cell and viral proteins. It contains a single open reading frame (ORF) flanked by 5' and 3' untranslated regions (UTR) of 341 and about 230 nucleotides, respectively. The ORF encodes a polyprotein of about 3000 amino acids. Both the 5' and 3' UTRs bear highly conserved RNA structures essential for poly-protein translation and genome replication (Penin et al. 2004). The 5' UTR is uncapped and contains an Internal Ribosomal Entry Site (IRES). The IRES is essential for the attachment of the HCV genome to host ribosomes (Bartenschlager R 2004) and for the recruitment of host proteins that initiate viral poly-protein translation. This function is highly dependent on the conservation of the IRES secondary structure (Odreman-Macchioli et al. 2000, El Awady et al. 2009). The poly-protein undergoes a complex series of co- and post-transcriptional cleavages in the endoplasmic reticulum, which is catalyzed by both host and viral proteases to yield 10 mature HCV proteins in infected cells (Penin et al. 2004). These proteins are divided into structural proteins, the core, envelope1 (E1), and envelope2 (E2), and non-structural proteins, including P7, NS2, NS3, NS4A, NS4B, NS5A, and NS5B. The primary host cells for HCV are hepatocytes (Moriishi K 2003), and the progeny virions leave the host cell by the constitutive secretory pathway (Lindenbach et al. 2005). Replication has also been described for peripheral blood mononuclear cells (PBMCs), as well as several T and B cell culture lines (Maggi et al. 1999).

1.3.2 Current therapeutic options

There is currently no approved vaccine available for HCV due to HCV heterogeneity and its ability to constantly mutate during infections (Prince et al. 2001, Simmonds 2004, Previsani Nicoletta et al. 2013, WHO 2011). All the developed vaccines are still under trials, and most of them are thus far targeting only genotype 1, subtypes a & b.

Standard alpha-interferon (IFN), PEGylated IFN, and the antiviral drug ribavirin were the only United States Food and Drug Administration (FDA)-approved medications for the treatment of hepatitis C (Manns Mp 2001). Recently, four novel anti-HCV drugs with high efficacy were approved by the

FDA. Treatment is accomplished when patients achieve a sustained virological response (SVR) 24 weeks after treatment termination, as evidenced by negative RT-PCR of the patient's blood sample. Because HCV infections have the aforementioned serious outcomes in addition to their genome heterogeneity, it is important to monitor responses to treatment. Diagnostic tests play a crucial role in addressing this aggressive viral disease. Moreover, the FDA recommended all baby boomers to get tested for HCV [i.e., 80 million people to be tested] (Smith et al. 2012, Nave 2013, Zagaria 2014). This will encourage more people to get tested.

1.3.3 Current diagnostic methods

Laboratory tests play a crucial role in management of HCV infection, and the heterogeneous nature of the infection augments the importance of HCV tests. Currently, several tests are used in the diagnosis and monitoring of HCV-infected patients. The tests fall into two main categories. Firstly, serological tests such as enzyme-linked immuno-assays (EIAs), which are used for screening, blood donations and diagnosis of symptomatic patients. Secondly, recombinant Immune Blot assays (RIBA), which are used primarily for confirmation of HCV infection (Atrah et al. 1996, Sarrazin 2004, Chevaliez et al. 2007). The second category comprises tests used for detection of HCV RNA (HCV viremia); including PCR-based assays (qualitative and quantitative including real-time PCR) and branched-DNA (b-DNA) assay. These tests are used mainly for therapeutic monitoring, prognostics, genotyping and mutational analysis for determination of adequate treatment regime, to reduce the treatment window period (Damen et al. 1995, Chevaliez et al. 2006, Scott et al. 2007).

1.3.3.1 Biochemical markers and serological tests

Elevation in serum liver trans-aminases, alanine amino-transferase (ALT) and aspartate amino-transferase (AST) usually accompany hepatic dysfunction and/or infection, including HCV infections. However, the serum ALT does not accurately predict the presence of HCV infection. Thus, extra serological tests should be done to detect anti-HCV antibodies within suspected individuals. Anti-HCV antibodies detection, which is accomplished using EIA, is the first line in HCV diagnosis. Three different generations of EIA have been developed, with improvement in the sensitivity of the assay in each generation. EIAs have an estimated specificity range of 98.8% to 100%

in immune-competent patients, while in immune-suppressed patients, the sensitivity of EIAs decreased in range from 50% to 95% according to the level of immune-suppression (Atrah et al. 1996).

RIBA is the second line in detecting anti-HCV antibodies, and it is usually used as a confirmatory test to avoid the false positives done of the EIA tests. It has also been developed in several waves, roughly leading to three generations of tests. Detection of mounted immune-reactivity against two or more HCV antigens is considered a positive test result. Immune-reactivity against only one HCV antigen (core, NS3 and/or NS4) is classified as an intermediate result and needs additional confirmatory tests. If no immune-reactivity is detected, the test is considered negative (Sarrazin 2004).

A clear drawback of the serological tests is that they are not suitable for detecting acute infections because antibodies can only be detected after at least three weeks of the onset of the infection. In addition, and as indicated above, they will not be suitable for the immune-suppressed patients.

1.3.3.2 Nucleic acid testing (NAT)

NAT provides a direct measure of the HCV RNA and, thus, an estimation of the viral load, disease progression, and the response to therapy. However, NAT has limitations, such as high cost and unreliability in point-of-care testing. Two main strategies are currently used for detecting HCV RNA in clinical specimens. The first is based on target amplification, such as PCR-based techniques and transcription-mediated amplification (TMA), while the second is based on signal amplification, including branched DNA technology (b-DNA).

TMA is based on the multiplication of viral RNA *in vitro*, and 100 to 1000 RNA copies are synthesized in one cycle. These amplicons re-enter the TMA cycle and become templates for the next replication cycle. Single-stranded fluorescently labeled probes are then hybridized to the RNA amplicons and the chemiluminescent signal of the target sequence is detected (Scott et al. 2007)

PCR -based techniques are classified into conventional PCR and real-time PCR. Both of them are dependent on the amplification of the most conserved region in the HCV genome, which is the 5' UTR, and the detection of the amplicons' fluorescence. Many commercial assays based on PCR techniques with different sensitivities and specificities are available (Germer et al. 2002).

Real-time PCR is more promising than the conventional method, as it is more sensitive, it is fully automated and it is based on the use of fluorescent probes that allows the monitoring of the amplified product on real time basis, without the need for post- amplification detection as e.g. ethidium bromide stained gel electrophoresis. The detection limit can reach 15 IU/ml (Halfon et al. 2006). Moreover, multiplexing is achievable using real-time PCR, and a number of assays have been applied for the simultaneous detection of several viral genomes (Read Sj 2001).

Finally, the **b-DNA** measures nucleic acid molecules through linear signal amplification. It is a sandwich HCV RNA hybridization in which the viral RNA is captured in a micro-well by a set of specific synthetic oligonucleotides (called capture probes) that are specific to the highly conserved HCV RNA region of the 5'UTR. A set of target specific probes called (label extenders and capture extenders) then hybridizes to both the viral RNA and the pre-

amplifier probes. The capture extenders are designed to hybridize to both the target nucleic acid and capture probes that are attached to the micro-well, while the label extenders are designed to hybridize to adjacent regions on the captured target and provide sequences for the preamplifier probes. The latter leads to the formation of a stable hybrid only if it hybridizes to 2 adjacent label extenders; it also has other regions to hybridize to multiple b-DNA amplifier molecules that create a branched structure.

Finally, multiple copies of alkaline phosphatase (AP)-labeled probes, which are complementary to b-DNA amplifier sequences, then hybridize to this immobilized complex. The AP bound complex is then incubated with a chemiluminescent substrate, and the signal is quantified by photon counting in a luminometer, which is directly related to the amount of HCV RNA present in each sample (Urdea et al. 1997, Scott et al. 2007). The b-DNA assay is highly specific and sensitive for HCV quantitation. Furthermore, as many as 18 b-DNA molecules are bound to each HCV RNA, and as many as 810 separate AP molecules per HCV RNA can be hybridized. This provides a decisive enhancement of the signal, leading to increase in the sensitivity of the test, which can reach a lower detection limit of 615 IU/ml. A prime advantage of the b-DNA is that it is based on signal rather than target amplification, thus minimizing the chances of contamination. Examples of commercial available HCV molecular assays are summarized in Table 1.2.

Table 1.2: Selected commercially available HCV RNA detection assays. 1 IU/ml equivalent to 2-5 copies/ml. RT-PCR: Reverse Transcriptase polymerase chain reaction, TMA: Transcription mediated amplification. b-DNA: branched-DNA

Assay	Method	Lower limit of detection (IU/ml)	Specificity	References
Amplicor HCV v2.0	RT-PCR	50	97.8%-100%	(Podzorski 2002, Chevaliez et al. 2006)
Cobas Amplicor HCV v2.0		50	100% at detection cutoff (50 IU/ml)	(Germer et al. 2002)
Amplicor HCV Monitor v2.0		600	98%	(Tsou et al. 2005)
Cobas Amplicor HCV Monitor v2.0		600	100%	(Eissa et al. 2014b)
Versant HCV RNA qualitative assay	TMA	9.6	96%- 100%	(Tarrytown 2002)
Versant HCV RNA 3.0 Assay	b-DNA	615	98.8% at detection cutoff (615 IU/ml)	(Germer et al. 2002)
Quantiplex HCV RNA 2.0		200,000 HCV equivalents/ml.	97%	(Germer et al. 2002, Trimoulet et al. 2002)
Cobas TaqMan HCV test	Real-time PCR	15	95%	(Chevaliez et al. 2006, Halfon et al. 2006)
Abbott Real Time HCV assay		30 or 12 based on use of 0.2 or 0.5 ml of plasma for analysis, respectively	≥99.5%	(Chevaliez et al. 2006, Halfon et al. 2006, Arnold et al. 2013)

Many aspects of HCV infection, such as diagnosis, monitoring, and treatment, have evolved rapidly in the last decade. However, the sustained response, and the factors involved in HCV persistence, as well as developing chronic disease are still under debate. Thus, much work is needed to assess many features, including the decision to initiate therapy, the early detection of HCV, and how chronic infections develop. Therefore, novel HCV RNA diagnostic techniques, which are simple, cheap, rapid, with acceptable sensitivity and specificity, are urgently needed.

This can open the door for introducing nanotechnology to HCV diagnosis and, thus, applying point-of-care testing in HCV diagnosis and therapeutic monitoring.

1.4 Tumor Markers

The development of non-invasive methods for the early and specific detection of different cancer types is urgently needed. The tumor markers field is highly dynamic, and reliable diagnostic and prognostic tumor markers are rapidly evolving as non-invasive methods for early cancer detection. The overall success is highly dependent on gathering information from various disciplines, such as genomics, proteomics, transcriptomics and epigenetics. There still is a major clinical need for a sensitive, specific, cheap, simple and non-invasive tumor biomarkers, and for techniques that could be used in the routine screening of individuals at high risk for cancer, as well as for the early diagnosis of low-grade tumors (Sanna Eissa et al. 2013). Nucleic acids (DNA, RNA and micro-RNA)-based assays of specific genes that are related to the cancer type could be a promising non-invasive method for the early detection of tumors, enabling the prediction of responses to treatment and the screening of high-risk individuals. In this work, we have selected two tumor markers for urinary bladder and breast cancer as examples of the development of novel nano-assays for their early detection.

1.4.1 Urinary Bladder Cancer

Bladder cancer is a significant public health problem worldwide, and is one of the five most common malignancies. It is the second most common tumor of the urogenital tract, and the second most common cause of death in patients with such malignancies (Eissa S. et al. 2014). The highest incidence rates are found in Europe, North America and Northern Africa

(Jemal et al. 2011). According to the annual report of the American Chemical Society (ASC) (Society 2014), in 2014, about 74,000 new cases are estimated to occur in the USA, with about 16,000 estimated deaths. In Egypt, urinary bladder cancer is the main cause of cancer in males and the second one in females (Salem et al. 2012).

Although the main symptom of bladder cancer is painless hematuria, no other symptoms are found in the early stage of tumors (Kaufman et al. 2009). Moreover, these tumors have a 30% to 70% recurrence rate and a strong tendency to progress to invasive cancers in 10% to 30% of patients, with an increased risk of metastasis and subsequent mortality (Howlader N et al. 2011). Thus, early detection of bladder cancer is urgently needed to improve its prognosis and long-term survival. Cystoscopy is considered the gold standard for detection of bladder cancer (Smith et al. 2013). It enables the direct visualization of the urothelium and the subsequent characterization of the tumor. However, cystoscopy is rather invasive, expensive and labor intensive (Avritscher et al. 2006, Margel et al. 2011). Finally, flexible cystoscopy has a definite false-negative rate, particularly for carcinomas *in situ* (Sapre et al. 2014). Urine cytology (microscopic examination of cells from urine specimens under light microscope to look for cancerous cells) is a non-invasive test widely utilized with cystoscopy for both screening and surveillance of tumor recurrence. It is generally acceptable for detecting high-grade bladder tumors. However, classical cytology has a low sensitivity and cannot be used to identify low-grade cancer cells. In addition, the accuracy of the diagnosis in urine cytology is dependent on the level of expertise of the cytopathologist (Vrooman et al. 2008).

In addition to cystoscopy and cytology, numerous urine tests have been developed for the detection of bladder cancer, including bladder tumor antigen (BTA), fibrin degradation products, nuclear matrix protein 22, Immunocyt, fluorescence *in situ* hybridization and hyalouronic acid/hyaluronidase. Most of these markers have a higher sensitivity than urine cytology, although their specificity is generally lower, and urinary tract infection, benign prostatic hypertrophy, and renal calculi can reduce their accuracy (Van Rhijn et al. 2005, Vrooman et al. 2008, Sapre et al. 2014). Although several urinary biomarkers have been investigated and have received FDA approval for diagnosis, none of these has been implemented

in practice guidelines due to an insufficiency of clinical evidence (Kamat et al. 2013). At present, there is no consensus regarding their role in enhancing or replacing cystoscopy and/or cytology (Yossepowitch et al. 2007).

Identifying novel biomarkers in urine has the great advantage in that urine specimens can be collected and obtained at high quantities. Moreover, investigation of RNA-based tumor markers (mRNA and/or micro RNA) in different samples is a rapidly evolving strategy not only in bladder cancer detection but also for the diagnosis of other tumors (Cortez et al. 2011).

1.4.1.1 Hepatoma Up-Regulated Protein (HURP)

Hepatoma up-regulated protein (HURP) is an important cell cycle regulator that plays a role in the carcinogenesis of different cancer types, including urinary bladder cancer cells (Chiu et al. 2002, Huang et al. 2003, Tsou et al. 2003, Tsou et al. 2005). Cells over-expressing HURP appear to have the characteristics of tumor cells, with a reduced dependence on extracellular growth factors and the potential to exhibit anchorage-independent growth. In a very recent study (Eissa et al. 2014b), HURP RNA was measured in the urine specimens of 211 patients with bladder cancer, 71 benign bladder lesions and 62 normal controls using semi-quantitative RT-PCR. The assay exhibited 78.7% sensitivity and 94% specificity for bladder cancer detection. Thus, HURP RNA could be considered as a potential non-invasive biomarker for urinary bladder cancer diagnosis.

1.4.2 Breast Cancer

Breast cancer still remains the most common cancer among women and the major cause of cancer mortality among women in both developed and developing countries (Zeeneldin et al. 2013). The ACS, in its 2014 annual report (Society 2014), estimated that about 232,670 (29% of cancer cases) new cases of breast cancer will occur in women, with about 40,000 (15%) estimated deaths in the USA in 2014. Worldwide, breast cancer is the leading cause of cancer deaths in females, accounting for about 14% of their cancer related mortality, and 23% of the total cancer diagnoses in females (Jemal et al. 2011, Ferlay et al. 2012). Also, it is considered one of the most four common cancers in Europe, and its incidence has increased in Western and Northern Europe in the last two decades (Arnold et al. 2013). In Egypt, it is the most common cancer in females, accounting for 37.7% of their total

cancer cases and 29% of their cancer-related deaths (Siegel et al. 2012). As for other cancer types, no signs or symptoms and/or pain are associated with breast tumors in their early stage, and even large tumors are painless, although they may appear as an internal swelling in the breast. The main problem in breast cancer is that even very small lesions or tumors could lead to metastasis (Misek et al. 2011).

There are many risk factors related to breast cancers, such as obesity, heavy smoking, and alcohol consumption, the use of combined estrogen and progestin pills and, most importantly, women having a family history with breast and/or ovarian cancer. Until now, the most effective method for breast cancer diagnosis and/or screening is the standard mammography; it usually detects cancer at early stages. However, the mammography technique has low specificity and/or sensitivity, and lesions less than 0.5 cm in size cannot be detected by mammography. Additionally, its sensitivity is lower in young women and those with dense breasts. A combination of digital mammography and magnetic resonance imaging may increase the sensitivity and specificity. However, for most women, with abnormal mammograms, the tissue biopsies provide the final decision of the diagnosis (Misek et al. 2011, Society 2014). The shift toward an earlier diagnosis of breast cancer due to improved imaging methods and screening programs highlights the need for new factors and combinations of biomarkers to quantify the residual risk to patients, and to indicate the potential value of additional treatment strategies (Bartlett et al. 2010). A broad range of protein biomarkers has been investigated as potential and predictive factors for breast cancer detection, including such well-established factors as Ki-67 and HER-2. Other investigational prognostic factors include mitosis, apoptosis-related proteins, cell cycle regulators, plasminogen activators and inhibitors, and angiogenesis-related proteins (Cecchini et al. 2012). On the other hand, genetic alterations, such as gene rearrangements and mutations, as well as their roles in regulating cancer cell growth and metastasis, are part of a highly evolving field of research for investigating novel genetic biomarkers, which are usually seem to be more reliable than most of the protein biomarkers (Bhatt et al. 2010). Therefore, nucleic acids (DNA, RNA and miR)-based assays of specific genes could be used as tools for breast cancer detection and/or screening, in addition to predicting responses to treatment.

1.4.2.1 Histidine-Rich Glycoprotein (HRG)

Histidine-rich glycoprotein (HRG) is a 75 kDa α 2-glycoprotein synthesized by the liver, and it is also found in plasma and platelets (Leung et al. 1983, Hulett et al. 2000). The human HRG gene is 12 Kbp long and maps to chromosome 3q27, and consists of seven exons (protein coding). HRG is a multi-domain protein that acts as a regulator of coagulation, fibrinolysis and angiogenesis (Jones et al. 2005). HRG has been identified as one of many serum proteins biomarkers for breast cancer identification (Schaub et al. 2009). In a very recent study, HRG RNA was detected and evaluated in breast tissue biopsies by RT-PCR, and HRG serum protein was evaluated by EIA (Matboli et al. 2014). In this study, the authors showed that HRG RNA expression increased in all subtypes of breast cancer, with 71.7% sensitivity and 93.3% specificity, while HRG serum protein detected by ELISA had 86.7% sensitivity and 80% specificity. These data suggest the prognostic value of HRG RNA in breast cancer tissue as a novel breast cancer biomarker.

1.5 Scope of the thesis

The global aim of my PhD research and this dissertation was to develop novel methods and techniques that can be used for the diagnosis of unamplified nucleic acids of infectious diseases and tumors in clinical specimens. The two major biological models that were chosen to apply the developed diagnostic methods to: were Hepatitis C Virus and tumor biomarkers (urinary bladder cancer and breast cancer), respectively.

The specific aims of the thesis were:

1. The development of a novel diagnostic assay prototype using unmodified, negatively charged gold nanoparticles for the direct detection of unamplified Hepatitis C Virus RNA in clinical serum specimens.
2. The development of a novel assay using magnetic nanoparticles and positively charged gold nanoparticles for the direct detection of unamplified Hepatitis C Virus RNA in clinical serum specimens.
3. The development of unmodified negatively charged gold nanoparticles and magnetic nanoparticles-based assays for the detection of selected urinary bladder and breast cancer tumor markers.

2 Direct Detection of Unamplified Hepatitis C Virus RNA Using Unmodified Gold Nanoparticles

^{1,2}Sherif M Shawky, ²Dirk Bald, and ¹Hassan ME Azzazy*

¹Department of Chemistry & Yousef Jameel Science & Technology Research Center, the American University in Cairo, P.O. Box 74 New Cairo 11835, Egypt; ²Department of Structural Biology, Faculty of Earth & Life Science, Free University, Amsterdam, the Netherlands.

*To whom correspondence should be addressed. E-mail: hazzazy@aucegypt.edu

Published in: Clinical Biochemistry, 2010 Sep; 43 (13-14):1163-8. PMID: 20627095

2.1 Abstract

Background: AuNPs exhibit a unique phenomenon known as Surface Plasmon Resonance, which is responsible for their intense red color. This color changes to blue upon aggregation of AuNPs. **Objective:** This work aims to develop a rapid, simple and cheap assay for direct detection of unamplified HCV RNA extracted from clinical samples using unmodified AuNPs. **Methods:** Serum samples were collected from healthy volunteers (n = 45) and chronic HCV patients (n = 30). Extracted RNA, hybridization buffer containing PBS, and a primer targeting the 5'UTR of HCV were mixed. The mixture was denatured, annealed, and then cooled to room temperature for 10 min followed by addition of AuNPs. **Results:** Salt, primer, AuNPs concentrations and annealing temperature and time were all optimized. In HCV positive specimens, the color of the solution changed from red to blue within 1 min. The assay has a sensitivity of 92%, a specificity of 88.9%, and detection limit of 50 copies/reaction. **Conclusions:** To our knowledge, this is the first assay that allows the detection of unamplified HCV RNA in clinical specimens using unmodified AuNPs. The developed assay is highly sensitive, has a turnaround time of 30 min, and eliminates the need for thermal cycling and detection instruments.

Key words: HCV RNA, gold nanoparticles, colorimetric assay.

2.2 Introduction

According to the World Health Organization, there are around 200 million people worldwide infected with hepatitis C virus (HCV), with three to four million newly infected patients annually (Who). HCV is a small enveloped single-stranded RNA virus that belongs to the *Flaviridae* family, *Hepacivirus* genus, which comprises a group of highly variable strains or isolates. HCV is a blood borne virus and infection has different clinical outcomes ranging from acute resolving hepatitis to chronic liver disease, including liver cirrhosis and hepatocellular carcinoma (Lauer et al. 2001, Higuchi et al. 2002, Strader et al. 2004). The acute viral infection resolves in 15% of infected patients but progresses in 85% of patients to chronic infection (Marcellin. 1999).

Currently HCV is detected using immuno-assays and confirmed by molecular assays. Immuno-assays such as enzyme linked immuno-assays (EIAs) and recombinant immune blot assays (RIBA) are used for detection of anti-HCV antibodies (Sarrazin 2004). Conventional RT-PCR is used for qualitative detection of HCV RNA while quantitative detection is achieved using real-time RT-PCR and/or branched DNA-based assays (Scott et al. 2007). Despite the high sensitivity and specificity of these methods, they are time-consuming, labor intensive, expensive, and require specialized equipment. Therefore, there is a great need to develop a low-tech assay for the direct detection of unamplified HCV RNA with acceptable sensitivity and specificity, short turnaround time, and cost-effectiveness. Such an assay would be critical to control HCV in developing countries with limited resources and high infection rates, such as Egypt.

Nanoparticles have been recently proposed as promising tools to develop the next generation of diagnostic assays. Because of their unique properties and ability to interact with biomolecules on one-to-one basis, various nanoparticles show great promise to meet the rigorous demands of the clinical laboratory for sensitivity and cost-effectiveness, and can be used in the future in point-of-care diagnosis (Jain 2005). Gold nanoparticles (AuNPs) are spheres with a typical diameter of approximately 2 – 50 nm. They exhibit a unique phenomenon known as Surface Plasmon Resonance (SPR), which is responsible for their intense red color. This color changes to blue upon aggregation of AuNPs (Jain et al. 2006). The addition of salt shields

the surface charge on the AuNPs, which are typically negatively charged owing to adsorbed negatively charged citrate ions on their surfaces, leading to aggregation of AuNPs and red-to-blue color shift (Li et al. 2004a). SPR is also responsible for the large absorption and scattering cross-sections of AuNPs which are 4-5 orders of magnitude larger than those of conventional dyes (Huang et al. 2007). These unique optical properties have allowed the use of AuNPs in simple and rapid colorimetric assays for clinical diagnosis offering higher sensitivity and specificity than current detection techniques (Li et al. 2004a, Radwan et al. 2009)

Li et al. developed a colorimetric assay using unmodified citrate-coated AuNPs (Li et al. 2004a, Li et al. 2004b). This method is based on the fact that single-stranded DNA (ssDNA) adsorbs on citrate-coated AuNPs. This adsorption increases the negative charge on the AuNPs leading to increased repulsion between the particles, thus preventing aggregation. The adsorption of ssDNA on AuNPs occurs due to the fact that ssDNA can uncoil and expose its nitrogenous bases. The attractive electrostatic forces between the bases and the AuNPs allow adsorption of the ssDNA. On the other hand, double-stranded DNA (dsDNA) does not adsorb on AuNPs due to the repulsion between its negatively-charged phosphate backbone and the negatively-charged coating of citrate ions on the surfaces of the AuNPs. Therefore, when AuNPs are added to a saline solution containing the target DNA and its complementary unlabeled primer, AuNPs aggregate (since the primers are not free to stabilize the AuNPs) and the solution color changes to blue. However, in the absence of the target or the presence of a non-complementary target, the primers are free to stabilize the AuNPs thus preventing their aggregation and the solution color remains red. This method has been used to detect single nucleotide polymorphisms in PCR-amplified genomic DNA extracted from clinical samples (Li et al. 2004b). Moreover, based on the same principle, AuNPs are capable of quenching fluorescent dyes and this property has been used for detection of synthetic HCV sequences with high sensitivity and selectivity (Griffin et al. 2009a, Griffin et al. 2009b). In this study, AuNPs-based colorimetric method has been used to directly detect unamplified HCV RNA extracted from clinical specimens (Figure 1). The colorimetric assay is simple, rapid, and sensitive. In addition, the hybridization of the unlabeled probe to the target takes place in a separate tube before addition of the AuNPs and therefore allows hybridization to take place under the desired optimum conditions without affecting the stability of the gold colloid.

Direct Detection of Unamplified Hepatitis C Virus RNA Using Unmodified Gold Nanoparticles

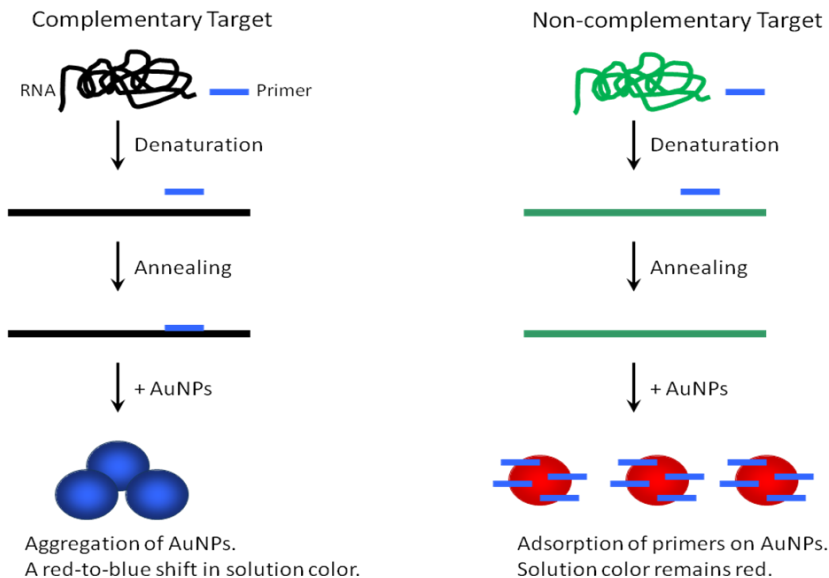


Figure 1. Schematic diagram of a colorimetric assay based on unmodified AuNPs for detection of full length HCV RNA. First, the tertiary structure of the target RNA is denatured and the complementary primer hybridizes to the target forming double strands. Upon adding AuNPs they will aggregate since there are no free primers to stabilize the AuNPs, and the solution color changes from red to blue. In the presence of a non-complementary target RNA, the primers will be free to bind and stabilize the AuNPs thus preventing their aggregation and the solution color remains red. The figure was modified with permission from the American Chemical Society.

2.3 Materials and Methods:

2.3.1 Synthesis of AuNPs

A colloidal solution of AuNPs with a diameter of $15 \text{ nm} \pm 2$ was prepared by citrate reduction of hydrogen tetrachloroaurate (III) ($\text{HAuCl}_4 \cdot 3\text{H}_2\text{O}$) as described elsewhere (Storhoff et al. 1998). Briefly, the reflux system was cleaned by aqua-regia and then rinsed with ultrapure water, and blown out with N_2 . An aqueous solution of $\text{HAuCl}_4 \cdot 3\text{H}_2\text{O}$ (1 mM, 100 mL) was brought to reflux while stirring, and then 10 mL of 1 % trisodium citrate (38.8 mM) were added quickly. This resulted in consequent change in solution color from yellow to clear to black to purple to deep red. Afterwards, the solution was refluxed for an additional 15 minutes and then allowed to cool to room temperature. The colloidal solution was then

filtered through 0.45 μm acetate filter, and transferred into a clean storage glass bottle.

2.3.2 Characterization of AuNPs

Size and distribution of the prepared AuNPs were characterized using field emission scanning electron microscopy (Model: Leo Supra 55). One drop of the AuNPs solution was added onto a silicon slide that was allowed to air dry before examination. The λ_{max} for AuNPs was measured using UV spectrophotometer (Jenway 6800). The concentration of the prepared AuNPs was calculated as described previously (Liu et al. 2007).

2.3.3 Serum Samples

Seventy five serum samples were collected from healthy volunteers ($n = 45$) and chronic HCV patients ($n = 30$). All samples were negative for hepatitis B surface antigen and hepatitis B antibody. All positive samples have elevated ALT and AST levels. Rapid HCV test was performed on all the samples. Viral load of HCV positive samples was determined by real-time PCR (Artus kit; Qiagen).

2.3.4 HCV RNA Extraction

Extraction of RNA from serum samples was assessed using three different kits: **1) QI-Amp Viral RNA kit** (Qiagen; Cat. No. 52904), **2) Absolute RNA Miniprep Kit** (Stratagene; Cat. No. 400800) according to standard manufacturer's instructions, and **3) SV total RNA isolation system** (Promega; Cat. No. Z3100) according to the modified manufacturer's protocol for HCV RNA isolation (Paul Otto et al. 1998). Cell free DNA may fragment and may interfere with the assay. These fragments lead to false negative results due to their adsorption onto the AuNPs. Therefore, the samples were treated with DNase to exclude cell-free DNA and/or genomic DNA in the sample. Qiagen viral RNA extraction kit as stated in the kit's instruction manual does not guarantee the absence of DNA within the final RNA eluted. Using this kit, we obtained false negative results with all samples, even at very high viral titers. The Stratagene total RNA kit and Promega RNA extraction kit both include a DNase treatment step. Reproducible results were obtained with Stratagene and Promega kits.

2.3.5 RT-PCR and Real Time RT-PCR

Amplification of RNA was done by using Qiagen one step RT-PCR enzyme mix (Cat. Number 210210) using primers targeting the 5'UTR region, forward primer: **5'GTGAGGAACTACTGTCTTCACG'3**, and the reverse primer **5'ACTCGCAGGCACCCTATCAGG'3**. The thermal cycling protocol was 50° C for 30 min (reverse transcriptase reaction), 95° C for 15 min (Taq activation), and 40 cycles of 1 min at 95° C, 1 min at 55° C, and 1 min at 72° C; 10 min at 72°C, and then held at 4°C yielding a product of 265 bp. Real-time RT-PCR was done by AgPath ID One Step RT-PCR kit (cat # AM1005; Ambion) where 8 µL of the sample were taken and completed to 10 µL with ultra-pure water. Amplification was done using a Stratagene Mx3005P.

2.3.6 Colorimetric AuNPs Assay for Detecting Full Length HCV RNA in Clinical Samples

One primer targeting 5'UTR of HCV RNA was added to 10 mM phosphate buffer saline solution (PBS, pH = 7.0; hybridization buffer). Different concentrations of NaCl in PBS buffer and primer concentrations were tested to determine the optimum concentrations for performing the assay. Hybridization buffer was prepared using 0.53 M NaCl and 6.66 µM (6.6 pmol/µL) primer. Different volumes of the AuNPs were tested, and 10 µL of the prepared AuNPs (10 nM) was selected for use in the final assay. As for the primer used in the assay, two primers were tested, both targeting the HCV RNA 5'UTR. The first primer was 22 nucleotides long and the second one was 27 nucleotides long. The second primer was finally used in this study due to its high specificity to all HCV genotypes and subtypes. In addition, it is not complementary to any human mRNAs as verified by blasting the primer using NCBI database.

The assay was performed as follows, 7 µL of the extracted RNA were placed in a sterile PCR tube and 3 µL of the hybridization buffer were added and mixed well (final concentration of the primer and NaCl after addition of AuNPs was 1 µM and 0.08 M, respectively). The mixture was then denatured at 95°C for 30 seconds, and annealed at 59°C for 30 seconds and then cooled to room temperature for 10 minutes. 10 µL of colloidal AuNPs were then added to the mixture, and the color was observed within one minute. For a

permanent record of the results, one μL of the final mixture was spotted onto a silica plate.

2.3.7 Detection Limit Measurements

HCV positive samples with known viral load, as determined by real-time PCR, were used to determine the detection limit of the colorimetric assay. Serial dilutions of the sample (25-2000 HCV RNA copies) were tested using the developed method to determine the detection limit of the assay.

2.4 Results

2.4.1 Size Distribution and Surface Plasmon Band of the Prepared AuNPs

Scanning electron microscope image of AuNPs (Figure 2) was analyzed using the Image 1.41J software package (Wayne Rasband, National Institutes of health, USA. [Http://: rsb.info.nih.gov/ij/Java1.6.0_05](http://rsb.info.nih.gov/ij/Java1.6.0_05)). The AuNPs were well dispersed as shown in figure 2 and the mean diameter was found to be 15 nm (Figure 3). The absorption spectrum of the prepared AuNPs displayed a single peak in the visible region with λ_{max} at 518-520 nm.

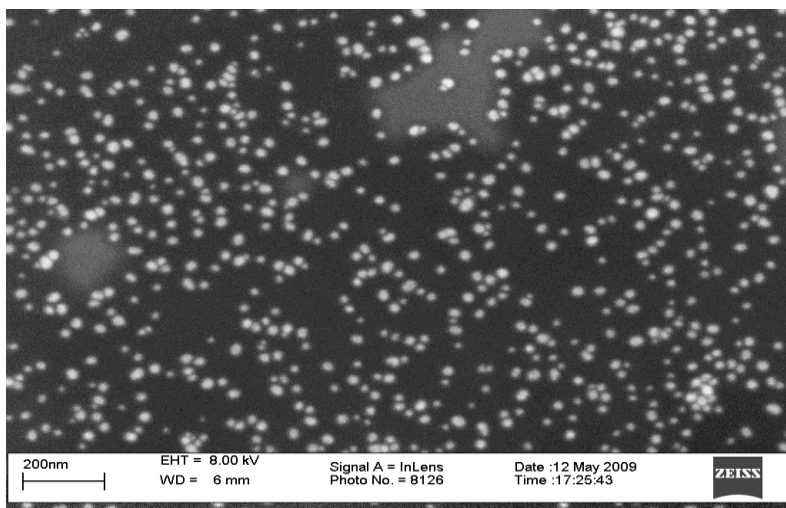


Figure 2. Scanning electron monographs of the prepared AuNPs. One drop of AuNPs was placed on silicon slide and left to dry then examined using field emission scanning electron microscopy (Model: Leo Supra 55).

Direct Detection of Unamplified Hepatitis C Virus RNA Using Unmodified Gold Nanoparticles

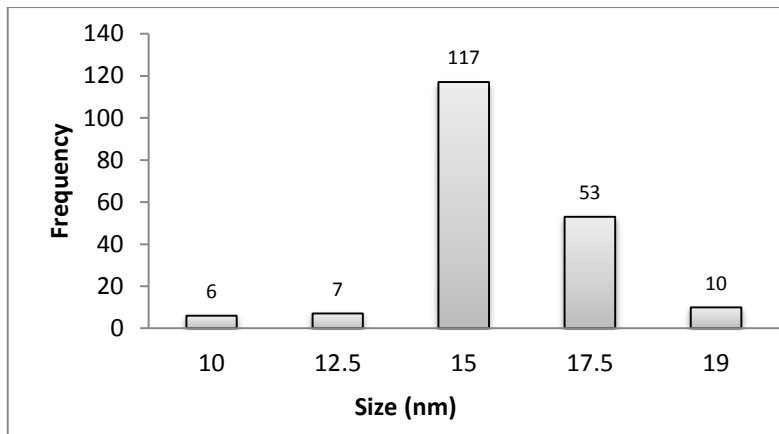


Figure 3. Analysis of the AuNPs size distribution. The scanning electron microscope image in Figure 2 was analyzed by Image J 1.4 software Wayne Rasband, National Institutes of Health, USA. http://rsb.info.nih.gov/ij/java 1.6.0_05.

2.4.2 Suitability of RNA Extraction Method

Serum samples may contain some lymphocytes, which contain human mRNA or genomic DNA. Moreover, serum also contains cell-free DNA, and nucleoproteins (Sisco 2001). Cell free DNA may fragment and may interfere with the assay. These fragments lead to false negative results due to their adsorption onto the AuNPs. Therefore, the samples were treated with DNase to exclude cell-free DNA and/or genomic DNA in the sample. Qiagen viral RNA extraction kit as stated in the kit's instruction manual does not guarantee the absence of DNA within the final RNA eluted. Using this kit, we obtained false negative results with all samples, even at very high viral titers. The Stratagene total RNA kit and Promega RNA extraction kit both include a DNase treatment step. Reproducible results were obtained with Stratagene and Promega kits.

2.4.3 Colorimetric AuNPs Assay: Development & Optimization

The color of AuNPs colloidal solution is affected by four main factors which should be adequately optimized for best results. These are concentrations of NaCl, AuNPs, and primer used, and the assay temperature.

AuNPs were prepared using the citrate reduction method which produces negatively charged nanoparticles due to citrate coating on their surfaces. This negative charge prevents their aggregation and a red color is obtained. Salt induces aggregation leading to a red-to-blue shift in solution color. The optimum final concentration of NaCl used was 0.08 M, which was sufficient for aggregation of AuNPs and visual detection of the color change, and at the same time, sufficient for proper annealing of the primer to its target.

Although ssDNA primers adsorb on AuNPs and prevent their aggregation, the concentration of the primers should be optimized. This is because, in the absence of the target, a very low primer concentration will not be sufficient to prevent aggregation leading to a false positive result. On the other hand, in the presence of the target, a very high primer concentration will prevent aggregation leading to a false negative result. In this study, at a final salt concentration of 0.08 M, a primer concentration less than 0.2 μ M was unable to prevent aggregation of 10 nM 15 nm AuNPs in

the absence of the target. On the other hand, a final primer concentration more than 3 μM was too high for any aggregation to occur in the presence of the target. Consequently, the optimal primer concentration was found to be 1 μM in the total assay volume.

The concentration of 15-nm AuNPs used in the assay was 10 nM in a total assay volume of 20 μL . This concentration is sufficient for visual detection of the color change, together with the primer and salt concentrations discussed above. Change in solution color was not clear and false results were obtained when lower concentrations of AuNPs were used.

Performing the assay without heating (that is essential for RNA denaturation and annealing of primers) lead to irreproducible results for most of the samples (positive and negative). Consequently, the denaturation and annealing steps were deemed necessary before the addition of the AuNPs to increase the specificity of the assay. It should be noted that the addition of AuNPs directly after removal of the tubes from the thermal cycler (while the tubes are still hot), resulted in false positive results. Therefore, the mixture must stand at room temperature for 10 to 15 minutes prior to addition of AuNPs in order to obtain reproducible results. Increasing the time of the denaturation and annealing steps also increases the percentage of false positive results. In our opinion, increasing the time of denaturation and annealing might increase the probability of the primer annealing non-specifically to some escaped nucleic acids other than HCV RNA that may be found in the nucleoprotein complexes in the serum.

Direct Detection of Unamplified Hepatitis C Virus RNA Using Unmodified Gold Nanoparticles

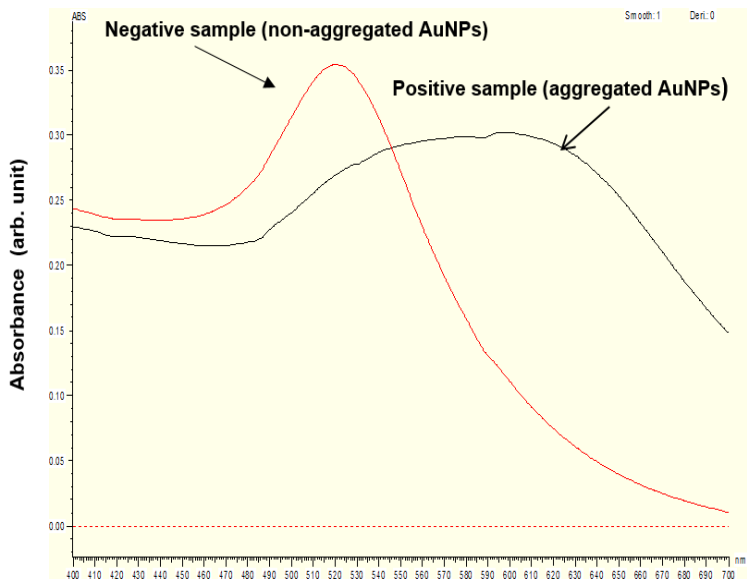


Figure 4. Extinction spectra of positive and negative samples. The absorption spectra of positive sample (aggregated AuNPs, black) and negative sample (non- aggregated AuNPs, red). Note the red shift and broadening of the peak of the positive sample due to aggregation of AuNPs. For the negative sample, the λ_{\max} was around 518-520 nm.

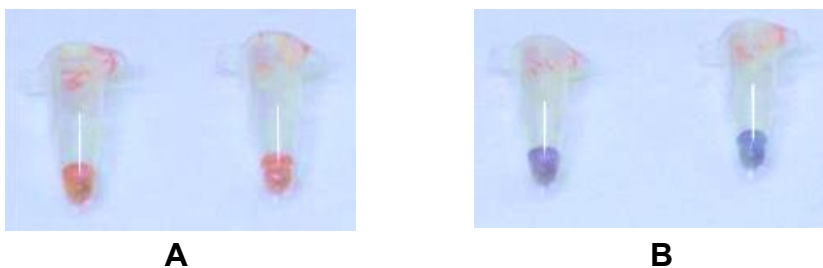


Figure 5. Colorimetric HCV RNA assay using unmodified AuNPs. Each tube contains 7 μL sample, 1 μM primer and 0.08 M NaCl. The samples were denatured at 95°C for 30 seconds and annealed at 59°C for 30 seconds and then 10 μL of 15 nm AuNPs was added after cooling the mixture at room temperature for 10 minutes. The photographs were taken after 1 minute from the addition of the AuNPs. (a) HCV RNA negative samples and (b) HCV RNA positive samples. Note the change in color from red to blue in the positive samples.

In summary, after adding the hybridization buffer to the extracted RNA, the mixture was subjected to denaturation at 95°C for 30 seconds, annealing at 59°C for 30 seconds, and then cooling to room temperature before the addition of the AuNPs. The change in color was visualized within only one minute. Also, change in the AuNPs absorption spectra was measured (Figure 4). 28 out of 30 HCV positive samples gave a blue color and 40 out of 45 HCV negative samples gave a red color (Figure 5). Based on these results, the assay has a sensitivity of 92% and a specificity of 88.9%.

Real-time RT-PCR was used to calculate the HCV viral load in clinical specimens that ranged from 43 IU/mL to 12,000 IU/mL. Serial dilutions of the HCV RNA (25–2000 HCV RNA copies) were prepared and assayed using the AuNPs as described above. The assay was capable of detecting 50 HCV copies/reaction.

2.5 Conclusions

A colorimetric assay has been developed using unmodified AuNPs for the direct detection of unamplified HCV RNA in biological fluids without the need for RNA amplification. The assay has a detection limit of 50 copies per reaction. The detection limit of the developed assay is better than that of the commercially available HCV core antigen test that detects HCV RNA levels above 20,000 IU/mL (one IU is typically equivalent to 3-5 copies) (Seme et al. 2005). The developed assay may be applied for tracking HCV replication even at low viral titers. The developed assay has several advantages including acceptable sensitivity, specificity, short turnaround time, and cost effectiveness. The cost of 1 gram of gold chloride is about 200 Euros that is enough to prepare 1 liter of 15 nm gold nanoparticles where only 10 μ L are needed per assay. Moreover, the use of AuNPs eliminates the need for expensive detection instrumentation. Furthermore, there is no need for functionalization of the AuNPs, the primer or the target. HCV RNA extraction is now easy and takes less than 20 min using commercial kits that are based on silica column extraction, magnetic beads, or organic extraction. The cost varies between kits but generally it is between 100-200 Euros for 50 extractions.

The detection limit of the proposed assay could be improved by increasing the starting serum volume used for RNA extraction. Moreover, it could be further developed into quantitative tests by spectrophotometric

quantification of the resulting blue color against a standard curve or developing a Fluorimetric version of the test by utilization of the size and distance nanoparticles surface energy transfer (NSET) properties of AuNPs. Also, this method may be further developed for detection of SNPs by manipulating the annealing temperature of the primers. This may have great implications for HCV genotyping, sub-typing, and monitoring of viral factors that have been correlated to patient's response to interferon therapy (El Awady et al. 2009). To our knowledge, this is the first study done using unmodified AuNPs for direct detection of unamplified HCV RNA in clinical specimens. Upon further developments and optimization, the assay may soon compete with commercial immunoassays and RT-PCR methods as routine tests for management of HCV patients.

3 Detection of Unamplified HCV RNA in Serum Using A Novel Two Metallic Nanoparticle Platform

Sherif M. Shawky¹, Bassem S. Guirgis¹ and Hassan M.E.Azzazy^{1,2i}

¹Youssef Jameel Science & Technology Research Centre and

²Department of Chemistry, the American University in Cairo, P.O. Box 74
New Cairo 11835, Egypt.

Running Title: HCV RNA detection using magnetic and gold nanoparticles

Corresponding author*: Hassan M. E. Azzazy, PhD, Department of Chemistry, School of Sciences & Engineering, the American University in Cairo, P.O. Box 74. New Cairo, Egypt 11835. E-mail: hazzazy@aucegypt.edu. Cell: +201000565727

Published in: Clinical Chemistry and Laboratory Medicine, 2014, 52 (4). PMID: 24158422

3.1 Abstract

Background: The unique properties of metallic nanoparticles have allowed their utilization in bio-sensing applications. A novel assay for the detection of Hepatitis C Virus (HCV) RNA in serum specimens has been developed using magnetic nanoparticles and unmodified cationic gold nanoparticles (AuNPs).

Methods: HCV RNA was extracted using magnetic nanoparticles functionalized with an oligonucleotide specific to HCV RNA. Extracted RNA is reacted with oligonucleotide sequence specific for HCV RNA in presence of unmodified cationic AuNPs. In positive samples, AuNPs are aligned onto the phosphate backbone of the RNA and their aggregation changes the solution color from red to blue. In the absence of target, solution colour remains red. The assay has been tested on 50 serum clinical samples (25 HCV positive and 25 controls).

Results: The dual nanoparticles assay detected HCV RNA in serum and generated comparable results to real-time PCR. The assay had specificity and a sensitivity of 96% and 96.5%; respectively, and a detection limit of 15 IU/ml.

Conclusions: The developed colorimetric dual nanoparticles HCV RNA assay is simple and inexpensive and can be used for rapid detection of unamplified HCV RNA in serum. Similar sensing platforms can be developed to detect other nucleic acid targets.

Keywords: Cationic AuNPs; Hepatitis C Virus (HCV); magnetic nanoparticles; nucleic acid Tests (NAT); Qualitative HCV RNA assay.

3.2 Introduction

Hepatitis C virus (HCV) is a major global health problem; it infects about 170 million worldwide, with about 3-4 million new infections annually (Lavanchy 2009, Miller et al. 2010, Negro et al. 2011, Previsani Nicoletta et al. 2013, WHO 2011). A variety of molecular assays are available for detection of HCV RNA in patients' blood. These tests can be based on target amplifications e.g. qualitative nested reverse transcription polymerase chain reaction (RT-PCR), transcription mediated amplification (TMA), and quantitative real-time RT-PCR. Signal amplification-based methods are also available such as quantitative branched-chain DNA amplification (Scott et al. 2007). Although these tests have high sensitivity and specificity, they are time consuming, labor intensive, expensive, and require specialized equipment and relatively sophisticated laboratory infrastructure. Therefore, the development of novel diagnostic assays that are simple, rapid, sensitive, specific and most importantly cost-effective is urgently needed to control HCV in developing countries with limited resources.

Gold nanoparticles (AuNPs) are among the most promising nanostructures which could be employed in diagnostic assays. Owing to their Surface Plasmon Resonance (SPR), AuNPs exhibit intense absorbance and scattering properties. SPR refers to the collective oscillation of the free electrons on the surface of AuNPs, when they are hit by light. The resonance frequency lies in the visible portion of the electromagnetic spectrum, and thus a colloidal solution of AuNPs (around 20 nm in diameter) would appear with an intense red color and will have absorbance maximum around 520 nm (Radwan et al. 2009), this value is affected by multiple factors including AuNPs' particle size; inter particle distance, and the ionic strength and refractive index of the medium. When AuNPs come close together e.g. due to electrostatic attraction by another moiety, or due to alteration of medium ionic strength, Plasmon-Plasmon coupling occurs and a shift in the absorbance peak maximum to a longer wavelength and a change in solution color from red to blue (Radwan et al. 2009, Larginho et al. 2012, Kumar et al. 2013). AuNPs can be conjugated to bio-molecules (such as proteins, antibodies, and nucleic acids) through electrostatic interactions to be employed in various biological assays (Radwan et al. 2009).

The signal generated in AuNPs-based molecular diagnostic assays can be detected by various strategies including colorimetric, scanometric, light-scattering, electrochemical and electrical, quartz-crystal microbalance, and Nanometal Surface Energy Transfer (NSET) (Ray et al. 2006, Griffin et al. 2009b), surface enhanced Raman scattering (SERS) and laser diffraction strategies (Radwan et al. 2009). AuNPs colorimetric methods are quite attractive in diagnostic applications and, usually employ negatively charged particles, and can be further categorized into cross-linking (Storhoff et al. 1998, Storhoff et al. 2004) (utilizing two oligonucleotide-functionalized AuNPs probes), non-cross-linking (Conde et al. , Huber et al. 2004, Baptista et al. 2005, Costa et al. 2009) [one probe], and non-functionalized [no probes] AuNPs (Li et al. 2004a, Li et al. 2004b, Shawky et al. 2010).

Positively charged (cationic) un-functionalized AuNPs were also explored for utility in diagnostic molecular assays. Sun et al (Sun et al. 2005) developed a microarray assay (solid support) for gene expression analysis using cationic AuNPs, while Hsiao et al (Hsiao et al. 2009)utilized them for the determination of DNA microarray chip quality prior to use. He et al developed a calorimetric assay for the detection of HIV in clinical specimens using gold nanorods and a label-free probe DNA (He et al. 2008).

In this study, we report for the first time the development of a two metallic nanoparticles based colorimetric platform (solution phase) which employs non-functionalized cationic AuNPs for the direct detection of unamplified HCV RNA extracted from serum specimens. The cationic AuNPs bind to the negatively charged phosphate backbone of nucleic acids extracted from patient serum. The cationic AuNPs align closely along these molecules and thus color change from red to blue. In the absence of the target, the positively-charged AuNPs repel each other and the solution color remains red. Prior to detection by cationic AuNPs, specific capturing of HCV RNA in serum was achieved using functionalized magnetic nanoparticles. The principle of the assay is shown in Figure 1. This method is simple, rapid, highly sensitive, specific and inexpensive and can replace the currently used NATs for the extraction and detection of HCV RNA. Also, the proposed assay could be expanded to be used in extraction and detection of other nucleic acids targets.

Detection of Unamplified HCV RNA in Serum Using A Novel Two Metallic Nanoparticle Platform

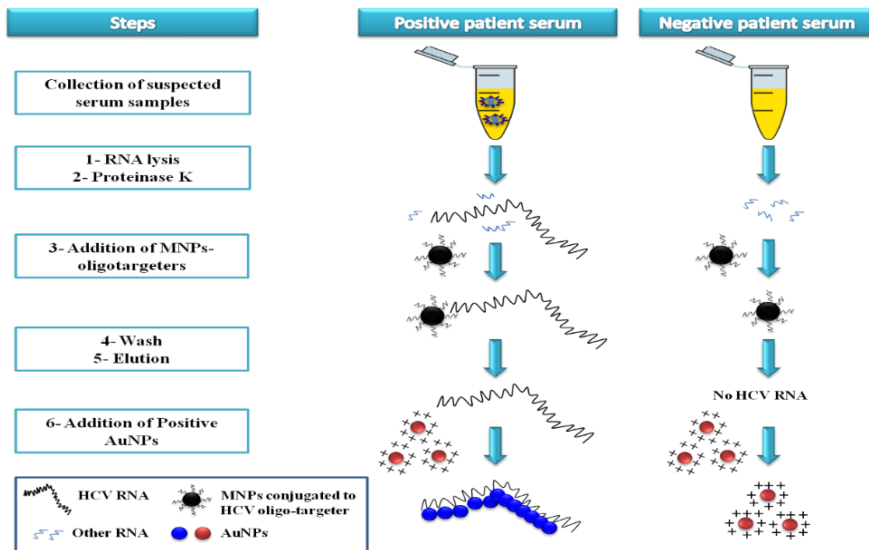


Figure 1. The principle of the developed AuNPs-based assay. HCV virions are first lysed with RNA lysis buffer, and then proteins are digested with proteinase K (steps 1& 2 respectively). In step 3, HCV RNA is captured with magnetic nanoparticles conjugated to oligonucleotide specific to HCV RNA. The captured RNA is then heated and eluted (step 5) for purification. The last step is the addition of AuNPs and phosphate buffer to the purified RNA and the color of the tube was observed within 5 min. In the presence of HCV RNA target, alignment of the positively charged AuNPs onto the negatively charged phosphate backbone of HCV RNA occurred leading to nanoparticles aggregation and solution color changed from red to blue. On the other hand, in case of negative samples, no nucleic acid was present for alignment of the AuNPs and thus nanoparticles remained separated from each other due to repulsion between their positive charges and the solution color remained red.

3.3 Materials and Methods:

3.3.1 Iron oxide magnetic nanoparticles: synthesis and functionalization

HCV RNA was extracted using homemade magnetic nanoparticles conjugated to an oligonucleotide specific to the 5'untranslated region of HCV RNA. First, 90 nm magnetic nanoparticles functionalized with amino groups were synthesized as described elsewhere (Kouassi et al. 2005, Kouassi et al. 2006). Magnetic nanoparticles synthesized by co-precipitation of ferric and ferrous chloride. Briefly, FeCl₂ and FeCl₃(1:2) were mixed with deionized water and then mixed with 10 wt.% of amino propyl tri-ethoxysilane (APES) with stirring and heating at 80°C. After 5 minutes, NaOH was added drop-wise to the mixture and pH adjusted to 10. Heating was turned off and the mixture stirred for 20 h with nitrogen gas flow. Washing was done with ethyl alcohol (70%) and deionized water and the particles were removed with a magnet and dried in vacuum oven at 50°C.

3.3.2 Characterization of Magnetic Nanoparticles (MNP)

The size and the morphology of the prepared magnetic nanoparticles were characterized by scanning electron microscope (SEM, LEO SUPRA 55; Carl Zeiss AG, Oberkochen, Germany). While, Fourier transform infrared spectroscopy (FT-IR) was used to record the IR spectra of the particles using potassium bromide (KBr) pellet technique.

3.3.3 Conjugation of HCV specific probe to the amino functionalized MNP

The prepared magnetic nanoparticles were conjugated to a synthetic HCV RNA specific probe using a hetero-bi-functional cross-linker (***3-maleimidobenzoic acid N-hydroxyl succinimide, MBS***), which has NHS ester at one end (which reacts with primary amine groups forming stable amide bond) and a maleimide group at the other end (which reacts with sulfhydryl groups forming stable thioether linkage).

For functionalization of the nanoparticles, the disulfide labeled probe was prepared as previously described (Hill et al. 2006, Rosi et al. 2006). Briefly, disulfide cleavage of the probe was done by lyophilization of

10 nmol of the probe and then re-suspended in 100 μ L of 0.1 M dithiothriitol prepared in disulfide cleavage buffer (170 mM phosphate buffer, pH= 8). The solution was wrapped in foil and allowed to stand at room temperature for 3 h with occasional vortexing. Desalting of the freshly cleaved probe was done using Nap-5 column (illustra NAP-5, GE Healthcare) according to the manufacturer's instructions. The amine functionalized magnetic nanoparticles were washed twice with di-methyl sulfoxide (DMSO), then MBS cross linker dissolved in DMSO was added to the nanoparticles. The mixture was mixed on a roller shaker for 1 hat room temperature. Then, the nanoparticles were washed twice with DMSO followed by coupling buffer (100 mM phosphate buffer and 0.2 M NaCl, pH= 7) twice. The particles were suspended again in coupling buffer and the cleaved probe added to the suspended particles and allowed to react on a roller shaker overnight. Finally, the supernatant was removed and the magnetic nanoparticles functionalized with HCV RNA specific probe were re-suspended in storage buffer (10 mM phosphate buffer, 0.1 M NaCl, pH= 7.4).

3.3.4 Synthesis of Positively Charged AuNPs

Positively charged spherical particles were synthesized as mentioned elsewhere with slight modifications (Huang 2006, Huang et al. 2007). Briefly, the seed solution was prepared by reducing HAuCl_4 (2.5 ml of 0.001 M HAuCl_4), in presence of CTAB (7.5 mL of 0.2 M), with ice-cold NaBH_4 (600 μ L; 0.01 M). The vials were then shaken vigorously (about 2 min) to produce brown seed suspensions. The seed (80 μ L) was then added to the centre of a solution containing HAuCl_4 (50 mL of 0.001 M HAuCl_4), 50 mL of 0.2 M CTAB, AgNO_3 (1.5 mL of 0.004 M AgNO_3) and ascorbic acid (700 μ L of 0.0788 M). The mixture was stirred for about 24 hours to produce the positively charged gold nanoparticles.

3.3.5 Characterization of synthesized AuNPs

The absorbance spectrum and concentration of the positively charged particles was determined using UV spectrophotometer (Jenway 6800) as previously reported (Link et al. 1999, Jain et al. 2006). The shape, size and the charge of the prepared AuNPs were analysed using field emission scanning electron microscopy (SEM, LEO SUPRA 55; Carl Zeiss AG, Oberkochen, Germany) and zeta sizer (Malvern Instrument Ltd., Zeta sizer Nano series, UK); respectively. For the SEM analysis, 5 μ L of the synthesized AuNPs were placed on silicon wafer and allowed to air dry prior to examination.

3.3.6 Serum specimens

Serum samples were collected from healthy volunteers (n= 25), who have tested negative for HCV antibodies, and from chronic HCV patients (n= 25). Rapid HCV test was performed on all the samples and positive HCV samples tested by real time RT-PCR. All positive samples had elevated ALT and AST levels. All samples were negative for hepatitis B surface antigen and hepatitis B antibody. HCV standards were included in the study with different concentrations. Each serum sample was divided into two portions one extracted by SV total RNA isolation system (Promega, cat. No. Z3100) following the modified protocol for HCV RNA isolation (Paul Otto et al. 1998) and the second portion was extracted using the functionalized magnetic nanoparticles prepared as described below. The RNA isolation using the functionalized magnetic nanoparticles was repeated twice by 2 different persons.

3.3.7 Real-time RT-PCR

Real-time RT-PCR was performed using AgPath ID One Step RT-PCR kit (cat # AM1005; Ambion) according to manufacturer's protocol for all the samples under study (positive and negative samples), and for the HCV standards included in the Real Time PCR kit. To 16.5 μ L master mix, 8.5 μ L of the extracted HCV RNA was added and amplification was performed using Stratagene (Mx3005P) under the following cycling conditions: 1 cycle of 45°C for 10 min, 1 cycle of 95°C for 10 min followed by 45 cycles of 95°C for 15s and 60°C for 45s.

3.3.8 Colorimetric two nanoparticles HCV assay:

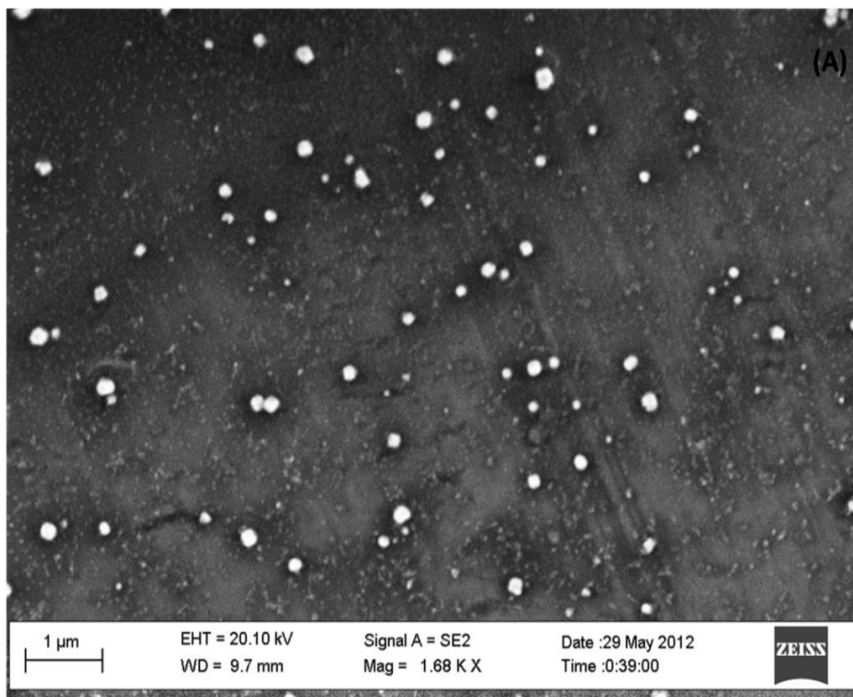
ADNA sequence specific for HCV RNA was synthesized and conjugated to magnetic nanoparticles and used to capture HCV RNA after virion lysis, digestion and precipitation of the proteins in patient sera. In a 1.5 mL micro-centrifuge tube, 100 μ L of the magnetic nanoparticles conjugated to HCV specific probe was washed twice with the assay buffer (10 mM phosphate buffer, 150 mM sodium chloride, pH= 7.4) and then re-suspended in 50 μ L assay buffer. In another 1.5 mL micro-centrifuge tube, 200 μ L of patient serum was added to 200 μ L of lysis buffer to break down the viral envelope. After mixing by inversion, 50 μ L proteinase K was added to digest the serum proteins and left to incubate for 10 min. Then, the mixture was centrifuged for 10 min at 21913 x g and the supernatant was taken and mixed with 300 μ L of iso-propanol. Then, the re-suspended magnetic nanoparticles were added to the previous mixture and heated at 90°C for 2 min to denature the target RNA. The mixture was shaken at a temperature \sim 15°C below the melting point of the conjugated probe for 45 min. Then, the tubes were placed on magnet until all solutions were clear and the supernatant was removed. Then, the particles were washed twice with washing buffer (60 mM potassium acetate, 10 mM Tris-HCl, 60% ethanol, pH=7.5). Supernatant was removed between each wash with the help of magnet. Elution was done by adding 50 μ L DEPEC –water, and heated at 95°C for 2 min. The tubes were placed on magnet until all solutions were clear and the eluted HCV RNA was transferred to new RNase free tube. The extracted HCV RNA was then assayed using the cationic AuNPs assay as described below.

To 5 μ L of the extracted HCV RNA, 5 μ L of 2M phosphate buffer was added followed by 30 μ L of the positively charged AuNPs. The sample was mixed by pipetting and the color of the solution was observed within 5 min.

3.4 Results:

3.4.1 Characterization of magnetic nanoparticles

The magnetic nanoparticles were well dispersed and the majority of the measured nanoparticles have a mean diameter of 90 nm as analyzed by scanning electron microscope (Figure 2A). The magnetic nanoparticles were functionalized by amino groups through their reaction with 3- aminopropyl tri-ethoxysilane (APTES) in a silanization reaction which includes hydrolysis and condensation steps (Mikhaylova et al. 2004, Yamaura et al. 2004a, Yang et al. 2009a). The FT-IR spectra (Figure2B) of the functionalized magnetic nanoparticles confirmed the synthesis and the functionalization procedures. The band at 583cm^{-1} corresponds to the Fe-O bond, the one at 1050cm^{-1} and 1380cm^{-1} corresponds to the vibrations of SiOCH_2 structure and Si-CH₂ scissoring vibrations respectively, while the N-H bending mode and stretching vibrations of the free amino groups are appeared at bands 1625cm^{-1} and 3436cm^{-1} respectively. Also, the anchored propyl group of the APTES is present at band 2923cm^{-1} .



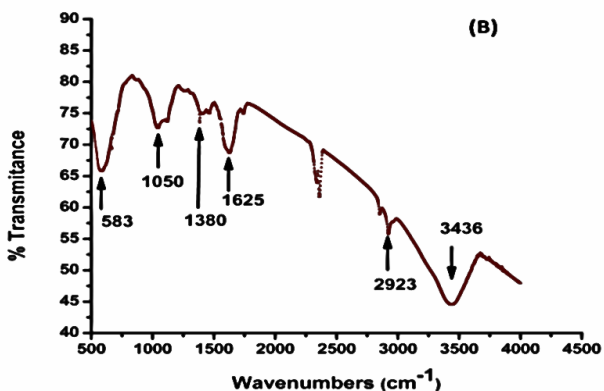


Figure 2. (A) Scanning Electron Microscope image (SEM) of the prepared magnetic nanoparticles. (B) FT-IR spectra of the prepared magnetic nanoparticles functionalized with amino Propyl tri-ethoxysilane (APES). The peaks showed by the arrows are described in the text.

3.4.2 Characterization of synthesized AuNPs

UV-Vis spectrum was performed for the prepared AuNPs. The spectrum shows a λ_{max} at 531 nm characteristic of spherical AuNPs with average diameter of about 46.43 nm and a positive charge of +52.1 mv have been confirmed by the zeta sizer analysis (Figure 3).

Detection of Unamplified HCV RNA in Serum Using A Novel Two Metallic Nanoparticle Platform

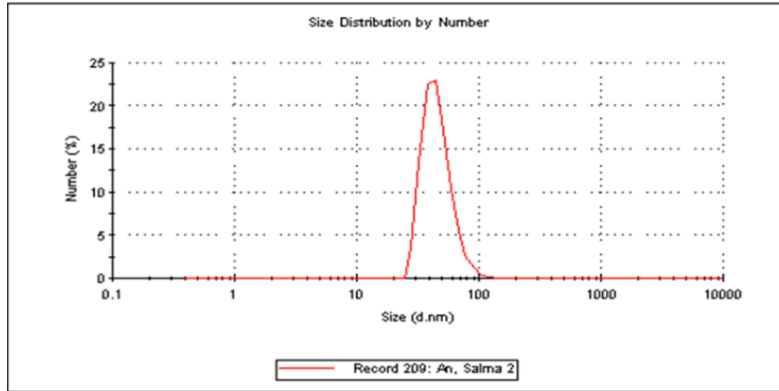
Results

(A)

Pdl:

0.145

	Size (d.nm):	% Number	Width (d.nm):
Peak 1:	46.43	100.0	13.51
Peak 2:	0.000	0.0	0.000
Peak 3:	0.000	0.0	0.000



(B)

Results

Zeta Deviation (mV): 20.2

Conductivity (mS/cm): 3.53

	Mean (mV)	Area (%)	Width (mV)
Peak 1:	52.1	62.4	11.9
Peak 2:	88.8	37.6	9.01
Peak 3:	64.3	17.3	4.03

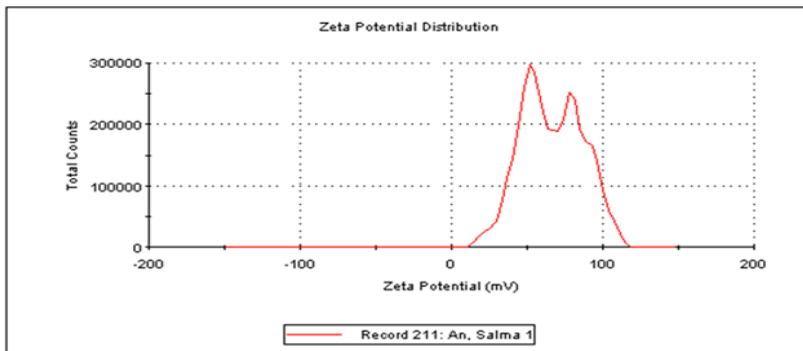


Figure 3. Analysis of cationic AuNPs size (A) and charge (B) using zeta sizer.

3.4.3 Detection of HCV RNA in Serum Using Real-time RT-PCR and Two Nanoparticles HCV Assay

Fifty serum samples were used in this study; 25 HCV positive and 25 samples from healthy individuals. All the samples were subjected to extraction by SV total RNA isolation kit. Extracted HCV RNA was detected and quantified using real-time RT-PCR as a standard method for HCV RNA detection.

The extracted RNA was also assayed using the developed two nanoparticles based assay. The color of the AuNPs colloidal solution of the negative samples remained red which indicates absence of target HCV RNA in the sample. On the other hand, the presence of HCV RNA in positive samples led to aggregation of the AuNPs and the color changed from red to blue (Figure 4). The intensity of the blue color correlated to the HCV viral load as quantified by real-time RT-PCR. Of the 25 HCV positive samples, 23 samples gave blue color which indicated the presence of the HCV RNA, while no change in color occurred in 2 samples (false negatives). On the other hand, 22 out of 25 negative samples gave red color which indicates the absence of HCV RNA in addition to any other nucleic acid, which reflected high purity of the sample and efficiency of HCV RNA extraction using the magnetic nanoparticles. Only three HCV negative samples gave blue color (false positive). The sensitivity and specificity of the assay were 96% and 96.5%; respectively. The negative predictive and positive predictive values were 91.6% and 88.5% respectively, while the assay accuracy was 90%.

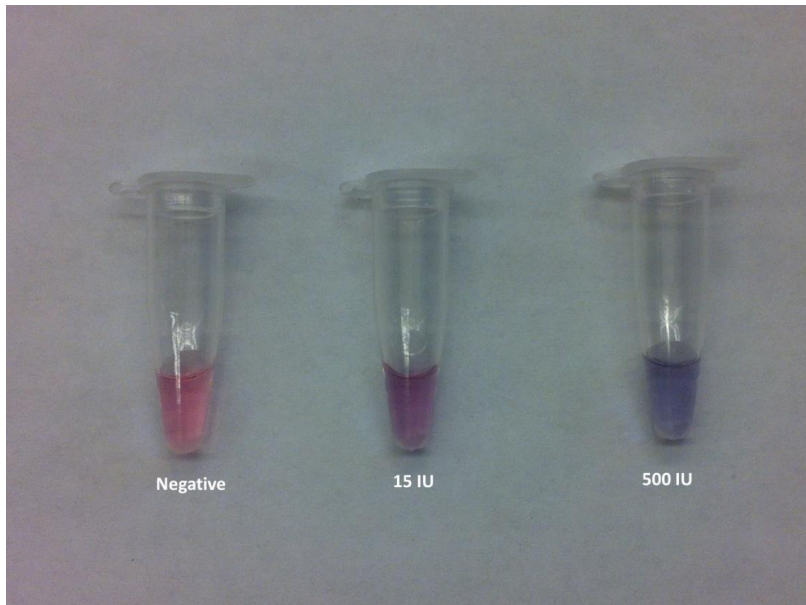


Figure 4. Detection of HCV RNA extracted from serum using the developed two metallic nanoparticles assay. In the absence of HCV RNA, the cationic AuNPs are repelled from each other and remain suspended in solution which retains its red color (left tube). On the other hand, in the presence of HCV RNA, direct alignment of the cationic AuNPs onto the negatively charged phosphate backbone of HCV RNA occurs, leading to change in the colour solution from red to blue (other two tubes). The intensity of blue colour is proportional to the HCV viral load.

It is important to note that the same principle can be used in extraction and purification of any other nucleic acid and/or protein by simply replacing the HCV RNA specific probe with the other target specific molecule (e.g. antibodies, lectins, aptamers, etc.), therefore the developed HCV RNA extraction method by the magnetic probe could be expanded to be used in many other targets. The main aim for capturing the HCV RNA is to remove other nucleic acids (DNA or RNA) that may interfere with the assay results and thus allowing an increase in assay specificity.

3.5 Discussion and Conclusions

We report the development of a two nanoparticles assay platform for direct detection of unamplified HCV RNA in serum. The assay employed magnetic nanoparticles functionalized with oligonucleotide specific for HCV RNA for its extraction from serum. Cationic AuNPs were then used to detect the presence of HCV RNA by generating a colorimetric signal. In case of positive samples, the CTAB capped cationic AuNPs bound to the negatively-charged phosphate groups of the HCV RNA target (Sun et al. 2005, Jain et al. 2006). The presence of phosphate buffer in the assay increased the aggregation capability of the AuNPs (for only the positive samples) where we propose that phosphate ions bound to the aligned cationic AuNPs on HCV RNA and then another row of AuNPs attaches to the phosphate ions which will be aligned on another phosphate backbone of another RNA molecule and so on. So, aggregation occurred by first alignment of AuNPs on phosphate backbone of one nucleic acid, which then binds to phosphate ions and the latter binds to other AuNPs which then binds to other nucleic acid phosphate backbones. Therefore, several layers (*1stRNA/AuNPs/Phosphate ions/AuNPs/2ndRNA*) were formed in the positive samples leading to AuNPs aggregation. These layers will result in forming a network of nucleic acid/AuNPs which lead to AuNPs aggregation and change of colour from red to blue (Wang et al. 2003, Koyfman et al. 2005). To confirm our hypothesis, SEM images were taken for a positive sample (Figure 5A) showing many layers of AuNPs aligned on RNA molecules.

In the absence of HCV RNA (absence of any nucleic acid), the AuNPs are far from each other (repulsion between positively-charged particles) and thus the solution colour remained red (Figure 4). A SEM image (Figure 5b) was taken for a negative sample which shows no aggregation of AuNPs. It is important to note that the red colour was stable even when left undisturbed for several days. Moreover, the prepared cationic AuNPs are stable for about 2 years and no change in their colour or charge occurred to the nanoparticles.

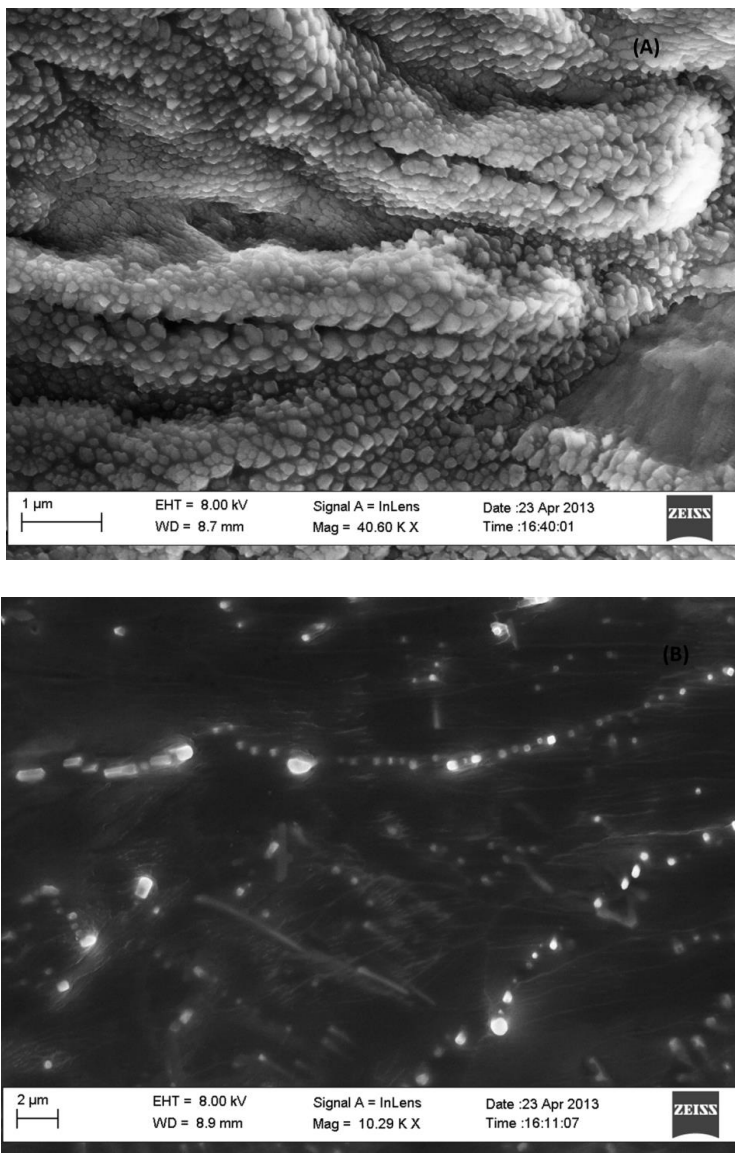


Figure 5. SEM analysis of AuNPs in positive and negative HCV assays. (A) SEM of AuNPs in positive HCV sample. AuNPs aggregate on RNA molecules in presence of phosphate buffer. (B) SEM of AuNPs in the absence of HCV RNA (no aggregation of AuNPs).

This study reports for the first time the development of a colorimetric solution-phase two nanoparticles assay for direct detection of unamplified HCV RNA extracted from clinical specimens. The assay has high sensitivity and specificity of >95%, and a detection limit of 15 IU/mL. The

Detection of Unamplified HCV RNA in Serum Using A Novel Two Metallic Nanoparticle Platform

turnaround time of the proposed assay is about 75 min (including RNA extraction) which is about one third the turnaround time of the standard real time PCR method. The assay costs about US\$10 per test, which is several folds cheaper than that of the real time PCR. Moreover, the test can be developed into a quantitative one since the intensity of the blue color generated correlated with the HCV viral load as determined by real time RT-PCR (Figure 4).

In conclusion, the developed assay is simple (adding cationic AuNPs solution to the extracted RNA in presence of phosphate buffer), rapid, sensitive, inexpensive, and similar platforms can be used for the detection of other RNA and/or DNA targets in solution.

Acknowledgments

This work has been funded by a grant from YJ-STRC to Dr. Hassan Azzazy. The authors acknowledge Mr. Kamel Eid (YJ-STRC) for preparing the magnetic nanoparticles.

Statement of funding or conflict of interest:

This work has been funded by a grant from YJ-STRC (AUC) to Dr. Hassan Azzazy. Authors of this paper have submitted a patent on the use of nanoparticles for detection of HCV RNA in clinical specimens. Dr. Azzazy is the President and Chief Technology Officer of D-Kimia, a LLC, which develops HCV nano-diagnostic assays.

4 Development and evaluation of gold nanoparticles assays for direct detection of urinary bladder and breast cancer biomarkers

This research has been developed into two papers:

- 1- Direct detection of unamplified Hepatoma up Regulated protein RNA in urine using Gold Nanoparticles for Bladder Cancer Diagnosis. Sanaa Eissa, **Sherif M. Shawky**, Marwa Matboli, Shymaa Mohamed and Hassan M.E. Azzazy. **Clinical Biochemistry** 2014, 47 (1-2): 104-110. **PMID: 24183881**

- 2- The prognostic value of Histidine-Rich Glycoprotein RNA in Breast Tissue using unmodified Gold nanoparticles assay. Sanna Eissa, Hassan Azzazy, Marwa Matboli **Sherif M. Shawky**, Hebatallah Said, Faten Anous. **Applied Biochemistry and Biotechnology**. 2014 August 2014. **PMID: 25091325**

4.1 Abstract

Objective: To develop an unmodified gold nanoparticles-based assay for the direct detection of unamplified HURP RNA in urine samples for early bladder cancer diagnosis. The second aim is to develop an unmodified AuNPs assay for the direct detection of unamplified HRG RNA in breast cancer tissues.

Methods: HURP RNA was extracted from urine samples (50 bladder carcinomas, 25 benign bladder lesions, and 25 controls). Also, HRG RNA was extracted from breast tissues (60 patients proven to have breast carcinomas, 30 with benign breast lesions and 30 controls). The extracted RNA for both markers was further purified using homemade magnetic nanoparticles functionalized with target-specific oligonucleotides. Real-time PCR (RT-PCR) was performed on the extracted RNAs before and after the magnetic purification step. The developed AuNPs assay was performed on the extra-purified RNA targets.

Results: The developed HURP RNA AuNPs assay had a sensitivity and specificity of 88.5% and 94%, respectively, with a detection limit of 2.5 nmol/L. The HRG AuNPs assay had a sensitivity and specificity of 90%, with a detection limit of 1.5 nmol/L.

Conclusion: The developed colorimetric assays for both biomarkers are sensitive, specific, simple, rapid and inexpensive. Moreover, the assays maybe further developed for the detection of other cancer biomarkers.

4.2 Introduction

Hepatoma Up regulated protein (HURP) RNA has been recently identified as a powerful biomarker in urine specimens that could be used for the early detection of bladder cancer (Kaufman et al. 2009, Eissa et al. 2014b). On the other hand, histidine-rich glycoprotein (HRG) is considered as a serum biomarker for breast cancer detection (Schaub et al. 2009). Moreover, HRG RNA has been found to be over-expressed in breast cancer tissues in comparison to normal tissues (Matboli et al. 2014). Increasing cancer patient survival rates and the prevention of cancer spread among high-risk individuals are directly proportional to the early detection of the disease and screening, respectively. In the past few years, the field of identifying, evaluating and employing novel biomarkers for accurate detection of different cancers has evolved rapidly (Choi et al. 2010). Meanwhile, advances in the field of nanotechnology as an emerging science in the last decade have allowed the development of many nanoparticles-based assays for direct detection of bio-molecules [RNA, DNA, proteins] (Jain 2005, Azzazy et al. 2006, Radwan et al. 2009, Alharbi et al. 2014). Nanoparticles have been recently proposed as promising tools for the development of the next generation of diagnostic assays. Because of their unique properties and ability to interact with biomolecules on a one-to-one basis, various nanoparticles show great promise to meet the needs of the clinical laboratory concerning simplicity, sensitivity, specificity and low cost. Information regarding the discovery of cancer biomarkers and the progress of nanotechnology in laboratory medicine is examined in this chapter to aid in the development of gold nanoparticles-based assays for the detection of RNA-based tumor markers in clinical samples from urinary and breast cancers.

Unmodified AuNPs-based colorimetric assays have been developed in two independent studies. The first one was for the direct detection of HURP RNA in urine samples for bladder cancer diagnosis (Eissa S. et al. 2014), while the second (Eissa et al. 2014a) have explored the role of the histidine-rich glycoprotein (HRG) RNA in tissue biopsies as a promising clinically useful biomarker for the prognosis of breast cancer patients. Prior to its detection by the unmodified AuNPs, specific capture of the target RNAs (HURP in urine samples and HRG RNA in tissues samples) was achieved using magnetic nanoparticles functionalized with target-specific probes. The two assays that

Development and evaluation of gold nanoparticles assays for direct detection of urinary bladder and breast cancer biomarkers

were developed were compared to the conventional RT-PCR and standard cytology and cystoscopy methods. Moreover, the use of the proposed assay was expanded to the purification and/or detection of other nucleic acids targets. In these assays, total RNA was first extracted from the sample, and then magnetic nanoparticles functionalized with target specific oligonucleotide were added to the extracted RNA to capture the target RNA. The captured RNA was then washed and eluted. A portion of the target RNA was mixed with hybridization buffer (NaCl and target-specific primers). After 1 minute for denaturation and annealing, AuNPs were then added and the color change was observed within 2 minutes. The assay was based on the fact that single stranded DNA (ssDNA) adsorbs to the citrate-coated AuNPs through its nitrogenous bases and, thus, stabilizes the AuNPs, thereby preventing their salt-induced aggregation. In contrast, double stranded DNA (dsDNA) does not adsorb to the surface of the nanoparticles due to the repulsion between its negatively charged phosphate backbone and the negatively charged surface of the AuNPs (Li et al. 2004a, Li et al. 2004b, Li et al. 2005, Li et al. 2007, Shawky et al. 2010). Therefore, when a colloidal solution of the AuNPs is added to a saline solution containing ssDNA (oligotargeter), the latter is free to stabilize the nanoparticles and prevent their aggregation, and the solution remains red. In the presence of a complementary target to the oligotargeter, the latter leaves the surface of the AuNPs, hybridizes to its target, and the AuNPs aggregate by the action of the salt in the solution. As a result, the solution turns blue. The principle of the assay is summarized in figure 1.

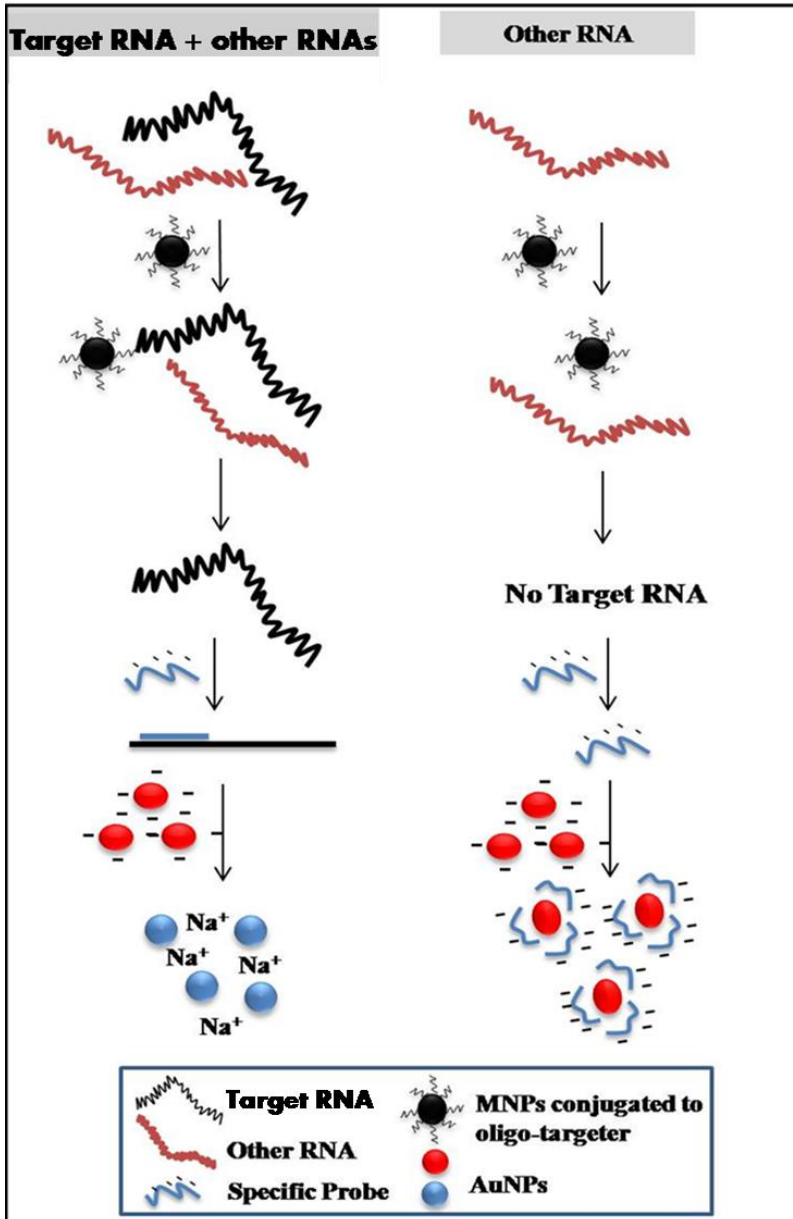


Figure 1: Schematic diagram of the developed unmodified AuNPs based assay. After extraction of the total RNA in the sample, the target RNA is captured using magnetic nanoparticles functionalized with the target probe. The target is then mixed with hybridization buffer (NaCl and target specific probe). After denaturation of the target and annealing to its specific probe (the straight black and blue lines respectively) AuNPs were then added to the mixture and color change was observed within 2 minutes.

4.3 Materials and methods

4.3.1 Study Population

Both studies were approved by Ain Shams University, faculty of medicine ethical committee. Samples collection and biopsies was performed at Ain Shams University, Faculty of Medicine, Cairo, Egypt.

4.3.1.1 Urinary Bladder Cancer

A prospective analysis was performed on 100 Egyptian subjects, 75 patients were selected from urology department, Ain Shams University, Egypt, in addition to 25 healthy normal volunteers as a control group between January 2011 and June 2012, after obtaining informed consent. Patients presented with hematuria and chronic irritative voiding symptoms were included in the study and patients with past history of bladder cancer or any other malignancy were excluded from the study. All patients provided a single voided urine sample before cystoscopy. Biopsy of any suspicious lesion was performed for histo-pathologic examination. Accordingly, the 75 patients included in the study were classified into malignant and benign groups. The malignant group included 50 patients (mean age 59.8 ± 9.3 years, and range from 37-79 years). Of those patients, 42 were diagnosed by histopathology with transitional cell carcinoma (TCC), and 8 with squamous cell carcinoma (SCC). Tumor staging and grading was determined according to TNM and World Health Organization classification 1973. The benign group included 25 patients with benign urological diseases: bilharzial dysplastic lesions, renal stone and urethral stricture (mean age 52.88 ± 9.4 years, and range from 25-68years). A group of 25 healthy volunteers (mean age 45.44 ± 11.9 years, and range from 28-79 years) recruited from the hospital laboratory staff.

4.3.1.2 Breast Cancer

A prospective analysis was performed on 120 Egyptian subjects, 90 patients were selected from General Surgery department, Ain Shams University Hospitals, Cairo, Egypt, in the period from November 2008 to June 2009 then was followed up for recurrence till december 2013, after obtaining informed consent.

Sample size (120 subjects: 60 cases and 60 controls) was calculated by Epi-info version 6 software using prevalence rate of breast disease: 29%, odds ratio of oral contraception: 2, α : 0.05, power: 80% and confidence level: 95%. Patients presented with breast mass and/or bleeding per nipple were included in the study and patients with past history of breast cancer or any other malignancy, inflammatory mastitis, chemotherapy or radiotherapy were excluded from the study. Tissue specimens were reviewed independently by histopathologists to grade and sub-classify the tumors based on established criteria. Subsequently, the 90 patients included in the study were classified into malignant and benign groups. The malignant group included 60 patients (mean age 52.47 ± 13.2 years, and range from 20-81yrs). 43 of which were histopathologically diagnosed as invasive duct carcinoma (**IDC**), 1 patient with invasive lobular carcinoma (**ILC**), 9 with mixed invasive duct and lobular carcinoma and 7 patients with rare histological types. Tumor staging and grading was determined according to TNM and World Health Organization classification. The benign group included 30 patients with benign breast diseases; (fibro adenoma,) (49.6 ± 14.11 years, and range from 20-67yrs). The third study group was represented by 30 healthy volunteers who underwent plastic breast reduction surgery (mean age 50.47 ± 11.64 yrs., and range from 36-77yrs) with matching age and sex to the patient' groups. Breast cancer patients were regularly followed up every 6 months. Local-regional relapses and the subsequent surgery during the 90-day post-surgery period were considered to be part of the primary management and distant recurrence during this time disqualified the patient from study. Relapses after 90 days were considered events. Relapses were dated and reviewed by two of three medical oncologists.

4.3.2 Amino functionalized MNP synthesis, functionalization and characterization

Amino functionalized homemade magnetic nanoparticles were prepared by chemical co-precipitation method as described previously with slight modifications (Kouassi et al. 2005, Kouassi et al. 2006). Briefly, ferrous chloride and ferric chloride in a 1/2 molar ratio were mixed with deionized water and then mixed with 10wt % of amino-propyl tri-methoxysilane (APMS) with slight heating. After 5 minutes ammonium hydroxide was added drop-wise to the above mixture and the pH adjusted

to 12. The heating was turned off and stirring continued for another 30 minutes. The resulting particles were washed thoroughly with ethyl alcohol 70% and deionized water to remove ammonia traces. The particles were then removed by a magnet and dried in vacuum oven overnight at 50 C. Size and morphology of the magnetic nanoparticles were characterized by scanning electron microscope (SEM, LEO SUPRA 55; Carl Zeiss AG, Oberkochen, Germany).

Conjugation of HURP and/or HRG RNA specific probes to the amino functionalized magnetic nanoparticles was carried out as described previously in chapter 3. The conjugation process was based on a hetero bi-functional cross linker (*3- maleimido benzoic acid N-hydroxyl succinimide, MBS*) that has an NHS ester at one end which reacts with primary amine groups on the magnetic nanoparticles forming stable amide bonds, the other end has a maleimide group that reacts with sulfhydryl conjugated probes forming a stable thioether linkage.

4.3.3 Synthesis and characterization of Gold Nanoparticles

Spherical gold colloid was prepared using citrate reduction method as described elsewhere (Hill et al. 2006). Briefly, an aqueous solution of hydrogen tetra chloroaurate (III) ($\text{HAuCl}_4 \cdot 3\text{H}_2\text{O}$) (1mM) (99.99% Sigma Aldrich, Germany) was brought to reflux and stirred followed by a quick addition of 1% tri sodium citrate solution. The solution color changed from yellow to wine red. The solution was then refluxed for an additional 15 min and left to cool at room temperature. The resulting spherical gold nanoparticles were filtered using a 0.25 μm syringe filter (Sigma), and transferred into a clean storage glass bottle. Size and distribution of the morphology of the AuNPs was characterized using field emission scanning electron microscopy (Model: Leo Supra 55). One drop of the AuNPs solution was added onto a silicon slide that was allowed to air dry before examination. The particle mean diameter was measured by dynamic light scattering (DLS, Malvern Instruments, UK). The λ_{max} for AuNPs was detected by scanning the colloidal AuNPs from 400-700 nm using UV spectrophotometer (Jenway 6800).

4.3.4 Total RNA extraction

Total RNA extraction procedures were done at Ain Shams University, Faculty of Medicine, laboratories, Cairo, Egypt. The detailed procedures are described below.

4.3.4.1 Urinary Bladder Cancer

Voided urine samples were obtained before cystoscopy and washed in phosphate-buffered saline (PBS, pH 7) and centrifuged at 1000 times gravity for 10 minutes. A portion of the pellet was taken for cytology examination and another portion was immediately processed for RNA extraction using Tri Fast kit (PeQ Lab Biotechnologie GmbH Corporation) according to the manufacturer's instruction (Sambrook J et al. 1989, Eissa et al. 2003). The extracted RNA was divided into two parts; the first part was used for detection of HURP by RT-PCR; while second part was further purified by magnetic nanoparticles.

4.3.4.2 Breast Cancer

After primary surgery, a representative part of the tumor tissue was immediately frozen and stored at -80 freezer for RNA extraction (Qiagen, Hilden, Germany). Total RNA was purified with TriFast™ (PeQ-Lab Biotechnologie GmbH Corporation) according to the manufacturer's instructions (Sambrook J et al. 1989, Hummon et al. 2007).

4.3.5 HURP & HRG RNA purification by MNP functionalized by a target specific probe

Hundred micro-liters of functionalized magnetic nanoparticles was taken and washed twice with the assay buffer (10 mM phosphate buffer, 150 mM sodium chloride, pH= 7.4) and then re-suspended in 50 µL assay buffer and mixed well with about 40 µL of the target and heated at 70°C for 2 min. The mixture was shaken for 45 min to allow hydrogen bond formation between the immobilized probe and target RNA to achieve proper capture. An external magnet was then placed at the bottom of the tube until the solutions were clear. The supernatant was then removed and the particles were washed twice with washing buffer (60 mM potassium acetate, 10 mM Tris-HCl, 60% ethanol, pH=7.5). The supernatant was removed between each

wash with the help of a magnet. Elution was done by adding 40 μ L deionized water, and heated at 95°C for 2 min. The tubes were placed on magnet until all solutions were clear and the eluted target mRNA (HURP or HRG) in the supernatant was transferred to new tube.

4.3.6 RT-PCR for HURP and HRG RNA

RT-PCR reactions were done in Hybaid thermal cycler (Thermo Electron [formerly Hybaid] Waltham, MA) using the Qiagen One Step RT-PCR Kit. Hepatoma up regulated (HURP) protein RNA primers were: sense primer: 5'-CCCATCTTCCTTGAGAAAG-'3, antisense primer: 5'-AGG AGA CAT CAA GAA CAT GC-'3 (Accession NM_001146015). The thermal cycling protocol was 42°C for 60 min, 95°C for 15 min, and 30 cycles of 1 min at 94°C, 1 min at 50°C, and 1 min at 72°C, and final extension step at 72°C for 10 min.

On the other hand, Histidine-rich glycoprotein (HRG) primers were: sense primer: 5'-GATCATCATCATCCCCACAAG-'3, antisense primer: 5'-GGGTACAAGGTCCATAGTC-'3, (accession NM_000412.2) (Sabbatini et al. , Koide et al. 1986). The thermal cycling protocol was 50°C for 30 minutes, 95°C for 15 minutes, and 30 cycles of 1 min at 94°C, 1 min at 50°C, and 1 min at 72°C, and final extension step at 72°C for 10 min.

Amplicons of both targets were run on 2% agarose gel electrophoresis. The quality of RNA was checked by amplification of c-DNA for β -actin to ensure successful completion of the c-DNA step using the primer pair; sense 5'-AGC GGG AAA TCG TGC GTG -3', and antisense 5'-CAG GGT ACA TGG TGC C -3' (Accession NM_001017992.2), (Smith et al. 2001).

4.3.7 The developed colorimetric AuNPs based assay for target RNA detection

One antisense primer (oligotargeter) targeting the purified RNA (HURP or HRG) was mixed with a NaCl solution to prepare the hybridization buffer. Different salt and primer concentrations were tested to determine their optimal concentrations for the assay. The hybridization buffer contained NaCl and anti-sense primer with final concentrations of 0.42 M and 9 μ M, respectively. The assay was done by mixing 5 μ L hybridization buffer, 5 μ L sample RNA and 20 μ L AuNPs. The color change was observed within 1 min.

4.3.8 Detection Limit Measurement

Serial dilutions of RNA sample of known concentration were tested using the AuNPs assay to determine its detection limit. RNA sample of known concentration (concentration was measured spectrophotometrically), was taken and serial dilutions for the sample were done, and the RNA was detected in the above mentioned dilutions using the developed AuNPs

4.3.9 Statistical Analysis

Univariate analyses were performed using a Chi square test of association of categorical variables. Sensitivity, specificity, positive predictive value (PPV), negative predictive value (NPV), and accuracy were calculated according to standard statistical methods. All analyses were performed using Statistical Package for the Social Sciences software (SPSS Inc., Chicago, IL).

4.4 Results

4.4.1 Size Distribution of amine functionalized magnetic nanoparticles

A scanning electron microscope image of the prepared magnetic nanoparticles (Figure 2), was analyzed using the 1.41 image J. software package (Wayne Rasband, National Institutes of health, USA. [Http://:rsb.info.nih.gov/ij/Java1.6.0_05](http://rsb.info.nih.gov/ij/Java1.6.0_05)). The particles were well dispersed and their mean diameter was $95 \text{ nm} \pm 5 \text{ nm}$. The magnetic nanoparticles were functionalized by amino groups through the reaction of the nanoparticles with 3- aminopropyl tri-methoxysilane (APMS) by a silanization reaction (Mikhaylova et al. 2004, Yamaura et al. 2004b, Yang et al. 2009b), that includes hydrolysis and condensation steps, the detailed reaction can be found in (Yamaura et al. 2004b).

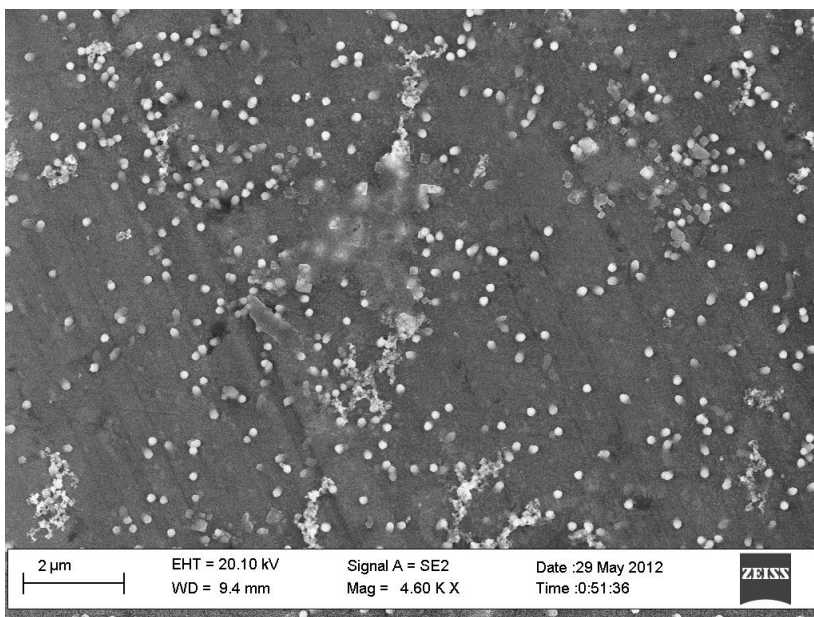
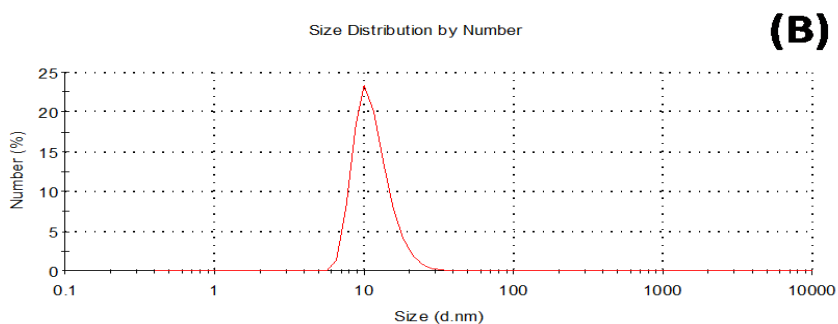
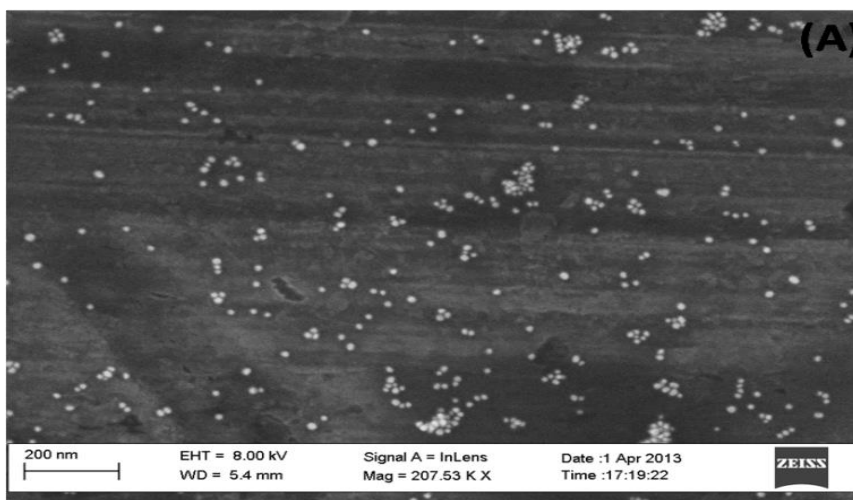


Figure 2. Scanning electron monograph (SEM) of the prepared magnetic nanoparticles, functionalized with amino groups

4.4.2 Size distribution and surface Plasmon band of the prepared AuNPs

Figure 3A shows the SEM image of the prepared gold nanoparticles. The mean particles diameter of the prepared AuNPs was found to be about $13 \text{ nm} \pm 2 \text{ nm}$ (Figure 3B). Figure 3C shows the absorption spectrum of the prepared AuNPs that displayed a single peak in the visible region with a λ_{max} at 518–520 nm which is typically the SPR of the AuNPs of this size (Hill et al. 2006, Rosi et al. 2006).



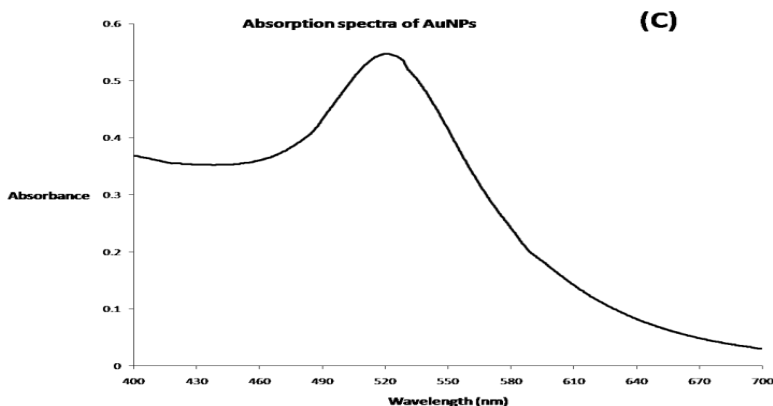


Figure 3. (A) Scanning electron monographs of the prepared AuNPs. (B) Size distribution of AuNPs and (C) the absorption spectra of AuNPs showing λ_{\max} at 518-520 nm.

4.4.3 RT-PCR for HURP and HRG

RT-PCR of HURP and HRG RNA was done as described in the methods section. RT-PCR of HURP yielded an amplicon of 258 base pair (Figure 4A), while that of HRG yielded an amplicon of 404 bp (Figure 4B). Amplification of c-DNA for β -actin yielding an amplicon of 309 bp. Introduction of an additional purification step using the functionalized magnetic nanoparticles improved the sensitivity of the HURP RT-PCR from 64% to 84%, while the HRG RT-PCR sensitivity was improved from 71.7% to 80%. Moreover, the specificity of the HURP RT-PCR was improved from 90% to 94% after magnetic purification, while no change in specificity occurred in the HRG RT-PCR.

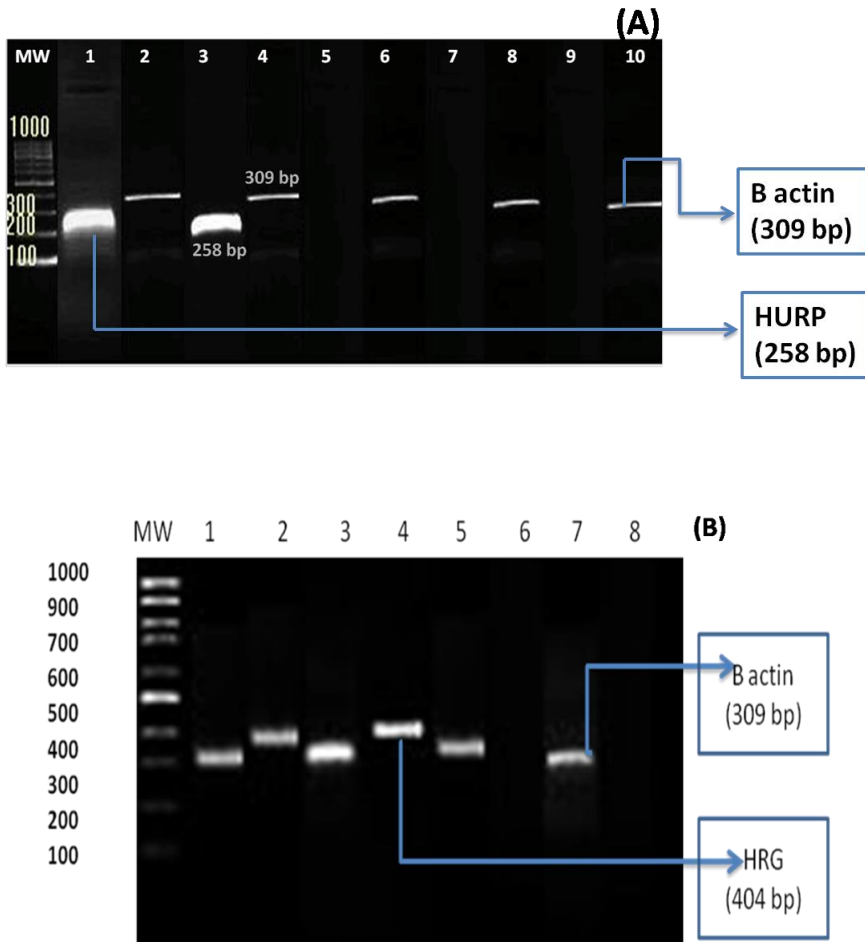


Figure 4. (A) Semi-quantitative RT-PCR of the urinary HURP and beta actin RNA using agarose gel electrophoresis that produced bands with 258 and 309 bp respectively. Lane 1-4: urine from bladder cancer patients, Lanes 5-8 urine from benign genitourinary conditions and Lane 9-10: urine from healthy normal individuals. **(B)** RT PCR analysis for Breast tissue HRG showing 309 bp. Lanes 1-4: biopsy from breast cancer patients showing positive HRG, Lanes 5-6: biopsy from benign breast conditions showing positive beta actin bands and negative HRG. Lanes 7-8: biopsy from normal breast showing positive beta actin bands and negative HRG. Lane MW: molecular weight ladder standard (100 bp).

4.4.4 AuNPs assay: development and optimization

The color of AuNPs colloidal solution is affected by three main factors which should be adequately optimized; those are the concentrations of NaCl, AuNPs, and ss DNA (primer) used. The final NaCl concentration was 0.07 M, while the final primer concentration was 1.5 μ M in the total assay volume, for 10 nM AuNPs which was sufficient to stabilize the AuNPs and prevent their NaCl induced aggregation. The sample was mixed with the hybridization buffer and then colloidal solution of AuNPs was added to the mixture, and the color change was observed within 1 min. The positive samples, had the color changed from red to blue, while, the color remained red in the negative samples (Figure 5).

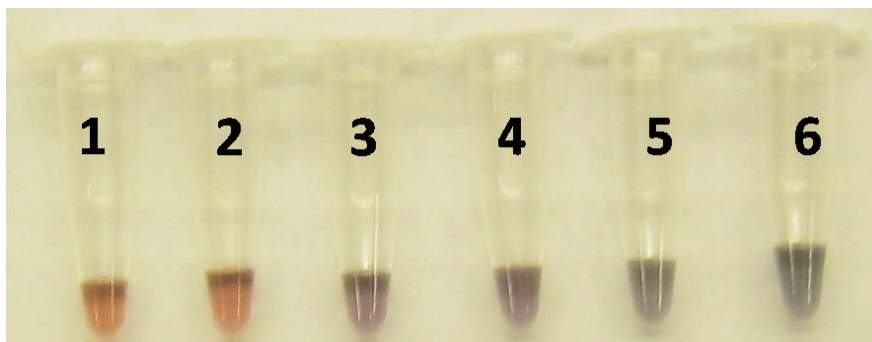


Figure 5: Unmodified AuNPs assay. The color of the colloidal AuNPs solution changed from red to blue within 2 minutes in positive samples (tubes 3-6), while in negative samples (tubes 1-2), the AuNPs color solution remains red.

4.4.5 AuNPs assay: performance characteristics

HURP RNA was detected in RNA extracted from urine samples by the developed AuNPs assay, 45 malignant samples out of 50 were positive, with a sensitivity of 90%. On the other hand, all 25 normal samples were negative, while 22 out of 25 benign samples were negative and 3 samples were false-positive. The specificity of the assay was 94%. The lower detection limit of the HURP RNA AuNPs assay was 2.4 nanomole/L. On the other hand, HRG RNA detection in tissues done by the developed AuNPs assay has a sensitivity and specificity of 90%, with a detection limit of 1.5 nmol/L. The optimization resulted in a reproducible and accurate assay for the direct detection of unamplified RNA targets in the samples.

4.5 Discussion

Discovery of new tumors biomarkers is a highly dynamic research field and aims at achieving highly sensitive and specific biomarkers for early cancer diagnostics and prognostics. Advances in genomics, proteomics and epigenetics, in addition to cancer cell research, have led to a deluge of novel biomarkers for cancer diagnosis and prognosis. However, many of these novel biomarkers have not yet been implemented in practice guidelines due to the lack of sufficient validation required to attain a significant level of evidence (Swellam et al. 2004, Cecchini et al. 2012, Smith et al. 2013, Xylinas et al. 2014). The unique properties of the emerging nanoparticles, such as gold and magnetic nanoparticles, made them attractive and promising for applications in molecular diagnostics, and they are showing great promise in the development of assays that are simple, rapid, sensitive, specific and cost-effective. Moreover, the National Cancer Institute is engaged in efforts to harness the power of nanotechnology to radically change cancer diagnosis and treatment (Azzazy et al. 2006). The magnetic separation of nucleic acids has several advantages compared to other techniques used for the same purpose. Nucleic acids can be purified from crude sample materials such as blood and tissue homogenates (Thaxton et al. 2005). Magnet particles can be removed relatively easily and selectively, even from viscous sample suspensions, by adjusting the magnetic properties of the solid materials. In fact, magnetic separation is the one of the best attainable method for the recovery of small particles (diameter approx. 50–1000nm) in the presence of biological debris, and high efficiency magnetic separation can be used for large-scale purifications to detect ultra-low concentrations of tissue-based genetic biomarkers (Franzreb et al. 2006). This is due to many reasons for example, magnetic nanoparticles at this size scale have high surface area so, they can capture more target. Also, its surface can be easily modified with many capping agents like streptavidin, amino and thiol groups. Moreover, magnetic nanoparticles could be easily separated from the sample after the purification and/or the washing steps by simply applying external magnet so, separation time is saved, and also effort if compared for example to the silica based columns used in purification of nucleic acids that need many centrifugation steps throughout the purification steps.

Magnetic nanoparticles are currently used commercially in nucleic acid and proteins purification, and are produced by many reagents

companies, such as Invitrogen and Miltenyi Biotec GmbH. However, the commercialized particles are expensive, have a low stability, and usually tend to aggregate and precipitate. We have succeeded in avoiding these drawbacks of the commercial magnetic nanoparticles, as our magnetic particles are stable, easy to synthesize, have a mono-distribution, and, most important, have a low preparation cost. In the current chapter, we report two nanoparticles (magnetic and gold nanoparticles) for the direct detection of unamplified HURP and HRG RNA for urinary bladder and breast cancers diagnosis and/or prognosis, respectively. The HURP RNA, as a urinary bladder cancer biomarker, was detected in urine samples by the developed AuNPs-based assay. Moreover, RT-PCR of HURP RNA was performed before and after the developed magnetic HURP RNA purification. All the methods were compared to the standard cystoscopy and cytology methods, and the data is shown in Table 1. The developed AuNPs assay detected HURP RNA in 90% of the urine samples of malignant cases and in 12% of the benign cases, and yielded negative results for the control samples. The combination of the developed AuNPs assay with urine cytology improved the sensitivity of urine cytology from 64% to 100%, even in low-grade and superficial bladder cancer, which confirms the possibility of using the developed assay in the early detection of urinary bladder cancer. Also, HURP RNA was detected using conventional RT-PCR, with a sensitivity and specificity of 63% and 90%, respectively. After the magnetic purification step, the sensitivity and specificity of the HURP RT-PCR assay improved to 85% and 94%, respectively.

Development and evaluation of gold nanoparticles assays for direct detection of urinary bladder and breast cancer biomarkers

Table 1: Clinical characteristics of the assay used for detection of urinary HURP RNA and cytology in superficial (Stage 0+1) and grade 1 bladder cancer patients. Abbreviations: AuNPs: gold nanoparticles, HURP: Hepatoma Up regulated protein, MP: magnetic nanoparticles, RT-PCR: reverse transcriptase polymerase chain reaction.

Parameter	Sensitivity	Specificity	NPV	PPV	Accuracy
Bladder cancer group (n=50)					
Cytology	62%	98%	72%	96%	80
RT-PCR before MP purification	64%	90%	71.4%	86.4%	77%
RT-PCR after MP purification	84%	94%	85%	93.3%	89%
HURP by nano assay	90%	94%	90.3%	93.3%	92%
RT-PCR before MP purification+ cytology	86%	90%	86.5%	89.9%	88%
RT-PCR after MP purification +cytology	100%	94%	100%	94.3%	97%
HURP by nano assay+ cytology	100%	94%	100%	94.3%	97%
Superficial bladder cancer (stage 0 &1)(n=28)					
Cytology	57.1%	98%	80.3%	94.4%	83.3%
RT-PCR before MP purification	64%	90%	81.8%	78.2%	80.7%
RT-PCR after MP purification	82.1%	94%	90.3%	88.4%	93.3%
HURP by nano assay	89.3%	94%	94%	89.2%	92.3%
RT-PCR before MP purification+ cytology	89.3%	90%	93.75%	83.3 %	89.7%
RT-PCR after MP purification +cytology	100%	94%	100%	90.3%	96%
HURP by nano assay+ cytology	100%	94%	100%	90.3%	96%
Grade 1 bladder cancer (n=8)					
Cytology	50%	98%	92.4%	80%	91.3%
RT-PCR before MP purification	62.5%	90%	93.75%	50%	86.2%
RT-PCR after MP purification	87.5%	94%	97.9%	70%	93.1%
HURP by nano assay	87.5%	94%	97.9%	70%	93.1%
RT-PCR before MP purification+ cytology	75%	90%	95.7%	54.5%	87.9%
RT-PCR after MP purification +cytology	100%	94%	100%	72.7%	94.8%
HURP by nano assay+ cytology	100%	94%	100%	72.7%	94.8%

Meanwhile, HRG RNA was detected in breast tissues of malignant, benign and normal individuals using the developed AuNPs assay. The assay had a sensitivity and specificity of 90%, with a detection limit of 1.5 nmol/L. Moreover, HRG RNA was detected using conventional RT-PCR. The sensitivity and specificity of RT-PCR were 71.7% and 93%, respectively. Upon the introduction of the magnetic purification before the RT-PCR, the sensitivity of the latter increased to 80%, which is still less than the proposed AuNPs assay, as shown above. The evaluation and comparison of the AuNPs results with RT-PCR and the histopathology finding, in addition to its relation to the cancer grade, are summarized in Table 2. As shown below in table 2, the developed AuNPs' assay sensitivity has been increased in the three stages and grades of the malignant groups, in addition to the different subtypes of the breast cancer. The data obtained in this study, may consider HRG RNA expression as an evolving independent biomarker prognostic factor for breast cancer that can be detected using the developed gold nanoparticles assay. Our results agreed with bioinformatics analysis of HRG transcript expression using data from GOBO tool (Ringner et al. 2011) that utilizes Affymetrics gene expression data collected from 1,881 breast cancer patients with associated stage, grade, nodal status and intrinsic molecular classification based on the paradigm first reported by the Perou Laboratory (Perou et al. 2000). All the above mentioned data are consistent with our findings that HRG expression is significantly increased in breast cancer and it is highly related to its progression. The role of HRG as an emerging prognostic tumor marker for breast cancer detection has been studied and reported by other research groups which reported that HRG induces progression of breast cancer cells (Simantov et al. 2001, Jones et al. 2005, Place et al. 2011, Rivas et al. 2012). In most of these studies, the authors have shown that HRG can modulate angiogenesis, the latter is a central step in the transition of benign tumors to malignant one. They also mentioned that HRG promote angiogenesis in breast cancer. Furthermore, in a PhD dissertation (Jones 2009) the author used proteomic mass spectrometry approaches for identifying and discovery of new biomarkers for breast cancer. The author stated that there is directly proportional relation between the HRG protein and the breast cancer especially in late stage (stage 4) breast cancer and obese patients.

Our primary focus was targeted on the evaluation of nano-molecular assays to validate the tissue expression of HRG RNA as a potential biomarker for breast cancer prognosis. Moreover, it is hoped that incorporation of nano-molecular diagnostics into the routine management of breast cancer patients will result in better disease classification, as well as assistance in discovery of targeted treatment. Such objectives are more likely to bring us to our ultimate goal, which is the personalized management of breast cancer.

Development and evaluation of gold nanoparticles assays for direct detection of urinary bladder and breast cancer biomarkers

Table 2: Sensitivity, Specificity, PPV, NPV & Accuracy of the assays used for breast tissue HRG RNA detection in different grades, stages and subtypes of Breast cancer. PPV: Positive Predictive Value, NPV: Negative Predictive Value, MNP: Magnetic Nanoparticles, AuNPs: Gold nanoparticles

Parameter	Sensitivity	Specificity	PPV	NPV	Accuracy
Breast cancer (n=60)					
RT-PCR before MNP purification	71.7%	93.33%	95.56 %	62.22 %	78.89%
RT-PCR after MNP purification	80%	93.33%	92.3%	72.7%	86.67%
AuNPs assay	90%	90%	94.7%	82.5%	91.11%
Early stage (0+ I) (n=26)					
RT-PCR before MNP purification	84.6%	93.33%	84.6%	93.33 %	90.7%
RT-PCR after MNP purification	88.5%	93.33%	85%	94.9%	91.86%
AuNPs assay	92.3%	90%	80%	96.4%	90.7%
stage 2 (n=28)					
RT-PCR before MNP purification	75%	93.3%	91.3%	80%	84.5%
RT-PCR after MNP purification	78.6%	93.3%	91.3%	90.3%	90.7%
AuNPs assay	85.7%	90%	88.9%	87%	87.9%
stage 3 (n=6)					
RT-PCR before MNP purification	33.3%	93.3%	50%	87.5%	83.3%
RT-PCR after MNP purification	50%	93.3%	60%	90.3%	86%
AuNPs assay	100%	90%	66.7%	100%	91.7%
Grade 1 (n=12)					
RT-PCR before MNP purification	83.3%	93.33%	71.4%	96.6%	91.67%
RT-PCR after MNP purification	91.6%	93.33%	73.3%	98.2%	93%
AuNPs assay	91.67%	90%	64.7%	98%	90.2%
Grade 2 (n=38)					
RT-PCR before MNP purification	68.4%	93.3%	92.8%	70%	79.4%
RT-PCR after MNP purification	76.3%	93.3%	93.5%	75.5%	83.3%
AuNPs assay	86.8%	90%	91.7%	84.3%	88.2%
Grade 3 (n=10)					
RT-PCR before MNP purification	70%	93.3%	77.7%	90.3%	87.5%
RT-PCR after MNP purification	80%	93.3%	80%	93.3%	90%
AuNPs assay	100%	90%	76.9%	100%	92.5%

Development and evaluation of gold nanoparticles assays for direct detection of urinary bladder and breast cancer biomarkers

Subtype: Luminal A (n=27)					
RT-PCR before MNP purification	81.5%	93.3%	91.7%	84.8%	87.7%
RT-PCR after MNP purification	88.9%	93.3%	92.3%	90.3%	91.2%
AuNPs assay	88.9%	90%	88.9%	90%	89.4%
Subtype: Luminal B (n=11)					
RT-PCR before MNP purification	45.5%	93.3%	71.4%	82.3%	80.5%
RT-PCR after MNP purification	45.5%	93.3%	71.4%	82.3%	80.5%
AuNPs assay	81.8%	90%	75%	93%	87.8%
Subtype: Triple negative (n=15)					
RT-PCR before MNP purification	80%	93.3%	85.7%	90.3%	88.9%
RT-PCR after MNP purification	93.3%	93.3%	87.5%	96.6%	93.3%
AuNPs assay	100%	90%	83.3%	100%	93.3%
Subtype: Her-2 overexpression (n=7)					
RT-PCR before MNP purification	71.4%	93.3%	71.4%	93.3%	89.2%
RT-PCR after MNP purification	71.4%	93.3%	71.4%	93.3%	89.2%
AuNPs assay	85.7%	90%	66.7%	96.4%	89.2%

In conclusion, we propose to use an unmodified AuNPs-based assay for the direct detection of unamplified HURP RNA in clinical urine samples and unamplified HRG RNA in breast tissue samples for the early diagnosis and prognosis of urinary bladder and breast cancers respectively. Both assays are sensitive, specific, simple, rapid, detect the target RNA in early-stage tumors and inexpensive. Moreover, we have introduced a magnetic nanoparticles purification step to increase the purity of the target RNA that will be used in downstream applications, such as the AuNPs assay or RT-PCR. Similar platforms could be developed for the detection of other cancer biomarkers, thereby making cancer diagnosis and screening of high-risk individuals more affordable and accessible to large patient populations.

5 Dissertation Discussion

The focus of this thesis was the development of novel techniques for the direct detection of unamplified nucleic acids in clinical specimens using nanoparticles. Gold and magnetic nanoparticles were the main nanoparticles used in our studies. It is obvious that the introduction of AuNPs and magnetic nanoparticles for the direct purification & detection unamplified of nucleic acids directly from clinical samples will dramatically enhance the detection parameters such as: speed (lower time), high sensitivity, high specificity, simplicity and the most important the total cost of the assay. Several methods have been developed for the detection of nucleic acids using AuNPs by many groups. Despite, the high sensitivity and specificity of these detection methods, more work still needs to be applied to real clinical specimens. In this thesis, our main focus was taking the advantages of AuNPs in nucleic acid detections, and magnetic nanoparticles for nucleic acids purification from the samples. We have used the unmodified negatively charged and positively AuNPs method for the development of colorimetric assays. The developed assays have been applied to detect of HCV RNA directly from serum samples, the detection of HURP RNA from urine samples as a urinary bladder cancer biomarker and finally for the detection of HRG RNA in tissues as a prognostic biomarker for breast cancer. The assays we developed have been optimized and compared to the currently used methods for the targets detection and promising results have been obtained.

5.1 Unmodified AuNPs in HCV RNA detection in serum samples

Unmodified AuNPs detection of nucleic acids was first developed (Li et al. 2004a, Li et al. 2004b). It is based on the adsorption of the small single stranded DNA (ssDNA) onto the negatively charged AuNPs that in turn increases their negative charge to prevent salt induced aggregation, while double stranded DNA (ds DNA) doesn't adsorb onto the AuNPs surface because the repulsion between their negatively charged phosphate backbone and the negatively charged AuNPs. When AuNPs are added to a saline solution containing the target nucleic acid and its complementary unlabeled oligotargeter (ss DNA), aggregation of AuNPs occurs and their color changes from red to blue, because the oligotargeter is not free to be

adsorbed onto the AuNPs surface to stabilize the nanoparticles against aggregation induced by the saline in the solution. On the other hand, in the absence of the target, the oligotargeter is free to stabilize the AuNPs colloidal solution against salt induced aggregation and the solution color remains red. In our study, we have used this principle for the development of a colorimetric assay for the direct detection of HCV RNA extracted from clinical serum samples. The main problem that we faced in developing this assay was working on serum samples of HCV infected patients. The serum may contain some cell free DNA which are small fragments of DNA, in addition to nucleoproteins (Sisco 2001). These short fragments of nucleic acids may interfere with the assay and stabilize the free AuNPs leading to false negative outcome. Therefore, many available commercial kits have been tried for HCV RNA extraction from serum, and we conclude that any available commercial extraction kit for total RNA purification can be used, but that it should be employed with a DNase step to remove the DNA molecules that could be in the final elution to prevent the generation of false negative results. The assay components are: AuNPs, the oligotargeter (ssDNA specific to HCV RNA), a sodium chloride solution, and the viral RNA (target). The first 3 components should be adequately optimized regarding their concentrations and/or amount, for example: if the concentration of the oligotargeter is very high and the target concentration is low, there will be enough oligotargeter in the solution to be adsorbed onto the AuNPs and prevent the aggregation and false results obtained, after hybridization of the oligotargeter with its complementary HCV RNA and vice versa. Consequently, the assay was performed by adding hybridization buffer (oligotargeter and sodium chloride with final concentrations of 1 μ M & 0.08M respectively) to the sample, followed by AuNPs to a final concentration of 10 nM and the color change was observed within 2 minutes. The assay has a sensitivity and specificity of 92% & 88.9% respectively, and a detection limit of 50 RNA copies/reaction. The proposed assay has many advantages as: (i) there is no need for RNA amplification. (ii) It is suitable for tracking an active infection even at low viral titers; (iii) It has acceptable sensitivity and specificity and, (iv) a short turnaround time (v) It is cost-effective as no expensive equipment is needed for the detection. The sensitivity and specificity could be improved by enhancing the purity of the extracted RNA by applying for example a specific capture of HCV RNA using magnetic nanoparticles. Also, it could be developed to be a quantitative test

by adding spectrophotometric quantification of the color outcome against a standard curve. Moreover, the assay could be easily optimized to detect SNPs in the HCV RNA, by proper selection of the oligotargeter and its annealing temperature. This will be essential when applied onto HCV genotyping which depends mainly on the detection of SNPs within the viral RNA. To our knowledge, this is the first study done using unmodified AuNPs for the direct detection of unamplified HCV RNA from serum samples, and upon fine tuning and optimization, it may be competitive with the available Hepatitis C Virus commercial immuno-assays and the RT-PCR methods. Moreover, it could be used in HCV screening especially in the early (acute) infection phase where the immuno-assays are inadequate, as it takes about 70 days for the HCV antibodies to appear in the blood, while the HCV RNA is detected in the serum within 21 days (Moller et al. 2003, Yoshizawa 2004, Fabris et al. 2008).

5.2 Cationic AuNPs in detection of HCV in serum samples

Cationic AuNPs have been used for diagnostic molecular assays, for example a microarray assay (solid support) for gene expression analysis using positively charged AuNPs (Sun et al. 2005). A colorimetric assay has also been developed for the detection of HIV in clinical samples using cationic gold nanorods and label free probe DNA (He et al. 2008). In chapter 3, we report the use of cationic gold nanoparticles for the detection of HCV RNA extracted from clinical serum samples. To increase the specificity of the assay, we have utilized a specific HCV RNA extraction using homemade magnetic nanoparticles functionalized with HCV RNA specific oligonucleotide. The assay is based on adding cationic AuNPs onto the sample, in the presence of phosphate buffer. In the presence of the target nucleic acid, the cationic AuNPs were aligned onto the negatively charged phosphate backbone of the target nucleic acid, the presence of phosphate buffer increases the aggregation of the cationic AuNPs in the case of positive samples only, where the phosphate ions bind to the AuNPs aligned onto the target RNA, then another row of AuNPs attached to the phosphate ions and then aligned to another RNA molecule and so on, until several layers of (RNA/AuNPs/phosphate ions/AuNPs/second RNA), and aggregation occurs changing the colloidal solution of AuNPs from red to blue. On the other hand, in the absence of any nucleic acid in the sample, the AuNPs are far from each

other and in the same time the amount of phosphate ions in the solution is insufficient for the nanoparticles to aggregate. To our knowledge, we were the first to propose and use cationic AuNPs in direct detection of unamplified RNA from serum clinical samples. The scanning electron microscope images obtained confirmed the principle we proposed. The introduction of a specific magnetic nanoparticles based extraction step prior to the assay increases the purity of the sample and ensures the presence of only the HCV RNA target in the sample. The assay could be utilized for the detection of any nucleic acid target, after specific extraction of the target nucleic acid. In conclusion, we report for the first time the development of colorimetric solution based assay using cationic nanoparticles for the direct detection of HCV RNA from clinical samples, the assay has sensitivity and specificity more than 95%, and a detection limit of 15 IU/ml. Moreover, the color obtained in the assay is very stable and does not change. It could be improved easily to become a quantitative assay for viral load measurements. Moreover the turnaround time of the assay including the RNA extraction is about 75 minutes, which is almost one third the time needed by standard Real time RT-PCR, and the cost of the assay does not exceed US\$10. The assay could be easily modified to be fully automated and can be used in routine screening and/or diagnosis of HCV RNA or any other nucleic acid target in solution after proper extraction.

5.3 Unmodified AuNPs in tumor marker detection

A major clinical need in cancer research is the development of non-invasive, simple, sensitive, specific and cheap methods for the early diagnosis and prognosis of tumors. Moreover, identifying novel biomarkers is a quickly growing field due to the accumulation of information from many disciplines as epigenetics, proteomics, transcriptomics, and genomics leading to the discovery of novel potential biomarkers for different tumors. We have tried the unmodified AuNPs assay on two emerging biomarkers: the first was Hepatoma Up Regulated Protein (HURP) RNA in urine samples for urinary bladder cancer diagnosis, and the second was Histidine-Rich Glycoprotein (HRG) in breast tissue for breast cancer prognosis. In these two independent studies, each biomarker RNA was extracted from clinical specimens, and then purified by our homemade magnetic nanoparticles for obtaining pure target. Then, the unmodified AuNPs assay was optimized and the results obtained were compared to the conventional RT-PCR method

and the standard methods used in tumors detection. For the detection of HURP RNA as a novel biomarker for urinary bladder cancer diagnosis, the urine samples were collected from patients, benign and normal individuals. The developed colorimetric assay has a sensitivity and specificity of 88.5% and 94% respectively, with a detection limit of 2.5 nmol/L. RT-PCR was done for all the samples before and after magnetic extraction step, the sensitivity of RT-PCR was increased from 64% to 84%. Upon combining, the nano assay with urine cytology improved the sensitivity of the standard cytology method, from 62% to 100%. Thus a colorimetric AuNPs based assay has been developed for the direct detection of HURP RNA in urine samples for the diagnosis of urinary bladder cancer even in the low grade and superficial bladder cancer. The assay is sensitive, specific, rapid and cost effective and non-invasive and could be developed easily for detecting SNPs by proper optimization of the oligotargeter-target annealing conditions. On the other hand, HRG RNA was detected in breast tissues from malignant, benign and normal individuals. The developed assay has a sensitivity and specificity of 90%, with a detection limit of 1.5 nmol/L. RT-PCR was done for all the samples before and after the magnetic extraction step. The RT-PCR sensitivity increased from 71.1% to 80%. Also, the sensitivity of the assay was 92.3% at the early stage cancer cases, while it was 84.6% using the conventional RT-PCR method. Herein, we are proposing a novel colorimetric assay for the detection of HRG RNA in breast tissues for prognosis and early diagnosis of breast cancer. In conclusion, Current molecular diagnostic methods have come a long way towards better, faster, cost-effective and reliable assays. Nevertheless, most are still time consuming and require expensive equipment (e.g. Real-time PCR, DNA sequencing), and/or reagents (e.g. fluorescent dyes, DNA polymerases), highly specialized laboratories and highly trained personnel. In the end, all these factors restrict their use at the point of care (POC) or in a larger number of laboratories, especially in countries with fewer resources available to healthcare. Developing novel assays based on nanoparticles will allow decreasing the costs associated with genetic tests with higher sensitivity and specificity, thus making them available to a broader population worldwide.

6 Bibliography

Alharbi, K. et al. (2014). "Role and implications of nanodiagnostics in the changing trends of clinical diagnosis." *Saudi J Biol Sci* 21(2): 109-117.

Ambrosi, A. et al. (2010). "Enhanced gold nanoparticle based ELISA for a breast cancer biomarker." *Anal Chem* 82(3): 1151-1156.

Amyn, S. et al. (2009). "Synthesis, properties, and applications of magnetic iron oxide nanoparticles." *Progress in Crystal Growth and Characterization of Materials* 55(1-2): 22-45.

Arnold, M. et al. (2013). "Recent trends in incidence of five common cancers in 26 European countries since 1988: Analysis of the European Cancer Observatory." *Eur J Cancer*.

Atrah, H. et al. (1996). "Hepatitis C virus seroconversion by a third generation ELISA screening test in blood donors." *J Clin Pathol* 49(3): 254-255.

Avritscher, E. et al. (2006). "Clinical model of lifetime cost of treating bladder cancer and associated complications." *Urology* 68(3): 549-553.

Azzazy, H. et al. (2006). "Nanodiagnostics: a new frontier for clinical laboratory medicine." *Clin Chem* 52(7): 1238-1246.

Baptista, P. et al. (2005). "Colorimetric detection of eukaryotic gene expression with DNA-derivatized gold nanoparticles." *J Biotechnol* 119(2): 111-117.

Baptista, P. et al. (2007). "Gold nanoparticles for the development of clinical diagnosis methods." *Anal Bioanal Chem*.

Baptista, P. et al. (2008). "Gold nanoparticles for the development of clinical diagnosis methods." *Anal Bioanal Chem* 391(3): 943-950.

Baptista, P. et al. (2006). "Gold-nanoparticle-probe-based assay for rapid and direct detection of *Mycobacterium tuberculosis* DNA in clinical samples." *Clin Chem* 52(7): 1433-1434.

Bartenschlager, R. et al (2004). "Novel insights into hepatitis C virus replication and persistence." *Adv. Virus Res.* 63: 71-80.

Bartlett, J. M. et al. (2010). "Predictive markers of anthracycline benefit: a prospectively planned analysis of the UK National Epirubicin Adjuvant Trial (NEAT/BR9601)." *Lancet Oncol* 11(3): 266-274.

Bartolome, J. et al. (2007). "Ultracentrifugation of serum samples allows detection of hepatitis C virus RNA in patients with occult hepatitis C." *J Virol* 81(14): 7710-7715.

Belloni, J. (1996). "Metal nanocolloids." *Current opinion in colloid interface science* 1(2): 184-196.

Bhambure, R. et al. (2009). "Extracellular Biosynthesis of Gold Nanoparticles using *Aspergillus niger*- its Characterization and Stability." *Chemical Engineering & Technology* 32(7): 1036-1041.

Bhatt, A. N. et al. (2010). "Cancer biomarkers - current perspectives." *Indian J Med Res* 132: 129-149.

Boyer, N. et al. (2000). "Pathogenesis, diagnosis and management of hepatitis C." *J Hepatol* 32(1 Suppl): 98-112.

Brown, K. et al. (1998). "Hydroxylamine Seeding of Colloidal Au Nanoparticles in Solution and on Surfaces." *Langmuir* 14(4): 726-728.

Brust, M. et al. (1995). "Synthesis and reactions of functionalised gold nanoparticles." *Journal of the Chemical Society, Chemical Communications*(16): 1655-1656.

Brust, M. et al. (1994). "Synthesis of thiol-derivatised gold nanoparticles in a two-phase Liquid-Liquid system." *Journal of the Chemical Society, Chemical Communications*(7): 801-802.

Busbee, B. D. et al. (2003). "An Improved Synthesis of High-Aspect-Ratio Gold Nanorods." *Advanced Materials* 15(5): 414-416.

Cao, M. et al. (2005). "Single-Crystal Dendritic Micro-Pines of Magnetic α -Fe₂O₃: Large-Scale Synthesis, Formation Mechanism, and Properties." *Angewandte Chemie International Edition* 44(27): 4197-4201.

Carrot, G. et al. (1998). "Gold nanoparticle synthesis in graft copolymer micelles." *Colloid and Polymer Science* 276(10): 853-859.

Castro, L. et al. (2010). "Extracellular biosynthesis of gold nanoparticles using sugar beet pulp." *Chemical Engineering Journal* 164(1): 92-97.

Catherine, C. et al. (2003). "Functionalisation of magnetic nanoparticles for applications in biomedicine." *J. Phys. D: Appl. Phys.* 36(13): R198-R206.

Cecchini, R. S. et al. (2012). "Body mass index and the risk for developing invasive breast cancer among high-risk women in NSABP P-1 and STAR breast cancer prevention trials." *Cancer Prev Res (Phila)* 5(4): 583-592.

Chen, S. (1999). "4-Hydroxythiophenol-Protected Gold Nanoclusters in Aqueous Media." *Langmuir* 15(22): 7551-7557.

Chen, S. et al. (1998). "Arenethiolate Monolayer-Protected Gold Clusters." *Langmuir* 15(3): 682-689.

- Cheng, M. et al.** (2006). "Nanotechnologies for biomolecular detection and medical diagnostics." *Curr Opin Chem Biol* 10(1): 11-19.
- Chevaliez, S. et al.** (2006). "Hepatitis C virus serologic and virologic tests and clinical diagnosis of HCV-related liver disease." *Int J Med Sci* 3(2): 35-40.
- Chevaliez, S. et al.** (2007). "Hepatitis C virus: virology, diagnosis and management of antiviral therapy." *World J Gastroenterol* 13(17): 2461-2466.
- Chin, A. et al.** (2007). "Synthesis and characterization of magnetic iron oxide nanoparticles via w/o microemulsion and Massart's procedure." *Journal of Materials Processing Technology* 191(1-3): 235-237.
- Chiu, A. W. et al.** (2002). "Potential molecular marker for detecting transitional cell carcinoma." *Urology* 60(1): 181-185.
- Choi, Y. E. et al.** (2010). "Nanotechnology for early cancer detection." *Sensors (Basel)* 10(1): 428-455.
- Choo, Q. L. et al.** (1989). "Isolation of a cDNA clone derived from a blood-borne non-A, non-B viral hepatitis genome." *Science* 244(4902): 359-362.
- Conde, J. et al.** "RNA quantification using gold nanoprobe - application to cancer diagnostics." *J Nanobiotechnology* 8: 5.
- Conde, J. et al.** (2010). "RNA quantification using gold nanoprobe - application to cancer diagnostics." *J Nanobiotechnology* 8: 5.
- Cortez, M. A. et al.** (2011). "MicroRNAs in body fluids--the mix of hormones and biomarkers." *Nat Rev Clin Oncol* 8(8): 467-477.
- Costa, P. et al.** (2009). "Gold nanoprobe assay for the identification of mycobacteria of the *Mycobacterium tuberculosis* complex." *Clin Microbiol Infect* 16(9): 1464-1469.
- Costa, P. et al.** (2010). "Gold nanoprobe assay for the identification of mycobacteria of the *Mycobacterium tuberculosis* complex." *Clin Microbiol Infect* 16(9): 1464-1469.
- Cui, X. D. et al.** (2002). "Changes in the Electronic Properties of a Molecule When It Is Wired into a Circuit." *The Journal of Physical Chemistry B* 106(34): 8609-8614.
- Damen, M. et al.** (1995). "Reliability of the third-generation recombinant immunoblot assay for hepatitis C virus." *Transfusion* 35(9): 745-749.
- Daniel, M. C. et al.** (2004). "Gold Nanoparticles: Assembly, Supramolecular Chemistry, Quantum-Size-Related Properties, and Applications toward Biology, Catalysis, and Nanotechnology." *Chem. Rev.* 104(1): 293-346.

- Daou, T. J. et al.** (2006). "Hydrothermal Synthesis of Monodisperse Magnetite Nanoparticles." *Chemistry of Materials* 18(18): 4399-4404.
- Doria, G. et al.** (2007). "Nanodiagnosics: fast colorimetric method for single nucleotide polymorphism/mutation detection." *IET Nanobiotechnol* 1(4): 53-57.
- Duan, L. et al.** (2005). "Rapid and simultaneous detection of human hepatitis B virus and hepatitis C virus antibodies based on a protein chip assay using nano-gold immunological amplification and silver staining method." *BMC Infect Dis* 5: 53.
- Dubertret, B. et al.** (2001). "Single-mismatch detection using gold-quenched fluorescent oligonucleotides." *Nat Biotechnol* 19(4): 365-370.
- Duff, D. G. et al.** (1993). "A new hydrosol of gold clusters. 1. Formation and particle size variation." *Langmuir* 9(9): 2301-2309.
- Eftink, M. R. et al.** (1981). "Fluorescence quenching studies with proteins." *Anal Biochem* 114(2): 199-227.
- Eissa, S. et al.** (2014a). "The prognostic value of histidine-rich glycoprotein RNA in breast tissue using unmodified gold nanoparticles assay." *Appl Biochem Biotechnol* 174(2): 751-761.
- Eissa, S. et al.** (2014b). "Evaluation of urinary HURP mRNA as a marker for detection of bladder cancer: relation to bilharziasis." *Medical Oncology* C7 - 804 31(2): 1-9.
- Eissa, S. et al.** (2003). "Diagnostic value of urinary molecular markers in bladder cancer." *Anticancer Res* 23(5b): 4347-4355.
- Eissa S. et al.** (2014). "Direct detection of unamplified hepatoma upregulated protein RNA in urine using gold nanoparticles for bladder cancer diagnosis." *Clin Biochem* 47(1-2): 104-110.
- El Awady, M. et al.** (2009). "Positional effect of mutations in 5'UTR of hepatitis C virus 4a on patients' response to therapy." *World J Gastroenterol* 15(12): 1480-1486.
- Elghanian, R. et al.** (1997). "Selective colorimetric detection of polynucleotides based on the distance-dependent optical properties of gold nanoparticles." *Science* 277(5329): 1078-1081.
- Fabris, P. et al.** (2008). "Acute hepatitis C: clinical aspects, diagnosis, and outcome of acute HCV infection." *Curr Pharm Des* 14(17): 1661-1665.
- Ferlay, J. et al.** (2012). "Breast and cervical cancer in 187 countries between 1980 and 2010." *Lancet* 379(9824): 1390-1391.

- Franzreb, M. et al.** (2006). "Protein purification using magnetic adsorbent particles." *Appl Microbiol Biotechnol* 70(5): 505-516.
- Frens, G.** (1973). "Controlled nucleation for regulation of particle size in monodisperse gold suspensions." *nature physical science* 241: 20-22.
- Germer, J. J. et al.** (2002). "Comparative evaluation of the VERSANT HCV RNA 3.0, QUANTIPLEX HCV RNA 2.0, and COBAS AMPLICOR HCV MONITOR version 2.0 Assays for quantification of hepatitis C virus RNA in serum." *J Clin Microbiol* 40(2): 495-500.
- Giri, S. et al.** (2005). "Magnetic properties of α -Fe₂O₃ nanoparticle synthesized by a new hydrothermal method." *Journal of Magnetism and Magnetic Materials* 285(1-2): 296-302.
- Griffin, J. et al.** (2009a). "Sequence-specific HCV RNA quantification using the size-dependent nonlinear optical properties of gold nanoparticles." *Small* 5(7): 839-845.
- Griffin, J. et al.** (2009b). "Size- and distance-dependent nanoparticle surface-energy transfer (NSET) method for selective sensing of hepatitis C virus RNA." *Chemistry* 15(2): 342-351.
- Grimm, J. et al.** (2004). "Novel nanosensors for rapid analysis of telomerase activity." *Cancer Res* 64: 639-643.
- Hahn, Y. K. et al.** (2007). "Magnetophoretic immunoassay of allergen-specific IgE in an enhanced magnetic field gradient." *Anal Chem* 79(6): 2214-2220.
- Haiss, W. et al.** (2007). "Determination of Size and Concentration of Gold Nanoparticles from UV-Vis Spectra." *Analytical Chemistry* 79(11): 4215-4221.
- Halfon, P. et al.** (2006). "Real-time PCR assays for hepatitis C virus (HCV) RNA quantitation are adequate for clinical management of patients with chronic HCV infection." *J Clin Microbiol* 44(7): 2507-2511.
- He, W. et al.** (2008). "One-step label-free optical genosensing system for sequence-specific DNA related to the human immunodeficiency virus based on the measurements of light scattering signals of gold nanorods." *Anal Chem* 80(22): 8424-8430.
- Higuchi, M. et al.** (2002). "Epidemiology and clinical aspects on hepatitis C." *Jpn J Infect Dis* 55(3): 69-77.
- Hill, H. D. et al.** (2006). "The bio-barcode assay for the detection of protein and nucleic acid targets using DTT-induced ligand exchange." *Nat Protoc* 1(1): 324-336.
- Hood, E.** (2004). "Nanotechnology: looking as we leap." *Environ Health Perspect* 112(13): A740-749.

Bibliography

Howlader, N. et al. (2011). "SEER Cancer Statistics Review." National Cancer Institute: 1975-2008.

Hsiao, C. R. et al. (2009). "Characterization of DNA chips by nanogold staining." *Anal Biochem* 389(2): 118-123.

Hu, X. et al. (2007). "Fast Production of Self-Assembled Hierarchical α -Fe₂O₃ Nanoarchitectures." *The Journal of Physical Chemistry C* 111(30): 11180-11185.

Huang, X. (2006). Gold Nanoparticles Used in Cancer Cell Diagnostics, Selective Photothermal Therapy and Catalysis of NADH Oxidation Reaction. Doctor of philosophy Doctor of Philosophy, Georgia institute of Technology.

Huang, X. et al. (2007). "Gold nanoparticles: interesting optical properties and recent applications in cancer diagnostics and therapy." *Nanomedicine (Lond)* 2(5): 681-693.

Huang, Y. et al. (2003). "Prognostic significance of hepatoma-up-regulated protein expression in patients with urinary bladder transitional cell carcinoma." *Anticancer Res* 23(3B): 2729-2733.

Huber, M. et al. (2004). "Gold nanoparticle probe-based gene expression analysis with unamplified total human RNA." *Nucleic Acids Res* 32(18): e137.

Hulett, M. D. et al. (2000). "Murine histidine-rich glycoprotein: cloning, characterization and cellular origin." *Immunol Cell Biol* 78(3): 280-287.

Hummon, A. B. et al. (2007). "Isolation and solubilization of proteins after TRIzol extraction of RNA and DNA from patient material following prolonged storage." *Biotechniques* 42(4): 467-470, 472.

Hyeon, T. et al. (2001). "Synthesis of Highly Crystalline and Monodisperse Maghemite Nanocrystallites without a Size-Selection Process." *Journal of the American Chemical Society* 123(51): 12798-12801.

Ibraimi, F. et al. (2006). "Rapid one-step whole blood C-reactive protein magnetic permeability immunoassay with monoclonal antibody conjugated nanoparticles as superparamagnetic labels and enhanced sedimentation." *Anal Bioanal Chem* 384(3): 651-657.

Ito, A. et al. (2005). "Medical application of functionalized magnetic nanoparticles." *J Biosci Bioeng* 100(1): 1-11.

Jain, K. K. (2005). "Nanotechnology in clinical laboratory diagnostics." *Clinica Chimica Acta* 358: 37-54.

Jain, K. K. (2007). "Applications of Nanobiotechnology in Clinical Diagnostics." *Clin Chem* 53(11): 2002-2009.

- Jain, P. et al.** (2007). "Au nanoparticles target cancer." *Nano Today* 2: 18-29.
- Jain, P. K. et al.** (2006). "Calculated Absorption and Scattering Properties of Gold Nanoparticles of Different Size, Shape, and Composition: Applications in Biological Imaging and Biomedicine." *The Journal of Physical Chemistry B* 110(14): 7238-7248.
- Jana, N. R. et al.** (2001). "Seeding Growth for Size Control of 50- 40 nm Diameter Gold Nanoparticles." *Langmuir* 17(22): 6782-6786.
- Jares-Erijman, E. A. et al.** (2003). "FRET imaging." *Nat Biotechnol* 21(11): 1387-1395.
- Jemal, A. et al.** (2011). "Global cancer statistics." *CA Cancer J Clin* 61(2): 69-90.
- Jennings, T. L. et al.** (2006). "Fluorescent lifetime quenching near $d = 1.5$ nm gold nanoparticles: probing NSET validity." *J Am Chem Soc* 128(16): 5462-5467.
- Jing, Z. et al.** (2004). "Synthesis and characterization of monodisperse hematite nanoparticles modified by surfactants via hydrothermal approach." *Materials letters* 58(27-28): 3637-3640.
- Jones, A. L. et al.** (2005). "Histidine-rich glycoprotein: A novel adaptor protein in plasma that modulates the immune, vascular and coagulation systems." *Immunol Cell Biol* 83(2): 106-118.
- Jones, K. J.** (2009). Identification of serum proteins biomarkers, indicative of breast cancer in postmenopausal women. PhD Doctor of Philosophy, Howard University.
- Jun, Y. W. et al.** (2008). "Nanoscaling laws of magnetic nanoparticles and their applicabilities in biomedical sciences." *Acc Chem Res* 41(2): 179-189.
- Byrappa, K. et al.** (2001). chapter 2: History of hydrothermal technology. *Handbook of Hydrothermal Technology* Noyes Publications, New york.
- Kamat, A. M. et al.** (2013). "ICUD-EAU International Consultation on Bladder Cancer 2012: Screening, diagnosis, and molecular markers." *Eur Urol* 63(1): 4-15.
- Kaufman, D. S. et al.** (2009). "Bladder cancer." *Lancet* 374(9685): 239-249.
- Kenji Suzuki, K. et al.** (2009). "Controlling the number and positions of oligonucleotides on gold nanoparticle surface." *Journal of American Chemical Society* 131(2): 2.
- Kimling, J. et al.** (2006). "Turkevich method for gold nanoparticle synthesis revisited." *J Phys Chem B* 110(32): 15700-15707.
- Koide, T. et al.** (1986). "Amino acid sequence of human histidine-rich glycoprotein derived from the nucleotide sequence of its cDNA." *Biochemistry* 25(8): 2220-2225.

Bibliography

- Kouassi, G. et al.** (2006). "Magnetic and gold-coated magnetic nanoparticles as a DNA sensor." *Anal Chem* 78(10): 3234-3241.
- Kouassi, G. K. et al.** (2005). "Activity of glucose oxidase functionalized onto magnetic nanoparticles." *Biomagn Res Technol* 3(1): 1.
- Koyfman, A. et al.** (2005). "Controlled spacing of cationic gold nanoparticles by nanocrown RNA." *J Am Chem Soc* 127(34): 11886-11887.
- Kumar, D. et al.** (2013). "Gold nanoparticles: an era in bionanotechnology." *Expert Opin Drug Deliv* 10(3): 397-409.
- LaConte, L. et al.** (2005). "Magnetic nanoparticle probes." *Materials Today* 8(5, Supplement 1): 32-38.
- Lakowicz, J.** (1999). *Quenching of Fluorescence. Principles of Fluorescence Spectroscopy.* Springer US: 237-265.
- Lakowicz, J.** (2006). *Quenching of Fluorescence. Principles of Fluorescence Spectroscopy.* Springer US: 277-330.
- Larginho, M. et al.** (2012). "Gold and silver nanoparticles for clinical diagnostics - From genomics to proteomics." *J Proteomics* 75(10): 2811-2823.
- Lauer, G. M. et al.** (2001). "Hepatitis C virus infection." *N Engl J Med* 345(1): 41-52.
- Lavanchy, D.** (2009). "The global burden of hepatitis C." *Liver Int* 29 Suppl 1: 74-81.
- Lee, J. H. et al.** (2007). "Artificially engineered magnetic nanoparticles for ultra-sensitive molecular imaging." *Nat Med* 13(1): 95-99.
- Leung, L. et al.** (1983). "Histidine-rich glycoprotein is present in human platelets and is released following thrombin stimulation." *Blood* 62(5): 1016-1021.
- Li, H. et al.** (2007). "Selective quenching of fluorescence from unbound oligonucleotides by gold nanoparticles as a probe of RNA structure." *RNA* 13(11): 2034-2041.
- Li, H. et al.** (2004a). "Colorimetric detection of DNA sequences based on electrostatic interactions with unmodified gold nanoparticles." *PNAS* 101(39): 14036-14039.
- Li, H. et al.** (2005). "Detection of specific sequences in RNA using differential adsorption of single-stranded oligonucleotides on gold nanoparticles." *Anal Chem* 77(19): 6229-6233.
- Li, H. et al.** (2004b). "Label-free colorimetric detection of specific sequences in genomic DNA amplified by the polymerase chain reaction." *J Am Chem Soc* 126(35): 10958-10961.

Liandris, E. et al. (2009). "Direct detection of unamplified DNA from pathogenic mycobacteria using DNA-derivatized gold nanoparticles." *J Microbiol Methods* 78(3): 260-264.

Liang, R. et al. (2004). "Colorimetric detection of protein microarrays based on nanogold probe coupled with silver enhancement." *J Immunol Methods* 285(2): 157-163.

Lindenbach, B. et al. (2005). "Unravelling hepatitis C virus replication from genome to function." *Nature* 436(7053): 933-938.

Link, S. et al. (1999). "Spectral Properties and Relaxation Dynamics of Surface Plasmon Electronic Oscillations in Gold and Silver Nanodots and Nanorods." *J. Phys. Chem. B* 103(40): 8410-8426.

Liu, W. T. (2006). "Nanoparticles and their biological and environmental applications." *J Biosci Bioeng* 102(1): 1-7.

Liu, X. et al. (2007). "Extinction coefficient of gold nanoparticles with different sizes and different capping ligands." *Colloids Surf B Biointerfaces* 58(1): 3-7.

Lucia, B. et al. (2006). "Size dependence of refractive index of gold nanoparticles." *Nanotechnology* 17: 1309.

Maeland, A. et al. (1964). "Lattice spacing of gold- palladium alloys." *Canadian Journal of Physics* 42(11): 2364-2366.

Maggi, F. et al. (1999). "Divergent evolution of hepatitis C virus in liver and peripheral blood mononuclear cells of infected patients." *J Med Virol* 57(1): 57-63.

Manns, M.P. et al. (2001). "Peginterferon alfa -2b plus ribavirin for initial treatment of chronic hepatitis C: a randomized trial." *Lancet* 358: 958-965.

Marcellin, P. (1999). "Hepatitis C: clinical spectrum of the disease." *J Hepatol.* 31: 9-16.

Margel, D. et al. (2011). "Stress proteins and cytokines are urinary biomarkers for diagnosis and staging of bladder cancer." *Eur Urol* 59(1): 113-119.

Matboli, M. et al. (2014). "Evaluation of histidine-rich glycoprotein tissue RNA and serum protein as novel markers for breast cancer." *Med Oncol* 31(4): 897.

Mikhaylova, M. et al. (2004). "BSA Immobilization on Amine-Functionalized Superparamagnetic Iron Oxide Nanoparticles." *Chemistry of Materials* 16(12): 2344-2354.

Miller, F. D. et al. (2010). "Evidence of intense ongoing endemic transmission of hepatitis C virus in Egypt." *PNAS* 107(33): 14757-14762.

Bibliography

- Misek, D. E. et al.** (2011). "Protein biomarkers for the early detection of breast cancer." *Int J Proteomics* 2011: 343582.
- Moller, J. M. et al.** (2003). "Diagnosis of acute hepatitis C: anti-HCV or HCV-RNA?" *Scand J Gastroenterol* 38(5): 556-558.
- Moriishi, K. et al.** (2003). "Mechanism of hepatitis C virus infection." *Antivir Chem Chemother.* 14: 285-297.
- Murphy, C. et al.** (2002). "Controlling the Aspect Ratio of Inorganic Nanorods and Nanowires." *Advanced Materials* 14(1): 80-82.
- Nave, R. L.** (2013). "Baby boomers and the hepatitis C boom." *Ann Emerg Med* 62(6): 19A-21A.
- Negro, F. et al.** (2011). "The global health burden of hepatitis C virus infection." *Liver Int* 31 Suppl 2: 1-3.
- Nikoobakht, B. et al.** (2001). "Evidence for Bilayer Assembly of Cationic Surfactants on the Surface of Gold Nanorods." *Langmuir* 17(20): 6368-6374.
- Odreman-Macchioli, F. E. et al.** (2000). "Influence of correct secondary and tertiary RNA folding on the binding of cellular factors to the HCV IRES." *Nucleic Acids Res* 28(4): 875-885.
- Paresh, C. R. et al.** (2007). "A gold-nanoparticle-based fluorescence resonance energy transfer probe for multiplexed hybridization detection: accurate identification of bio-agents DNA." *Nanotechnology* 18(37): 5504.
- Paul, O. et al.** (1998). Separate Isolation of Genomic DNA and Total RNA from Single Samples Using the SV Total RNA. *promega notes.* 69: 6.
- Penin, F. et al.** (2004). "Structural biology of hepatitis C virus." *Hepatology* 39(1): 5-19.
- Perou, C. M. et al.** (2000). "Molecular portraits of human breast tumours." *Nature* 406(6797): 747-752.
- Perrault, S. D. et al.** (2009). "Synthesis and Surface Modification of Highly Monodispersed, Spherical Gold Nanoparticles of 50~200 nm." *Journal of the American Chemical Society* 131(47): 17042-17043.
- Place, A. et al.** (2011). "The microenvironment in breast cancer progression: biology and implications for treatment." *Breast Cancer Research* 13(6): 227.
- Podzorski, R. P.** (2002). "Molecular testing in the diagnosis and management of hepatitis C virus infection." *Arch Pathol Lab Med* 126(3): 285-290.

- Previsani, N. et al.** (2013). "HCV global alert and response.", 2013
<http://www.who.int/csr/disease/hepatitis/whocdscsrlyo2003/en/index4>.
- Prince, A. M. et al.** (2001). "Immunoprophylaxis of hepatitis C virus infection." *Clin Liver Dis* 5(4): 1091-1103.
- Narayanan, R. et al.** (2008). "Cetyltrimethylammonium Bromide-Modified Spherical and Cube-Like Gold nanoparticles as extrinsic Raman labels in surface enhanced Raman spectroscopy based heterogeneous immunoassays." *Analytical Chemistry* 80(6): 2265-2271.
- Radwan, S. H. et al.** (2009). "Gold nanoparticles for molecular diagnostics." *Expert Rev Mol Diagn* 9(5): 511-524.
- Rao, C.N. et al.** (2004). *Moving nanoparticles around: phase – transfer processes in nanomaterials synthesis. The chemistry of nanomaterials: synthesis, properties and applications*, Weinheim: Wiley – VCH(Edt), 1:31-49
- Ray, P. C. et al.** (2006). "Gold nanoparticle based FRET assay for the detection of DNA cleavage." *J Phys Chem B* 110(42): 20745-20748.
- Read, S.J. et al.** (2001). "Light cycler multiplex PCR for the laboratory diagnosis of common viral infections of the central nervous system." *J Clin Microbiol.* 39: 3056-3059.
- Ringner, M. et al.** (2011). "GOBO: gene expression-based outcome for breast cancer online." *PLoS One* 6(3): e17911.
- Rivas, M. A. et al.** (2012). "Downregulation of the tumor-suppressor miR-16 via progesterin-mediated oncogenic signaling contributes to breast cancer development." *Breast Cancer Res* 14(3): R77.
- Rochelle, M. C. et al.** (2003). *The iron oxides: Structure, Properties, Reactions, Occurrences and Uses. (sec.edition)*, Wiley-VCH GmbH & Co. KGaA.
- Rockenberger, J. et al.** (1999). "A New Nonhydrolytic Single-Precursor Approach to Surfactant-Capped Nanocrystals of Transition Metal Oxides." *Journal of the American Chemical Society* 121(49): 11595-11596.
- Rosi, N. L. et al.** (2006). "Oligonucleotide-modified gold nanoparticles for intracellular gene regulation." *Science* 312(5776): 1027-1030.
- Rosi, N. L. et al.** (2005). "Nanostructures in biodiagnostics." *Chem Rev* 105(4): 1547-1562.
- Rupcich, N. et al.** (2006). "Quenching of fluorophore-labeled DNA oligonucleotides by divalent metal ions: implications for selection, design, and applications of

signaling aptamers and signaling deoxyribozymes." *J Am Chem Soc* 128(3): 780-790.

Shawky, S.M. et al. (2009). Rapid colorimetric method for detection of HCV RNA using gold nanoparticles. Hepatitis C Virus-3rd International conference, Dublin Castle, Ireland.

Wuanget, S.G. et al. (2006). "Heparinized Magnetic Nanoparticles: In-Vitro Assessment for Biomedical Applications." *Advanced Functional Materials* 16(13): 1723-1730.

Sabbatini, A. R. et al. (2011) "Evidence that muscle cells do not express the histidine-rich glycoprotein associated with AMP deaminase but can internalise the plasma protein." *Eur J Histochem* 55(1): e6.

Salem, H. K. et al. (2012). "Changing patterns (age, incidence, and pathologic types) of schistosoma-associated bladder cancer in Egypt in the past decade." *Urology* 79(2): 379-383.

Sambrook, J. et al. (1989). *Molecular cloning: A laboratory manual* (2nd edition). Cold Spring Harbor Laboratory Press, NY: 42-59.

Eissa, S. et al. (2013). "Integrated technologies in the post-genomic era for discovery of bladder cancer urinary markers." *World J Clin Urol* 2(3): 20-31.

Sapre, N. et al. (2014). "Gene-based urinary biomarkers for bladder cancer: an unfulfilled promise?" *Urol Oncol* 32(1): 48 e49-17.

Sarrazin, C. (2004). "Diagnosis of hepatitis C: update 2004." *Journal of Gastroenterology and Hepatology* 19: S88-S93.

Sau, T. K. et al. (2010). "Properties and applications of colloidal nonspherical noble metal nanoparticles." *Adv Mater* 22(16): 1805-1825.

Schaub, N. P. et al. (2009). "Serum proteomic biomarker discovery reflective of stage and obesity in breast cancer patients." *J Am Coll Surg* 208(5): 970-978; discussion 978-980.

Schleicher, E. (2006). "The clinical chemistry laboratory: current status, problems and diagnostic prospects." *Anal Bioanal Chem* 384(1): 124-131.

Schroter, M. et al. (2001). "Quantitative detection of hepatitis C virus RNA by light cycler PCR and comparison with two different PCR assays." *J Clin Microbiol* 39(2): 765-768.

Schulman., S. G. (1985). *Molecular Luminescence Spectroscopy: Methods and Applications. Part 1.* New York

- Scott, J. D. et al.** (2007). "Molecular Diagnostics of Hepatitis C Virus Infection: A Systematic Review." *JAMA* 297(7): 724-732.
- Seme, K. et al.** (2005). "The role of core antigen detection in management of hepatitis C: a critical review." *J Clin Virol* 32(2): 92-101.
- Shawky, S. M. et al.** (2011). "Fluorimetric nanodiagnostic assay for detection of hepatitis C virus RNA in serum." *Clinical Biochemistry* 44(7): 522.
- Shawky, S. M. et al.** (2010). "Direct detection of unamplified hepatitis C virus RNA using unmodified gold nanoparticles." *Clin Biochem* 43(13-14): 1163-1168.
- Shen, Y. et al.** (2005). "Characterization of a fluorescence-signaling and RNA-cleaving deoxyribozyme." *Nucleic Acids Symp Ser (Oxf)*(49): 55-56.
- Shinkai, M. et al.** (2004). "Functional magnetic particles for medical application." *Adv Biochem Eng Biotechnol* 91: 191-220.
- Shiyng H. et al.** (2007). "Biosynthesis of gold nanoparticles using the bacteria *Rhodospseudomonas capsulata*." *Materials letters* 61(18): 3984-3987.
- Siegel, R. et al.** (2012). "Cancer statistics, 2012." *CA: A Cancer Journal for Clinicians* 62(1): 10-29.
- Simantov, R. et al.** (2001). "Histidine-rich glycoprotein inhibits the antiangiogenic effect of thrombospondin-1." *The Journal of Clinical Investigation* 107(1): 45-52.
- Simmonds, P.** (2004). "Genetic diversity and evolution of hepatitis C virus--15 years on." *J Gen Virol* 85(Pt 11): 3173-3188.
- Simmonds, P. et al.** (1993). "Classification of hepatitis C virus into six major genotypes and a series of subtypes by phylogenetic analysis of the NS-5 region." *J Gen Virol* 74 (Pt 11): 2391-2399.
- Sisco, K. L.** (2001). "Is RNA in serum bound to nucleoprotein complexes?" *Clin Chem* 47(9): 1744-1745.
- Slavoff, S. A. et al.** (2011). "Imaging protein-protein interactions inside living cells via interaction-dependent fluorophore ligation." *J Am Chem Soc* 133(49): 19769-19776.
- Smith, B. D. et al.** (2012). "Recommendations for the identification of chronic hepatitis C virus infection among persons born during 1945-1965." *MMWR Recomm Rep* 61(RR-4): 1-32.
- Smith, S. D. et al.** (2001). "Urine detection of survivin and diagnosis of bladder cancer." *JAMA* 285(3): 324-328.

- Smith, Z. L. et al.** (2013). "Urinary markers for bladder cancer." F1000Prime Rep 5: 21.
- Society, A. C.** (2014). cancer facts and figures 2014. American Chemical society. Atlanta.
- Solans, C. et al.** (2005). "Nano-emulsions." Current Opinion in Colloid & Interface Science 10(3-4): 102-110.
- Somogyi, B. et al.** (1985). "A double-quenching method for studying protein dynamics: separation of the fluorescence quenching parameters characteristic of solvent-exposed and solvent-masked fluorophors." Biochemistry 24(23): 6674-6679.
- Stanislaw, S. et al.** (2011). Terminology of polymers and polymerization processes in dispersed systems (IUPAC Recommendations 2011). Pure and Applied Chemistry. 83: 2229.
- Storhoff, J. J. et al.** (1998). "One-Pot Colorimetric Differentiation of Polynucleotides with Single Base Imperfections Using Gold Nanoparticle Probes." Journal of the American Chemical Society 120(9): 1959-1964.
- Storhoff, J. J. et al.** (2004). "Homogeneous detection of unamplified genomic DNA sequences based on colorimetric scatter of gold nanoparticle probes." Nat Biotechnol 22(7): 883-887.
- Strader, D. B. et al.** (2004). "Diagnosis, management, and treatment of hepatitis C." Hepatology 39(4): 1147-1171.
- Sun, K. et al.** (2009). "Preparation and characterization of gold nanoparticles using ascorbic acid as reducing agent in reverse micelles." Journal of Materials Science 44(3): 754-758.
- Sun, S. et al.** (2002). "Size-Controlled Synthesis of Magnetite Nanoparticles." Journal of the American Chemical Society 124(28): 8204-8205.
- Sun, Y. et al.** (2005). "Microarray gene expression analysis free of reverse transcription and dye labeling." Anal Biochem 345(2): 312-319.
- Swellam, M. et al.** (2004). "Emerging role of p53, bcl-2 and telomerase activity in Egyptian breast cancer patients." IUBMB Life 56(8): 483-490.
- Tarrytown, N. B.** (2002). VERSANT HCV RNA Qualitative Assay (TMA) [package insert].
- Thaxton, C. S. et al.** (2005). "A bio-bar-code assay based upon dithiothreitol-induced oligonucleotide release." Anal Chem 77(24): 8174-8178.

- Titirici, M. et al.** (2006). "A Generalized Synthesis of Metal Oxide Hollow Spheres Using a Hydrothermal Approach." *Chemistry of Materials* 18(16): 3808-3812.
- Tourinho, F. et al.** (1990). "Aqueous ferrofluids based on manganese and cobalt ferrites." *Journal of Materials Science* 25(7): 3249-3254.
- Trimoulet, P. et al.** (2002). "Evaluation of the VERSANT HCV RNA 3.0 assay for quantification of hepatitis C virus RNA in serum." *J Clin Microbiol* 40(6): 2031-2036.
- Tsou, A. P. et al.** (2005). Expression of hepatoma-up-regulated protein (HURP) in resectable hepatocellular carcinoma: dual function and clinical significance. ACR Meeting Abstracts.
- Tsou, A. P. et al.** (2003). "Identification of a novel cell cycle regulated gene, HURP, overexpressed in human hepatocellular carcinoma." *Oncogene* 22(2): 298-307.
- Turkevich, J.** (1985a). "Colloidal gold. Part I." *Gold Bulletin* 18(3): 86-91.
- Turkevich, J.** (1985b). "Colloidal gold. Part II." *Gold Bulletin* 18(4): 125-131.
- Turkevich, J. et al.** (1951). "A study of the nucleation and growth processes in the synthesis of colloidal gold." *Discussions of the Faraday Society* 11(0): 55-75.
- Urdea, M. S. et al.** (1997). "Hepatitis C--diagnosis and monitoring." *Clin Chem* 43(8 Pt 2): 1507-1511.
- Van Rhijn, B. W. et al.** (2005). "Urine markers for bladder cancer surveillance: a systematic review." *Eur Urol* 47(6): 736-748.
- Vidal-Vidal, J. et al.** (2006). "Synthesis of monodisperse maghemite nanoparticles by the microemulsion method." *Colloids and Surfaces A: Physicochemical and Engineering Aspects* 288(1-3): 44-51.
- Vrooman, O. P. et al.** (2008). "Urinary markers in bladder cancer." *Eur Urol* 53(5): 909-916.
- Vu, T. B. et al.** (1998). "Nanotips and nanomagnetism." *Applied Surface Science* 130: 803-814.
- Wang, J. et al.** (2003). "One-step hydrothermal process to prepare highly crystalline Fe₃O₄ nanoparticles with improved magnetic properties." *Materials Research Bulletin* 38(7): 1113-1118.
- Wang, S.B. et al.** (2007). "Synthesis and Magnetic Properties of Uniform Hematite Nanocubes." *The Journal of Physical Chemistry C* 111(9): 3551-3554.
- Weissleder, R. et al.** (2005). "Cell-specific targeting of nanoparticles by multivalent attachment of small molecules." *Nat Biotechnol* 23(11): 1418-1423.

West, J. L. et al. (2003). "Engineered nanomaterials for biophotonics applications: improving sensing, imaging, and therapeutics." *Annu Rev Biomed Eng* 5: 285-292.

WHO. "http://www.who.int/vaccine_research/diseases/hepatitis_c/en/."

WHO. "http://www.who.int/vaccine_research/diseases/hepatitis_c/en/."

WHO. (2011). "World Health Organization , Factsheet No.164.
<http://goo.gl/5m3sY>, accessed 31.12.2012."

Woo, K. et al. (2004). "Easy Synthesis and Magnetic Properties of Iron Oxide Nanoparticles." *Chemistry of Materials* 16(14): 2814-2818.

Wu, W. et al. (2008). "Magnetic iron oxide nanoparticles: synthesis and surface functionalization strategies." *Nanoscale Res Lett* 3(11): 397-415.

Xie, H. (2004). Preparation, characterization and intracellular targeting of biomolecule-Gold nanoparticle complex. Doctor of philosophy dissertation, North Carolina state university.

Xylinas, E. et al. (2014). "Urine markers for detection and surveillance of bladder cancer." *Urol Oncol* 32(3): 222-229.

Yamaura, M. et al. (2004a). "Preparation and characterization of 3-aminopropyltriethoxysilane-coated magnetite nanoparticles." *Journal of Magnetism and Magnetic Materials* 279(2-3): 210-217.

Yamaura, M. et al. (2004b). "Preparation and characterization of (3-aminopropyl)triethoxysilane-coated magnetite nanoparticles." *Journal of Magnetism and Magnetic Materials* 279(2-3): 210-217.

Yang, P. et al. (2009a). "A magnetic, luminescent and mesoporous core-shell structured composite material as drug carrier." *Biomaterials* 30(27): 4786-4795.

Yang, P. et al. (2009b). "A magnetic, luminescent and mesoporous core-shell structured composite material as drug carrier." *Biomaterials* 30(27): 4786-4795.

Yeh, H. C. et al. (2005). "Single-molecule detection and probe strategies for rapid and ultrasensitive genomic detection." *Curr Pharm Biotechnol* 6(6): 453-461.

Yoshizawa, K. (2004). "[Early diagnosis of acute hepatitis C--detection of anti-HCV antibody and HCV-RNA]." *Nihon Rinsho* 62 Suppl 7(Pt 1): 353-356.

Yossepowitch, O. et al. (2007). "Use of urinary biomarkers for bladder cancer surveillance: patient perspectives." *J Urol* 177(4): 1277-1282; discussion 1282.

Zagaría, M. A. E. (2014). "Hepatitis C Alert: Baby Boomers Should Be Tested." *US Pharm.* 39(4): 18-20.

- Zeeneldin, A. A. et al.** (2013). "Clinico-pathological features of breast carcinoma in elderly Egyptian patients: a comparison with the non-elderly using population-based data." *J Egypt Natl Canc Inst* 25(1): 5-11.
- Zhang, H. et al.** (2004). "Emulsion-Templated Gold Beads Using Gold Nanoparticles as Building Blocks." *Advanced Materials* 16(1): 27-30.
- Zhao M. et al.** (2002). "Differential conjugation of tat peptide to superparamagnetic nanoparticles and its effect on cellular uptake." *Bioconjug Chem* 13(4): 840-844.
- Zheng, J. et al.** (2004). "Highly fluorescent, water-soluble, size-tunable gold quantum dots." *Phys Rev Lett* 93(7): 077402.
- Zheng, Y. et al.** (2006). "Synthesis and magnetic properties of Fe₃O₄ nanoparticles." *Materials Research Bulletin* 41(3): 525-529.
- Zhenxin, W. et al.** (2009). "Gold nanoparticle probes." *Coordination Chemistry Reviews* 253(11): 1607-1618.

7 Summary

Advances in molecular diagnostic technologies have led to substantial progress in the understanding and detection of a multitude of diseases including infectious, genetic diseases and cancer. These technologies have become a cornerstone in modern clinical diagnostics, and can be broadly classified into either nucleic acid amplification techniques (NAT) or signal amplification techniques, or direct detection using a labeled probes (e.g. using a fluorescent dye or a radioisotope). These molecular detection strategies have the advantage of being sensitive and specific; however, they are all relatively costly, labor-intensive, and require a sophisticated laboratory infrastructure. Moreover amplification based assays suffer from the risk of amplicon cross- contamination. There, is therefore a need to develop simpler and more cost-effective molecular diagnostic assays for the direct purification and detection of unamplified nucleic acids in clinical samples with acceptable sensitivity and specificity, short turnaround time, and suitable for low resource settings. This is particularly true for the poorer countries with less developed health care systems.

Nanotechnology is a powerful and rapidly evolving field whose integration into the molecular diagnostics arena would have a positive impact on the development of simpler effective nucleic acid testing. The utilization of nanoparticles would also allow assay miniaturization development of “at point of care” assays. One of the most promising nano-structures are gold nanoparticles (AuNPs) which exhibit a unique phenomenon known as Surface Plasmon Resonance (SPR) that is responsible for their characteristic optical properties such as large molar extinction coefficients. Due to SPR, AuNPs in colloidal solution have an intense red color which changes to blue upon aggregation of the AuNPs. Both positively and negatively charged AuNPs exhibit their unique optical properties and have been utilized in the development of simple, sensitive, specific, rapid and cheap colorimetric assays for nucleic acids detection that can compete with the currently used molecular assays. Another type of nanoparticles that is demonstrating high potential for utility in molecular assays is iron oxide magnetic nanoparticles (MNPs). These nanoparticles are characterized by Superparamagnetic properties, and with proper functionalization, can be used for the selective and efficient capture of the target bio-molecule. The combined use of MNPs with other signal-generating nanoparticles would allow the highly sensitive and accurate detection of target nucleic acids in clinical samples.

Summary

Here we have developed two applications for direct detection of unamplified nucleic acids in clinical samples. One application was the direct detection of unamplified Hepatitis C Virus (HCV) RNA. This was done using two approaches; the first employed negatively charged unmodified AuNPs and the other a combination of MNPs for RNA capture, and cationic AuNPs for detection. Both approaches were tested on clinical serum samples from HCV infected patients. The second application was the detection of cancer biomarkers. We combined MNPs specific capture with unmodified citrate AuNPs for detection of two novel biomarkers. One biomarker, Hepatoma Up Regulated Protein (HURP) RNA, was detected in clinical urine samples from urinary bladder cancer patients. The other target was the RNA for the breast cancer biomarker, Histidine-Rich Glycoprotein (HRG), which was detected in breast tissue.

In chapter 2: An assay prototype using AuNPs unmodified was developed for the direct detection of HCV RNA extracted from clinical serum sample. The results obtained are comparable to the currently used standard detection method; real Time RT-PCR. The novel assay has a sensitivity and specificity of 92% and 89.9% respectively, with a detection limit of 50 copies/reaction. The assay is simple, rapid, sensitive and specific and requires no detection equipment. Moreover, it could be further developed to be quantitative using a spectrophotometer.

In chapter 3: In this chapter, we present a prototype for a homogenous solution based assay (not solid based assay) for the detection of unamplified nucleic acid detection using cationic AuNPs, which align onto the negatively charged phosphate backbone of the long nucleic acid resulting to a change in color from red to blue. To increase the specificity of this assay, in-house MNPs functionalized with HCV specific oligonucleotides were prepared to selectively capture the viral RNA after total RNA extraction. The assay prototype has a sensitivity and specificity of 96.5% and 96% respectively, with a detection limit of 15IU/ml blood (1 IU corresponds to 2-5 copies). In addition to its simplicity, cost effectiveness, and its short turn-around time (75 min), this assay is amenable to automation

In chapter 4: Negatively charged unmodified AuNPs were employed for the detection of selected tumor biomarkers. The first was HURP RNA in urine which is an emerging biomarker for the early detection of urinary bladder carcinoma. The second is a novel biomarker of breast cancer; HRG RNA, in breast tissue. We have used magnetic nanoparticles conjugated to an oligonucleotide specific to the respective marker's RNA to selectively capture it and enhance the sample purity. This was followed by detection using the same concept of the previously described assay using negatively charged AuNPs. The sensitivity and specificity of HURP AuNPs

Summary

developed assay were 90% & 94% respectively, while that of the HRG was 90% for both sensitivity and specificity.

Moreover, incorporation of a MNP purification step with conventional RT-PCR has improved the HURP RT-PCR sensitivity from 64% to 84%, and the specificity from 90 to 94% while the sensitivity for the HRG RT-PCR has been improved from 71.7% to 80%. The magnetic purification step improved the unmodified citrate AuNPs assay on both HURP RNA and HRG RNA. Thus, the use of magnetic nanoparticles in the target purification has generated assays (unmodified AuNPs, and RT-PCR) with a high specificity and sensitivity.

In summary the assay prototypes described in this work illustrate the effectiveness and versatility of diagnostic platforms using different AuNPs and MNPs. The nanoparticles based assay platforms have high potential for the detection of high burden infections as well as cancers. These assays could aid in complex disease management due to their low cost, simplicity and short turnaround time.

8 Samenvatting

De vooruitgang in moleculair diagnostische technieken hebben gezorgd voor een aanzienlijke verbetering in het begrijpen en detecteren van vele ziekten, infectie ziektes, genetische ziektes en kanker. Deze technologie heeft zich ontwikkeld tot een hoeksteen van moderne klinische diagnostiek en kan ruwweg worden onderverdeeld in nucleïnezuuramplificatie technieken (NAT) of signaal amplificatie technieken of rechtstreekse detectie gebruikmakend van probes (bijv. d.m.v. fluorescentie of radioactiviteit).

Moleculaire detectie technieken hebben het voordeel dat ze selectief en specifiek zijn, echter ze zijn vrij duur, arbeidsintensief, en hebben een geavanceerde laboratorium infrastructuur nodig. Verder lopen amplificatie technieken het gevaar van amplicon kruis-contaminatie. Het is daarom noodzakelijk een eenvoudige en goedkope diagnostische methodes te ontwikkelen om niet geamplificeerde nucleïnezuren in klinische samples met een goede specificiteit en gevoeligheid in korte tijd te detecteren in een eenvoudige omgeving.

Nanotechnologie is een krachtig en snel ontwikkelend veld, waarvan de integratie in het moleculair diagnostisch veld een positieve invloed zou hebben op de ontwikkeling van effectieve testen voor de detectie van nucleïnezuren. Daarbij komt dat het gebruik van nanopartikels een miniaturisatie mogelijk zou kunnen maken van “op de [lek van zorg]” metingen. Een van de veel belovende nanostructuren zijn goud nanopartikels (AuNPs) die de unieke eigenschap Surface Plasmon Resonantie (SPR) hebben die verantwoordelijk is voor de karakteristieke optische eigenschappen zoals een hoge extinctie coëfficiënt. Vanwege SPR hebben AuNPs een intens rode kleur in een colloïdale oplossing die verandert naar blauw als de AuNPs aggregeren. Zowel positief als negatief geladen AuNPs hebben hun unieke optische eigenschappen en zijn gebruikt om een eenvoudige, gevoelige, specifieke, snelle en goedkope kleur detectie te ontwikkelen van nucleïnezuren, die de huidige moleculaire detectie methodes kan vervangen. Een ander soort nanopartikel dat groot potentieel heeft voor moleculaire diagnostiek zijn ijzer oxide magnetische partikels (MNPs). Deze nanopartikels worden gekarakteriseerd door superparamagnetische eigenschappen, die met de juiste functionele groepen, gebruikt kunnen worden voor de selectieve en efficiënte binding van het te detecteren bio-molecuul. Het gecombineerde gebruik van MNPs met andere signaal afgevend nanopartikels zou een zeer gevoelige en nauwkeurige meting toestaan van de te meten nucleïnezuren in klinische monsters.

Wij hebben twee methodes ontwikkeld voor de detectie van niet geamplificeerde nucleïnezuuren in klinische monsters. De eerste methode is de directe detectie van niet geamplificeerd Hepatitis C virus (HCV) RNA. Dit is gedaan door middel van twee benaderingen; één omhelst negatief geladen niet gemodificeerde AuNPs, de ander een combinatie van MNPs voor de binding van RNA en cationische AuNPs voor de detectie van het RNA. Beide benaderingen zijn getest op klinische samples van patienten geïnfecteerd met HCV. De tweede toepassing was het detecteren van kanker biomarkers. Een biomarker die werd gedetecteerd in klinische urine monsters was het RNA voor de blaaskanker marker Hepatoma Up Regulated protein (HURP). De ander marker was een borsttumor marker Histidine Rich Glycoprotein (HRG) in borstweefsel.

Hoofdstuk 2 beschrijft de ontwikkeling van een prototype assay met niet gemodificeerde AuNPs voor de detectie van HCV RNA geëxtraheerd uit serum uit de kliniek. De resultaten zijn vergelijkbaar met de huidige standaard detectie methode, real time RT-PCR. De nieuwe methode heeft een gevoeligheid van 92% en een specificiteit van 89,9% met een detectielimiet van 50 kopieën per reactie. De methode is eenvoudig, snel, gevoelig en specifiek en heeft geen meetapparatuur nodig. De methode zou verder kunnen worden ontwikkeld tot een kwantitatieve methode door het gebruik van spectrofotometrie.

Hoofdstuk 3 beschrijft een prototype methode om niet geamplificeerd nucleïnezuur te meten met AuNPs, die zich rangschikken op de negatief geladen fosfaatketen van het nucleïne zuur, hetgeen resulteert in een verandering van kleur van rood naar blauw. Om de specificiteit van de methode te verhogen zijn zelf gemaakte MNPs gefunctionaliseerd met HCV specifieke oligonucleotiden om selectief het virale RNA af te vangen na een extractie van het totale RNA. Het prototype heeft een gevoeligheid van 96,5% en een specificiteit van 96% met een detectie limiet van 15 IU/ml bloed (1 IU komt overeen met 2-5 kopieën). Vanwege zijn eenvoud, geringe kosten en snelle doorlooptijd (75 min.) is de methode geschikt voor automatisering.

Hoofdstuk 4 beschrijft het gebruik van negatief geladen ongemodificeerde AUNPs voor de detectie van specifieke kankermerkers. De eerste was HURP RNA in urine hetgeen een in opgang zijnde biomarker is voor de vroege detectie van een blaascarcinoom. De tweede is een nieuwe biomarker in borstkanker, HRG RNA. We hebben gebruik gemaakt van nanopartikels die geconjugeerd zijn aan een oligonucleotide die specifiek is voor het merker RNA om dat RNA af te vangen en de zuiverheid van het te meten monster te verhogen. Vervolgens wordt hetzelfde concept gebruikt voor detectie als hierboven beschreven voor negatief geladen

Samenvatting

AuNPs. De gevoeligheid en specificiteit van de HURP AUNPs waren respectievelijk 90% en 94%, terwijl die van HRG AuNPs beiden 90% waren.

Daarbij komt dat het inbouwen van een MNP zuiveringsstap met conventionele PCR de HURP RT-PCR gevoeligheid verbeterd heeft van 64% naar 84% en de specificiteit van 90 naar 94%, terwijl die van HRG RT-PCR verbeterd is van 71,75 naar 80%. Bovendien is de detectie van HURP en HRG RNA verbeterd door de magnetische zuiveringsstap voor de meting met niet gemodificeerde AuNPs. Dus het gebruik van magnetische nanopartikels in een zuiveringsstap heeft een methode (ongemodificeerde AuNPs en RT-PCR) opgeleverd met een hoge specificiteit en gevoeligheid.

In conclusie, de hier beschreven prototype assays illustreren de effectiviteit en veelzijdigheid van diagnostische methodes, die gebruik maken van verschillende AuNPs en MNPs. De op nanopartikels gebaseerde methodes hebben potentieel een hoge waarde voor de detectie van infectie ziektes en kanker. De hier ontwikkelde methodes zouden kunnen helpen in de management van complexe ziektes vanwege hun lage kosten, eenvoud en snelle doorlooptijd.

9 Curriculum vitae

Personal Data

Full name Sherif Mohamed Shawky Abdou

Date of Birth November 17, 1977

Place of Birth Cairo, Egypt

Education

- **2014** PhD student at Erasmus Medical Center, Rotterdam under the supervision of Prof.dr Frank Grosveld and The American University in Cairo, under the supervision of Prof. dr. Hassan Azzazy
- **2006** MSc degree in Bimolecular Sciences from Vrije Universiteit, Amsterdam
- **2001** BSc degree in pharmacy and pharmaceutical Sciences from Misr University For Science & Technology, Cairo, Egypt
- **1995** High School Certificate (Science Department), from Patriarchal College, Cairo, Egypt

Specialized Training

- **2010** National Institute For Material Science (NIMS), Material Research Lab for Environmental and Energy, Tsukuba, Japan
- **02-03** Naval American Medical Research Unit #3(NAMRU#3), Development of HCV novel diagnostics kits, Cairo, Egypt
- **2002** DNA Finger-printing Workshop, Vascera company, Cairo, Egypt
- **2001** Marketing Concepts, Pfizer Pharmaceutical Company, Cairo, Egypt

Employment

- **2006** Research assistant in Youssef Jameel Science &Technology Research Center (STRC), The American University in Cairo, Egypt
- **2001** Teaching assistance in Faculty of Pharmacy, Biochemistry Department, in Misr University For Science & Technology

Publications

2014 Shojaei TR, Tabatabaei M., Shawky S.M., Salleh M.A., Bald D. **A review on emerging diagnostic assay for viral detection: the case of avian influenza Virus.** *Mol Biol Rep.* **2014 Sep.23.** [Epub ahead of print]. PMID: 25245956.

2014 Sanna Eissa, Hassan Azzazy, Marwa Matboli Sherif M. Shawky, Hebatallah Said, Faten Anous. **The prognostic value of Histidine-Rich Glycoprotein RNA in Breast Tissue using unmodified Gold nanoparticles assay.** *Applied Biochemistry and Biotechnology.* 2014 August 2014. PMID: 25091325.

2014 Sherif M. Shawky, Bassem S. Guirgis and Hassan M.E. Azzazy. **Detection of unamplified HCV RNA in serum using a novel metallic nanoparticles platform.** *Clinical Chemistry and Laboratory Medicine*, 52(4). PMID: 24158422.

2014 Sanaa Eissa, Sherif M. Shawky, Marwa Matboli, Shymaa Mohamed and Hassan M.E. Azzazy. **Direct detection of unamplified Hepatoma up Regulated protein RNA in urine using Gold Nanoparticles for Bladder Cancer Diagnosis.** *Clinical Biochemistry* 47 (1-2) PMID: 24183881.

2012 Wael M., Li Y., Sherif M. Shawky, Hassan M. Azzazy, Liu C.J. **Influence of glow discharge plasma as an external stimulus on the self-assembly, morphology and binding affinity of gold nanoparticles-streptavidin conjugates.** *International Journal of molecular sciences* 13 (6), PMID: 22837648.

2010 Sherif M. Shawky., Dirk Bald, Hassan M. E. Azzazy. **Direct detection of unamplified Hepatitis C virus RNA using unmodified gold nanoparticles.** *Clinical Biochemistry* 43(13-14). PMID: 20627095.

2009 Mostafa K El Awady, Hassan M Azzazy, Ahmed M Fahmy, Sherif M Shawky, Noha G. Badreldin, Samar S Yossef, Moataza H Omran, Abdel Rahman N. Zekri, and Said A Goueli. **Positional effect of mutations in 5'UTR of hepatitis C virus 4a on patients' response to therapy.** *World Journal of Gastroenterology*15 (12). PMID: 19322922.

10 PhD Portfolio

Personal Data

Name Sherif Mohamed Shawky Abdou

PhD Period Jul 2008- Oct 2014

Department Cell Biology

Promoter Prof. Dr. F. Grosveld (EMC)

Co-Promoter Prof. Dr. H. M. E. Azzazy (AUC)

Conferences Abstracts & Posters

2011 Sherif M. Shawky and Hassan M.E. Azzazy. Fluorimetric nano diagnostic assay for detection of unamplified HCV RNA in serum samples. Abstracts/ clinical Biochemistry 44(7).

2009 Sherif M. Shawky, Sarah Radwan, Hassan M. E. Azzazy. Rapid colorimetric method for detection of HCV RNA using gold nanoparticles. Poster presentation at the Hepatitis C Virus- 3rd International Conference (Dublin 17-19 June 2009).

2008 Hassan M. E. Azzazy, N.G. Bader El-Din, S.M. Shawky, A. Fahmy, M.M. El Hefnawy, and M. K. El Awady. Chronic Hepatitis C virus clearance is associated with an internal ribosomal entry site (IRES) II Id stem loop structure variant. Clinical chemistry, vol.54, no.6, supplements.

2010 Sherif M. Shawky, Hassan M.E. Azzazy. Rapid Detection of Unamplified HCV RNA in Clinical Specimens Using Unmodified Gold Nanoparticles. Clinical Chemistry, vol. 56, no. 6.

Patents

Hassan M.E. Azzazy, Sherif M. Shawky. **Direct detection of unamplified hepatitis c virus RNA using unmodified gold nanoparticles.** PCT/US2011/020676, filed January 2011. Publication number: WO2012/096646.

Hassan M.E. Azzazy, Tamer M. Samir, Sherif M. Shawky. **Detection of Nucleic Acids Using Unmodified Gold Nanoparticles.** PCT/US2012/032778, filed April 2012. Publication number: WO2012/139122A1.

Hassan M.E. Azzazy, Sherif M. Shawky, Kamel M. Eid, and Bassem G. Shenouda. **Direct detection of disease biomarkers in clinical specimens using cationic nanoparticles based assays and versatile and green methods for synthesis of anisotropic silver nanostructures.** PCT/ US2013/024136, filed January 2013. Publication number: WO/2013/116513.

Awards

- **Intel Global Challenge, UC Berkeley, California, USA, November 2011.**

Was member of the team NanoDiagX, winner of the 3rd place, at the internal entrepreneurship competition; Intel Global challenge. After qualification by finishing in the 1st place in 7th Arab Technology Business Plan Competition, our team NanoDiagX became the first Arab team to ever make it to the top three places at the Intel Global Challenge. Our business plan for set up a company for novel nanodiagnostics of high burden diseases made to the finalists after competing with 28 other teams from 20 different countries.

- **7th Arab Technology Business Plan Competition, 2011.**

Was member of the team NanoDiagX, winner of the 1st place, for our business plan for establishing a company for development of novel nanodiagnostics platforms for direct, rapid, inexpensive, and sensitive detection of active infections. The competition was organized by the Arab science and Technology Foundation (ASTF) in collaboration with the United Nations Industrial Development Organization (UNIDO) and Intel, and had over 50 competing team from 12 Arab countries. Being of the top three teams qualified our team to represent the Arab World in the UC Berkeley Technology Entrepreneurship forum in the world wide finals of the Intel Global Challenge.

- **Second place in Annual Meeting of clinical Chemistry conference**

(Rapid detection of unamplified HCV RNA in clinical specimens using unmodified gold nanoparticles). **California, July 2010.**

11 Acknowledgements

My journey through post graduate studies has given me the opportunity to interact and collaborate with many wonderful people, who have strongly supported my research endeavors. It is through this interaction that I have acquired the essential value of being a team player in scientific research, and learnt firsthand how good productive scientific research work is a product of extensive practical and mental collaboration between researchers and colleagues.

First of all, I would like to thank my promoter Prof. dr. F. Grosveld for accepting me as a PhD candidate. I will be forever indebted to you for your belief in my work and the genuine support you have provided me on so many levels. Words cannot serve me enough to express my appreciation and gratitude for your efforts and helping me pursue my research passion.

I am very grateful to my co-promoter Prof. dr. H. Azzazy for giving me the opportunity to join his research group and participating in his research projects. Prof. Azzazy you have hosted me in your laboratory for the past 8 years, treating me as a PhD holder and not just a PhD student. You have given me the freedom for exploring and pursuing my research interests and you were always pushing me to convert the ideas into reality. The most important and critical thing I have learnt from working with you, is how to think out of the box and to truly believe nothing is impossible and to push forward towards greater goals. Moreover, I acquired skills for working independently; which is a precious asset for building up a real scientist or researcher. All these things will be valuable assets for me in the future, both in my professional and personal life, for this I truly thank you.

I would also like to express my appreciation for my committee members; Prof. dr.D.F.E. Huylebroeck, Dr. T.L. M. Hagen, Dr. N.J. Galjart, who invested their valuable time and effort in reading my thesis. Their feedback was a very valuable addition to the dissertation.

I am also grateful to Prof. dr. Sanna Eissa for her remarkable guidance and insights into clinical research, especially in the area of tumor biomarkers. Furthermore, I would like to express my genuine thanks to Dr. Marwa Matboli for her support and precious input, particularly in aspects related to cancer biology.

I could not forget Prof. dr. Elziény Ebied, who was the first one to draw my attention to the field nanotechnology and its biomedical applications, back when I was undergraduate student. This impressive scientist and dedicated mentor to his

Acknowledgements

students, has been a great source of guidance and support throughout the course of my studies.

I am greatly thankful to Dr. Khaled Alyan, who gave my first introduction into molecular biology. You have provided me with the remarkable opportunity to train and do research just after graduation in the reputable, US Naval Medical Research Unit (NAMRU #3). The 2 years I spent there were the base of my research career.

I am greatly indebted to Dr. Tamer Samir, my mentor and friend since my undergraduate studies. You were always there for me to answer my questions, and our discussions were always fruitful and provided me with new insights. Also, thank you for all your help with the formatting, writing and helping with vivid figures and illustrations.

Bassem Guirguis, I particularly enjoyed working with you as team. I will never forget staying in the lab till midnight, struggling together with the gold nanoparticles and Hepatitis C Virus RNA. I believe that you'll excel in whatever career you'll pursue and should you chose research you'd make a great scientist.

Mai Mansour, our team would have suffered greatly without you. I think I would never find a teammate like you. You were like a young sister and a mature mother at the same time to all of us.

Sarah Radwan, the hidden and a primary trigger in colleague in this research work. You are the one who shed the light for me on the potential of on unmodified AuNPs techniques. I will never forget your help and support. You have the makings of a remarkable scientist and/or teacher, and whichever you choose, any student who crosses your path would greatly benefit.

I would also like to tell my AUC colleagues: Marwa Hussein, Kamel Eid, Salma Tammam, Dr. Mahmoed Abd Elaty, Samir Nabhan, Karim Abd Elhady, Dr. Ahmed Ebrahim and Faten Farok, that it was very nice to work with you all. Each one of you has added a lot to me. I enjoyed our time in the lab working, discussing, laughing, and drinking coffee together.

Heba Adel, thank you for your care, valuable pieces of advice, and overall your support over the last year. I appreciate everything you have provided to me.

Dr. Parham Solaimani, no words could express my gratitude to you. You turned my career and my PhD around. It is an honor to have a friend like you and a privilege to have you as my paranymp. I hope someday we could conduct

Acknowledgements

research together, perhaps we can bring to reality some of your science fiction ideas, which I truly believe in.

Atef Kamel, my Godfather in Netherlands. Thank you for providing me the support, guidance and care which I needed most during my stay there.

Most of all, I am very grateful to my parents for their unconditional love and support, in all aspects of my life, through all these years, with all their ups and downs. You gave me the strength and power to continue during hard times, and drove me on when I thought I couldn't carry on. This thesis is for you Mama, I specially dedicate this work to you. You have made my dreams and aspirations your own, and spared no effort ensuring that I reach them. Your only reward is to see that I was happy. What you've done for me is beyond what can be expressed with words. You are my anchor and my motivation and strength. Thank you for all your sacrifices. I cannot ever thank you enough for what you have done for me.

My beloved daughters', Maryam and Farida, you are the joy of my heart and the sparkle in my smile, I thank God each day for blessing me with such two cute, lovely daughters like you and I believe that you will be great girls in the future, and you will have bright future. Be assured as you go through life, which you'll always have my support in whatever endeavors I undertake to see that you become the best you can.

Finally, I thank God for the life I have and its blessings and instilling the passion for science in my heart and putting me on the path to actively pursue it. I pray that He always allows me to be of good for human knowledge, to accept my efforts and continue to grant me strength in my future.

As prophet Mohamed said (PBUH): "The best person is the one who benefits all human being"

Based on prophet Mohamed's advice: PhD means, that it is time for me to work and to explore science for the benefit of mankind.